

ABSTRACT

In the evaluation of various theoretical approaches describing gas absorption in turbulent liquids, the effect of molecular diffusivity on mass transfer coefficient is a key factor which can shed light on the hydrodynamics of the boundary of the turbulent liquid. This effect is determined experimentally in a batch type stirred vessel with an unbroken liquid surface. Chemical absorption methods are used in measuring the absorption rate, which are used to calculate the mass transfer coefficients. Sulphite oxidation and allyl alcohol hydrogenation are the reactions taking place in the chemical absorption processes of oxygen and hydrogen respectively into the electrolyte solutions.

The results show that the dependence of the absorption coefficient, k_L , on the diffusivity, D , varies with changing stirrer speed. The variation of the dependence of k_L on the exponent of D is within the values of $1/2$ and $3/4$ and is in agreement with the prediction of the damped eddy diffusivity model of King.

The experiment is considered being performed in the transition region between the steady state transfer and the penetration asymptotes in the King's model. A new procedure is developed in evaluating model parameters. By comparison of the present experimental result with the result of previous workers, the geometry of the absorption system is found important to the mass transfer mechanism.

It is also found that the degree of dependence of k_L on the energy dissipation rate or stirrer speed may be different in a given geometry if different transfer asymptotes are considered. An examination of King's model shows that the usual forms of the relation $k_L \propto D^m$ and the correlation $N_{Sh} \propto N_{Sc}^\sigma N_{Re}^\delta$ are inadequate in an absorption experiment, such as in the present study, performed in the region of transition.

ACKNOWLEDGMENT

The author is deeply indebted to Professor John A. Ruether for his direction, advice, and inspiration during the course of this work.

The author wishes to acknowledge Mr. P. S. Puri for his providing the solubility data and for helpful discussions and suggestions in hydrogenation kinetics.

The author is also grateful to Mr. K. T. Heng for his help in making the graphs and drawings and to Mr. G. Gasperetti for his technical assistances.

Financial assistance from the National Research Council of Canada is gratefully acknowledged.

TABLE OF CONTENTS

		<u>Page</u>
	Abstract	i
	Acknowledgment	iii
	Table of Contents	iv
	List of Tables	vi
	List of Figures	vii
I	Introduction	1
II	Theories	6
	1. General concepts of gas absorption	6
	2. Mass transfer models	10
	3. Chemical absorption	15
	4. Chemical kinetics	22
III	Experimental	27
	1. Apparatus Description	27
	2. Experimental procedures	30
IV	Method of Calculation and Results	37
	(a) Oxygen-sulphite system	41
	(b) Hydrogen-allyl alcohol system	49
	(c) Dependence of k_L on D	50
	(d) Parameter evaluation in King's model	57
V	Discussion	67
	1. Transport mechanism	67
	2. Specific energy dissipation rate and stirring speed effects	73
	3. Correlation of data on k_L	76
VI	Conclusions and Recommendations	79

	<u>Page</u>
VII Nomenclature	82
VIII Bibliography	86
IX Appendices	90
A. Heterogeneous mass transfer with reaction: condition for diffusional regime	91
B. Supporting experiments	96
C. Experimental results	107
D. Sample calculations	129
E. Abstract of King's model	135

LIST OF TABLES

<u>Table</u>		<u>Page</u>
1	Oxygen absorption coefficients	47
2	Hydrogen absorption coefficients	51
3	The values of apparent exponent m for various stirring speeds	56
4	The parameters of King's model	63
5	Values of specific energy dissipation rate at various stirring speed	64
6	Summary of measurements of m values	70
B-1'	Values of t' in various material added solutions	100
C-1	Experimental results for oxygen-sulphite system	125
C-2	Experimental results for hydrogen-allyl alcohol system	127

LIST OF FIGURES

<u>Figure.</u>		<u>Page</u>
1	Concentration profile of diffusing solute a. Film theory b. Penetration theory	12
2	Concentration profiles for gas absorption with and without chemical reaction	21
3	Schematic representation of the vessel and the stirrer	28
4	Apparatus for H ₂ absorption studies	29
5	Solubilities of O ₂ and H ₂ in 0.1 M sodium sulphate solution	42
6	The influence of stirring speed upon k_L	53
7	General model for uniform lifetime surface age distribution	64
8	The dependence of parameters a and \bar{t} on ϵ	65
9	Dependence of mass transfer coefficient on diffusivity	77
B-1	Propanol concentration vs. time for hydrogenation of allyl alcohol at a condition where $C_B \neq 0$	103
B-2	Determination of mass transfer coefficient for absorption of hydrogen according to Equation (B1)	104
B-3	Mass transfer coefficient vs. amount of Raney nickel used	106

FigurePage

C-1	Sulphite concentration vs. time for oxidation of sodium sulphite at a stirring speed of 109 rpm	108
C-2	Sulphite concentration vs. time for oxidation of sodium sulphite at a stirring speed of 125 rpm	109
C-3	Sulphite concentration vs. time for oxidation of sodium sulphite at a stirring speed of 132 rpm	110
C-4	Sulphite concentration vs. time for oxidation of sodium sulphite at a stirring speed of 153 rpm	111
C-5	Sulphite concentration vs. time for oxidation of sodium sulphite at a stirring speed of 164 rpm	112
C-6	Sulphite concentration vs. time for oxidation of sodium sulphite at a stirring speed of 181 rpm	113
C-7	Sulphite concentration vs. time for oxidation of sodium sulphite at a stirring speed of 225 rpm	114
C-8	Sulphite concentration vs. time for oxidation of sodium sulphite at a stirring speed of 240 rpm	115
C-9	Sulphite concentration vs. time for oxidation of sodium sulphite at a stirring speed of 258 rpm	116
C-10	Sulphite concentration vs. time for oxidation of sodium sulphite at a stirring speed of 272 rpm	117

<u>Figure</u>		<u>Page</u>
C-11	Propanol concentration vs. time for hydrogenation of allyl alcohol at a stirring speed of 132 rpm	118
C-12	Propanol concentration vs. time for hydrogenation of allyl alcohol at a stirring speed of 153 rpm	119
C-13	Propanol concentration vs. time for hydrogenation of allyl alcohol at a stirring speed of 181 rpm	120
C-14	Propanol concentration vs. time for hydrogenation of allyl alcohol at a stirring speed of 225 rpm	121
C-15	Propanol concentration vs. time for hydrogenation of allyl alcohol at a stirring speed of 240 rpm	122
C-16	Propanol concentration vs. time for hydrogenation of allyl alcohol at a stirring speed of 258 rpm	123
C-17	Propanol concentration vs. time for hydrogenation of allyl alcohol at a stirring speed of 272 rpm	124
D-1	Calibration of propanol concentration	133
D-2	Typical analysis of propanol by gas chromatography	134
E-1	General model for free surface mass transfer	139
E-2	Exponent on diffusivity vs. dimensionless surface age	139

I INTRODUCTION

Gas-liquid interfacial mass transfer has, in the recent years, proved of continuing importance to chemical engineers both theoretically and practically. Many industrial processes involve gas absorption which has been studied from many points of view in various types of equipment.

For most industrial applications, the diffusion of substance from gas to the liquid phase is often accompanied by complex hydrodynamic conditions. In turbulent mass transfer problems, estimations of operation efficiency and performance continue to be based on empirical correlations. On the other hand, numerous approximate and simplified theories have been proposed to interpret experimental data and to predict transfer rate in terms of relatively few transport properties and parameters.

All of the well known theories for gas absorption except the film model of Lewis and Whitman (1) are based on turbulence effects on the liquid. Each model describes a different picture of the mechanism of transport in the liquid boundary adjacent to the gas-liquid interface. Certain of these existing models are capable of interpreting important experimental observations in one system, but do not correspond to any reasonably well defined physical quantities in others. Such models may provide the correct picture of transport mechanism to a particular case, but

do not give a general description to the phenomena of gas absorption. There is still no such a model with the detailed features of the theory generally confirmed. As Rozen and Krylov (2) have clearly pointed out, a number of problems in this area have not been solved.

The ultimate aim of fundamental mass transfer studies such as this one is to allow mass transfer coefficients, needed for design, to be predicted with increased accuracy. To accomplish this, correlation must be developed which can be used for extrapolation to conditions that have not been measured experimentally. A correlation is developed by postulating that the system can be described by a particular mathematical model. The quality of the correlation naturally is limited by the ability of the postulated model to describe the actual physical phenomena. If an unrealistic model has been used, the resulting correlation will give unreliable results when used for prediction.

For a model to be used in mass transfer coefficient correlation, the mechanisms of transport in theory must conform reasonably well with the system. A good selection and development of a model requires knowledge of hydrodynamic conditions near the gas-liquid interface and the understanding of which basic absorption concepts govern the transport process. It is generally accepted that there are three transport mechanisms for gas absorption in turbulent liquids: molecular diffusion, eddy diffusion, bulk

transport (i.e. surface renewal, or surface rejuvenation). Transport by molecular diffusion is the only mechanism that depends on the diffusivity, D . However, all models, with the exception of Kishinevsky's (3), postulate that the total resistance to diffusion contains a significant part attributable to molecular diffusion. Many of these theories postulate that a molecular diffusion resistance acts in series with turbulent transport mechanism. For the steady state molecular diffusion part of the total resistance, the dependence of flux on diffusivity is to $D^{1.0}$. However, since the overall resistance depends also on turbulent transport, the flux based on bulk concentration differences depends on D to some power less than unity. Different models postulate different degree of relative importance of resistance due to unsteady state molecular diffusion, steady state molecular diffusion, and turbulent transport. Each model therefore predicts a value (or for multiparameter models, a range) of the dependence of k_L on the power of D . By measuring the dependence of k_L on the power of D we gain information enabling us to judge which models more closely describe the physical situation.

Previous investigations for this purpose have been studied. Unfortunately, little agreement within the available data was found. For the studies of gas absorption or desorption in a vessel with mechanical agitation (3-6),

values of degree of dependence of mass transfer coefficient k_L on diffusivity D have been reported to be lying between 0 and 1. Other studies on various contactors, such as packed column (7), wetted-wall column (8), and turbulent jets (9), reported their results showing different dependence of k_L on D . These results were interpreted according to different models.

A confirmed model which can interpret well in experimental results and can predict transfer coefficients is necessary in understanding the mechanism of liquid phase mass transfer adjacent to a free surface. Well set-up experiments on gas absorption can be a source of valuable information on determination of transport mechanisms. All the previous experimental work concerned with determination of diffusivity effect on mass transfer coefficient used the physical absorption method. Various gas-liquid contacting systems and experimental techniques have been employed. In some of these works, the variation in the diffusivity was mainly brought about by varying the temperature (10) or viscosity (11) of the liquid in the experiments. However, since there were associated changes in the hydrodynamics of the flow field near the interface, the effect of diffusivity could not be definitely ascertained. As suggested by most of the other workers, a comparison of the mass transfer coefficients of absorption of various slightly soluble gases having a wide range of diffusivities under

the same controlled hydrodynamic conditions is a powerful tool for determining the effect of D on k_L without altering other variables in the system. Owing to the fact that at least two gases must be used in such an experimental method, oxygen and hydrogen, which give low values of solubility and a significant difference in diffusivity, were chosen in this work. The batch absorption technique was used in a stirred vessel with absorption rate measured by the chemical method. Oxygen was absorbed in a sodium sulphate solution accompanied with sulphite oxidation in the solution, while hydrogen was absorbed also in sulphate solution with identical hydrodynamic conditions. Hydrogenation of allyl alcohol took place in the solution.

The aim of this work was to find experimentally the influence of diffusivity upon mass transfer coefficient at a free turbulent interface. The results will be interpreted in light of an appropriate model, and this in turn will shed light on the mechanism of transfer. The inability of a particular model to correlate the data would also be evidence that the model was inadequate.

II THEORIES

1. General Concepts of Gas Absorption

In physical gas absorption, in which no chemical reaction takes place between the dissolved gas and liquid, there are individual-phase resistances to the passage of gas into liquid. In each phase, resistance is considered to exist primarily in a region adjacent to the interface. Inside this region, most of the change in concentration between the interface and the bulk liquid occurs. Beyond this region, convective transport is predominant and perfect mixing is assumed. In addition, it is assumed that there is no resistance across the gas-liquid surface, and that the concentration at the interface of liquid phase, C_I , is always in equilibrium with the concentration at the surface of the gas phase. The resistances encountered in both phases near the phase boundary are additive, and each is represented as the reciprocal of the individual transfer coefficient, k_L or k_G . The flux of material across the interface is

$$q_I = k_L(C_I - C_B) = k_G(p_G - p_I) \quad (1)$$

If Henry's Constant is used, the above equation can be rewritten to show all the driving forces represented by concentration differences as,

$$q_I = k_G H(C_G - C_I) = k_L(C_I - C_B) \quad (2)$$

where C_G is the hypothetical liquid phase concentration that would be in equilibrium with gas of partial pressure P_G , and C_B is the bulk concentration of liquid phase.

In general, the gas phase offers relatively little resistance to the absorption of slightly soluble gases, for which the Henry's Constant, H , is large and the liquid phase resistance $1/k_L$ is large compared with the gas phase resistance $1/(k_G H)$. The term involving the gas phase resistance in Equation (2) need not be considered, since it offers a negligible resistance to absorption. This is the case of liquid phase mass transfer control, and C_I is the concentration at saturation.

To explain the above stated mass transfer coefficient concept in turbulent liquids, one must consider molecular transport and turbulent transport. Molecular transport, as the term implies, depends upon the motion of individual molecules for the transport of mass, heat, and momentum. The rate in molecular diffusion is determined by diffusivity and the concentration gradient. The equation in a one-dimensional case with negligible bulk flow is

$$q = - D \frac{\partial C}{\partial y} \quad (3)$$

The general unsteady state molecular diffusion equation can be obtained by material balance:

$$\frac{\partial C}{\partial t} = D \frac{\partial^2 C}{\partial y^2} \quad (4)$$

Although in a turbulent system, the mechanism is more complex, the general concept of molecular transport is of fundamental importance.

Equating Equation (2) and (3) at the interface, the mass transfer coefficient can be shown, as a definition, in the form:

$$k_L = - D \left(\frac{\partial C}{\partial y} \right)_I / (C_I - C_B) \quad (5)$$

Turbulent transport is due to the random movement of large groups or clusters of molecules which are called eddies. The transfer of solute by random turbulence eddies is analogous to the transfer of matter by molecular diffusion. The existence of a concentration gradient in a fluctuating agitated fluid leads to a net transfer of matter in the direction of decreasing concentration, thus the flux transported by turbulence eddies in a one-dimensional system may be stated

$$q = - D_e \frac{\partial C}{\partial y} \quad (6)$$

where D_e represents the eddy diffusivity. Turbulent fluid motion varies with distance from the surface. Therefore, the transfer of matter by turbulence eddies also varies

with the distance. Thus, the eddy diffusivity must be a function of the distance from the surface. The eddy diffusivity is sometimes expressed as:

$$D_e = ay^n + b \quad (7)$$

As proposed by Levich (12), it is reasonable to expect b to be equal to zero for liquids of high surface tension because eddy diffusivity would be damped out at the surface.

The effects of turbulent transport are usually treated analytically by assuming that molecular and turbulent diffusion work in parallel. Thus Equation (3) and (6) were combined to give the following expression for mass transfer in turbulent liquids:

$$q = - (D + D_e) \frac{\partial C}{\partial y} \quad (8)$$

Since D_e is proportional to the macroscopic scale of turbulence eddies, it greatly exceeds the molecular diffusivity D in a fluid with developed turbulence. The large value of D_e ensures a virtually constant concentration of the solution down to very small distances from the interface. At short distances from the surface, however, the retarding effect of the surface begins to be felt.

The transport mechanism in a turbulent liquid is a combination of molecular and turbulent processes whose re-

relative effects are difficult to predict. As a result it is necessary to combine theory with experimental evidence to obtain an adequate picture of gas absorption.

2. Mass Transfer Models

As an effort to establish some theoretical bases for describing the mechanism of gas absorption into a turbulent liquid, a number of models have been proposed. The earliest model is the film theory of Lewis and Whitman (1), which assumes the existence of a stagnant film next to the boundary of the liquid with a thickness L . According to this model, gas absorption is a steady state process under a uniform concentration gradient across the film. Beneath the film perfect mixing is assumed and the solute concentration is constant throughout. This concentration profile is shown in Figure 1a. Molecular transport is the only process, and the rate equation is obtained from Equation (3):

$$q = \frac{D}{L}(C_I - C_B) \quad (9)$$

The relation $k_L = D/L$ gives a conclusion that there is a linear dependence between mass transfer coefficient and molecular diffusivity.

Higbie (13) proposed the penetration theory, in which uniform exposure time for all eddies is relatively short

at the surface, so that the transient molecular transport occurs as if into a liquid of infinite depth. The rate equation was derived starting with the general unsteady state molecular diffusion equation. The result is

$$q_I = \sqrt{2D/(\pi\theta)} (C_I - C_B) \quad (10)$$

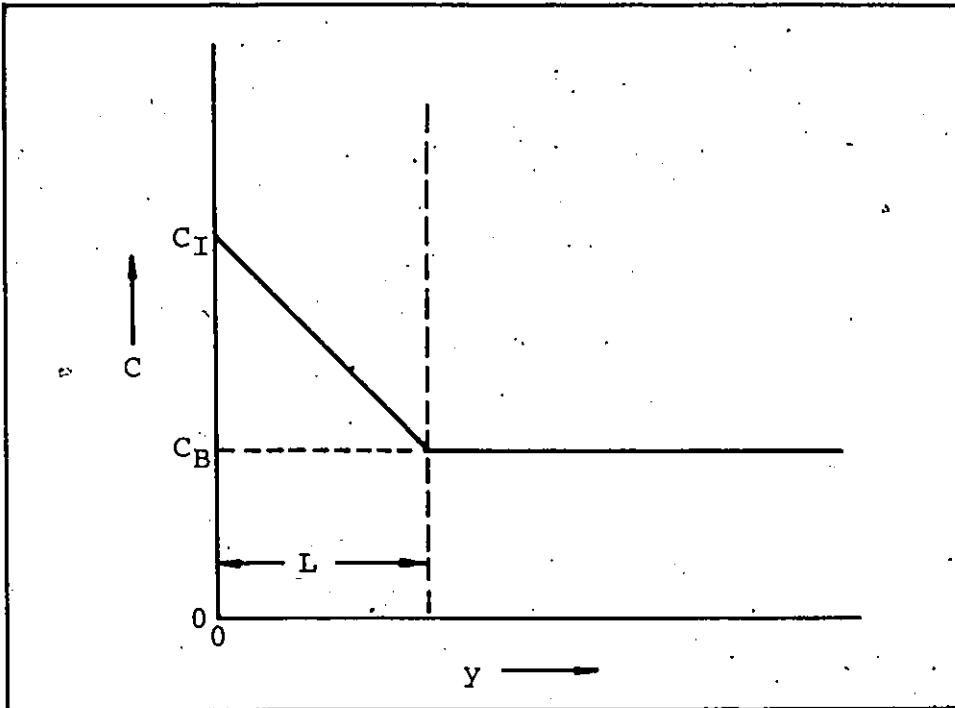
The mass transfer coefficient of this model is given by $k_L = \sqrt{2D/(\pi\theta)}$ where θ is the exposure time for eddies.

The random surface renewal concept was originally applied by Danckwerts (14) to absorption into a turbulent liquid. According to this model all surface eddies had an equal probability of being replaced regardless of their age. The unsteady state diffusion process of gas into liquid surface elements of various ages is similar in concept to that of Higbie. Fresh surface is continually created by the random motion of the eddies. The mean rate of production of fresh surface is constant for a given degree of turbulence and equal to s . The rate of absorption for the turbulent liquid with random surface renewal is

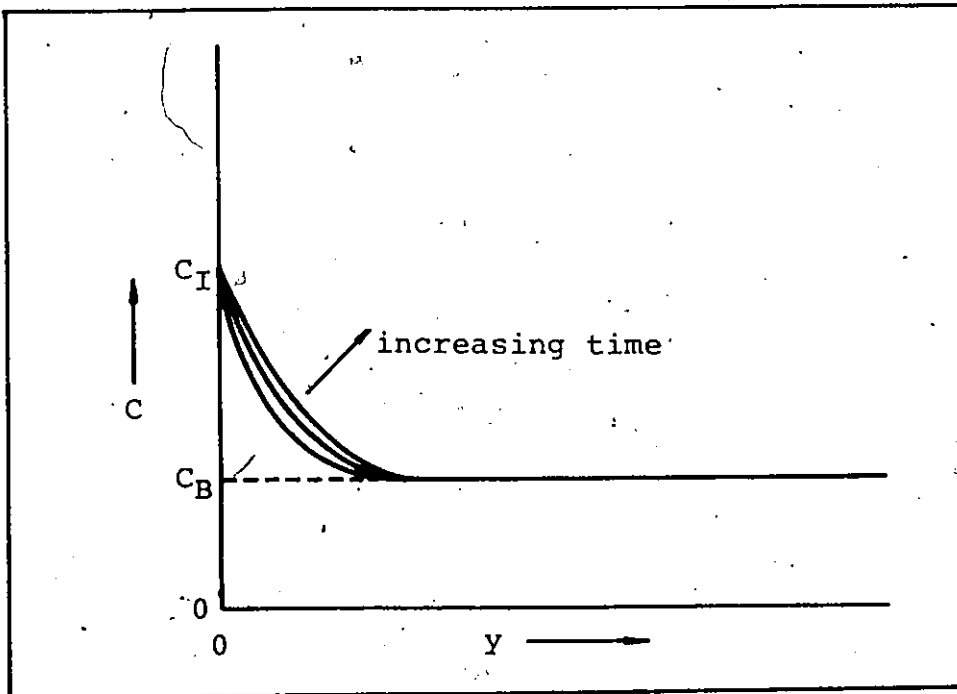
$$q_I = \sqrt{Ds} (C_I - C_B) \quad (11)$$

Both Higbie and Danckwerts models give a square root dependence of k_L on D . The concentration profile of these penetration models is given in Figure 1b.

The above described models form the basis of modern theory of gas absorption. Many modifications and exten-



a. Film theory



b. Penetration theory

Figure 1. Concentration profile of diffusing solute

sion of these models have been proposed, such as Perlmutter's (15) various imperfect mixing models, and the normalized surface renewal theory of Hanratty (16). Kishinevsky (3) has put forward the postulate of turbulence controlled mass transfer. He introduced the eddy diffusivity which, in addition with the molecular diffusivity, appears in the expression $k_L = 2\sqrt{(D + D_e)/\pi\theta}$ resulting from the penetration theory type model. At high turbulence levels the eddy diffusivity would be much larger than the molecular diffusivity, and the mass transfer coefficient would be independent of molecular diffusivity. Levich (12), and Davies (17) treated resistance to transfer by proposing different mechanisms controlling in different sublayers in the surface boundary. Transfer fluxes of these sublayers are all equal, and a steady state analysis gives a square root diffusivity dependence.

In addition to models that predict a constant value of dependence of mass transfer coefficient on diffusivity, there are others according to which the value of dependence changes continuously with the turbulent intensity.

Film-penetration theories have been presented by Toor and Marchello (18), and Dobbins (19). According to these models, the resistance to mass transfer in the phase considered is confined within a film at the interface, as in the film theory. However, the fluid elements of the film, or surface elements, are constantly renewed as in the

penetration theory. If Danckwerts' type of surface renewal is used, the mass transfer coefficient can be written in the form: $k_L = \sqrt{D} \text{scoth}/(sL^2/D)$. In addition to the transfer being produced by molecular diffusion in the interval between eddies, Harriott (20) started from the concept that eddies arriving at random times come to within random distances from the surface, sweeping away the accumulated solute. All three models just described predict the dependence of k_L on D to the power varied from 0.5 to 1. King (21) proposed a model which suggests surface fluid element renews with parallel molecular and eddy diffusion from the surface within each element. A damped eddy diffusivity is incorporated in the rate equation which predicts the mass transfer coefficient depending on the diffusivity to a varying degree, from 0.5 to 0.75 for free surface mass transfer.

Since the above described models involve one or more characteristic parameters which cannot be determined from known experimental conditions, difficulties remain in their use for predicting the transfer rate. For a model to be useful its parameters must be related to experimentally measurable quantities. Recently, eddy cell models have been proposed using the fundamental specific energy dissipation rate ϵ as a link to the theory of turbulent fields. This is an attempt to eliminate any empirical determined parameter and give a result to relate k_L to ϵ .

To this group of models Fortescue and Pearson (22) considered that large scale eddies control the transfer rate, yet Lamont and Scott (23) assumed that small scale motions should be most important.

3. Chemical Absorption

Chemical absorption methods have been used widely in recent years to determine the absorption coefficient of various gas-liquid contactors. Besides the possibility of evaluating the interfacial area independently, these methods provide some more advantages which have been stated by Sharma and Danckwerts (24). In addition, Kozinsky and King (5) stated that there are some problems about the determination of mass transfer coefficient by a physical batch absorption technique. Under conditions of high agitation the liquid tends to approach saturation very quickly, thus reducing the time available for measurements. Also, some gases, such as hydrogen, are highly insoluble gases, consequently the total volume of gas absorbed is quite small. There is thus a possibility of significant error due to small temperature changes or to leaks. These problems were solved by using continuous flow system in their experiment. However, a certain liquid flow rate is required in the flow system to reduce the problems of short run times and low total absorption. A substantial agitation is afforded by the flow process itself even in

the absence of stirring, thus the measurements of mass transfer coefficient are limited in the high range of turbulence levels only. The use of chemical absorption method can avoid the above problems, and experiments are allowed to operate at low turbulent intensities.

The general theory for chemical absorption was published in literature (25, 26). Gas dissolves in the liquid and there undergoes a reaction with another reactant dissolved in the liquid. A rate of reaction term has to be added in the general unsteady state continuity equation for absorption to represent the reaction effect. The equation becomes

$$D \frac{\partial^2 C}{\partial y^2} = \frac{\partial C}{\partial t} + r \quad (12)$$

The unsteady state form of penetration theory is used for convenience, but the conclusions do not depend on the model chosen.

From the asymptotic solutions of this equation, As-tarita (25) has proposed different regimes of chemical absorption which are identified by the resulting equations for the total absorption rate and by the conditions required. The work presented here concerns the diffusional gas absorption regime only. The concept of determining the mass transfer coefficient by chemical absorption in this regime is described as follows:

In a chemical absorption process, the diffusion of gas molecules in liquid is accompanied by chemical reaction. If the proportion of the gas reacted in the vicinity of the gas-liquid interface is very small, the process is essentially one of physical absorption followed by reaction in the bulk liquid. The condition required to satisfy this has been proposed by Astarita that the reaction time, t_r , must be much larger than the diffusion time, t_D . The reaction time is the time required for the reaction to proceed to an appreciable extent, and the diffusion time is the average time available for diffusion. They are defined as:

$$t_r = \frac{C_I - C_e}{r_{C_I}} \quad (13)$$

$$t_D = D/k_L^2 \quad (14)$$

where C_e is the chemical equilibrium concentration of gas solute and r_{C_I} is the reaction rate with concentration C_I . The condition can then be expressed as:

$$\frac{C_I - C_e}{r_{C_I}} \gg D/k_L^2 \quad (15)$$

The same condition can be obtained by applying the concept of the film theory. It is obvious that r_{C_I} represents the maximum local reaction rate in the film. The condition that the amount of reaction in the film can be

negligible compared to the amount of reaction in the bulk liquid thus can be expressed as:

$$1 \gg \frac{r_{C_I} V_f}{r_{C_B} V_B}$$

where V_f and V_B are the liquid volume of the film and the bulk respectively. The fraction of liquid in the diffusion film V_f/V_B can be expressed in terms of the film thickness L , and the liquid volume per unit interfacial area ϕ . With $L = D/k_L$, the condition becomes

$$1 \gg \frac{r_{C_I} D}{\phi r_{C_B} k_L}$$

It can be shown that in chemical absorption, $k_L(C_I - C_e)$ is always larger than ϕr_{C_B} . Therefore, the term ϕr_{C_B} can be replaced by $k_L(C_I - C_e)$ in the condition.

$$1 \gg \frac{r_{C_I} D}{k_L^2 (C_I - C_e)}$$

or,

$$\frac{C_I - C_e}{r_{C_I}} \gg D/k_L^2$$

In the situation under consideration, an insignificant amount of reaction occurs in the liquid surface boundary; and two phenomena, physical gas absorption and chemical reaction in the bulk liquid occur in series in the absorption process. In steady state, all the absorbed gas

is consumed by reaction in the liquid. The absorption rate at the interface is equal to the reaction rate in the bulk liquid.

$$q_I = k_L(C_I - C_B) = \phi r_{C_B} \quad (16)$$

If another condition, which represents the reaction rate being much faster than the mass transfer rate when both have the same total driving force,

$$\phi r_{C_I} \gg k_L(C_I - C_e) \quad (17)$$

is also fulfilled, the driving force for mass transfer, $C_I - C_B$, must be much larger than the driving force for reaction, $C_B - C_e$, or, $C_B \approx C_e$ in Equation (16). If such is the case, the reaction rate is high enough to keep the bulk gas solute concentration, C_B , practically equal to the equilibrium value C_e . The rate-controlling phenomenon is diffusion, so that the overall driving force is entirely used by the diffusion process. This condition will subsequently be called the "diffusional regime". The flux across the interface in the diffusional regime is given by

$$q_I = k_L(C_I - C_e) \quad (18)$$

In summary, under certain conditions the reaction is fast enough to keep the concentration of gas solute in the bulk of the liquid phase equal to C_e , while it is not fast enough for any appreciable amount of gas to react in the

thin layer at the surface of the liquid phase where the absorbing gas concentration passes from its interfacial to its bulk value. Under these conditions the overall absorption rate is that for physical transfer with its bulk concentration equal to C_e . For irreversible reactions, $C_e = 0$, and the equation becomes

$$q_I = k_L C_I \quad (19)$$

Figure 2 shows the comparison of concentration profiles between an absorption process with reaction occurring in the diffusional regime and a physical absorption process. The combined condition to be fulfilled for this regime can be expressed in the following form:

$$\frac{k_L^2}{D}(C_I - C_e) \gg r_{C_I} \gg \frac{k_L}{\phi}(C_I - C_e) \quad (20)$$

Many absorption processes with chemical reaction involve solid catalyst in finely divided particles. Absorbed gas molecules react with liquid reactants significantly only when they have reached the surface of the suspended particles. This three-phase reaction system has the added consideration of transfer resistance between the liquid and the solid phases. In the case of gas absorption with first order or pseudo-first order heterogeneous catalytic reaction it is again possible to operate in the diffusional regime. In this case the intraparticle resistance (for

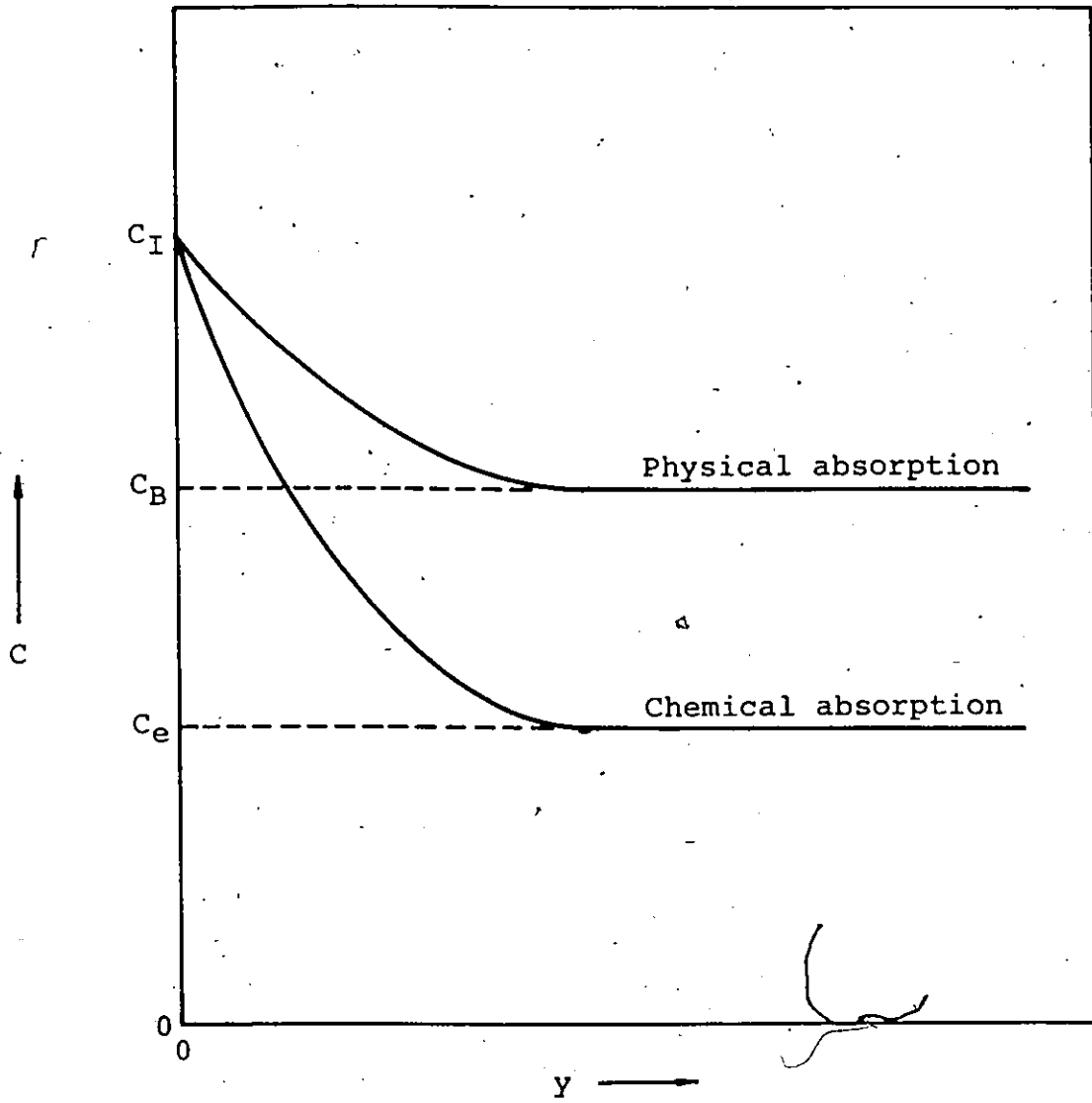


Figure 2. Concentration profiles for gas absorption with and without chemical reaction

diffusion and reaction) and the particle-liquid resistance are both negligible, so that essentially the entire available driving force is used for gas absorption. Details are shown in Appendix A, and the resulting condition necessary for operation in the diffusional regime is

$$\frac{k_L^2}{D} \gg k'w \gg \frac{k_L}{\phi} \quad (21)$$

where

$$k' = \frac{k_p a_p k_1 \eta}{k_p a_p + k_1 \eta}$$

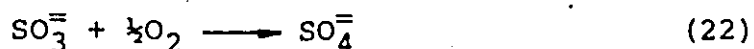
and w is the catalyst mass per unit volume of liquid.

4. Chemical Kinetics

(a) Oxygen-sulphite system

The oxidation of aqueous sulphite solution is one of the few reactions being proved to be a convenient model reaction suitable for evaluating the performance of gas absorbers. The reaction of sulphite to sulphate has been used widely for the determination of interfacial areas and mass transfer coefficients (27, 28). The applicability of the regime conditions of the chemical absorption method depends on the reliability of the kinetic data used. The existing data reported on the chemical kinetics of sulphite oxidation are rather contradictory. Many discrepancies in measurements were published for the reaction orders with respect to both reactants. Recent findings (29, 30) showed

that the kinetics of this reaction are rather complex and the reaction order changes as conditions altered. The reaction rate depends on many factors, such as temperature, PH, oxygen partial pressure, sulphite concentration, catalyst concentration, purity of reagents, etc. The reaction stoichiometric equation of sulphite oxidation can be shown as:



Yagi and Inoue's equation of kinetics, (31) was chosen to estimate the reaction rate because the reaction conditions are close between their experiment and the present work. They reported that the reaction of oxidation of sodium sulphite solution with or without cobalt ions catalyst was first order with respect to both oxygen and sulphite concentration, and the rate equation at 20°C is

$$\frac{d\text{CO}_2}{dt} = -1.4(1 + 1.46 \times 10^7 C_{\text{CoSO}_4}) C_{\text{Na}_2\text{SO}_3} C_{\text{O}_2} \quad (23)$$

By using the energy of activation of the reaction found by Wesselingh and Van't Hoog (30), the equation can be corrected to 25°C and the resulting second order reaction rate constant k_2 at 25°C is

$$k_2 = 1.9(1 + 1.46 \times 10^7 C_{\text{CoSO}_4}) \quad (24)$$

In order to determine the mass transfer coefficient from the oxygen reaction rate, the previous stated condi-

tion of diffusional regime has to be fulfilled. By substituting the expression $r_{C_I} = k_2 C_{Na_2SO_3} C_I$ to Condition (20), the condition for oxygen absorption in diffusional regime is

$$\frac{k_L^2}{D} \gg k_2 C_{Na_2SO_3} \gg \frac{k_L}{\phi} \quad (25)$$

Combination of Equation (24) and (25) shows that the required reaction condition can be controlled by the amount of $CoSO_4$ and Na_2SO_3 used.

The results of preliminary experiments showed that even at the highest stirring speed, 272 rpm, used in the present experiment, the reaction rate was fast enough to keep the oxygen content in the bulk liquid equal to zero without using any catalyst. All experimental runs used no catalyst in this work. The reaction kinetics can then be simplified to

$$\frac{dC_{O_2}}{dt} = -1.9 C_{Na_2SO_3} C_{O_2}$$

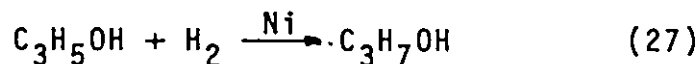
or, $k_2 = 1.9$ (26)

(b) Hydrogen-allyl alcohol system

In liquid phase hydrogenation over solid catalysts, the added steps of external and internal mass transfer between the liquid and solid phases make the reaction mechanism of the whole system more complex compared to the homogeneous oxidation system. Reliable kinetic data are dif-

difficult to be obtained from literature for hydrogenation of allyl alcohol which was employed in the present work.

Tests have been performed for catalysts selection with Raney nickel and palladium on carbon. For the reasons of the catalytic activity being unstable and the possibility of affecting the absorption mechanism in the solution (see Appendix B), palladium on carbon was abandoned. Raney nickel catalyst was used for the hydrogenation reaction of allyl alcohol.



To set up an experiment with conditions which can fulfill the requirements of gas-liquid diffusional regime, information concerning various resistances for chemical reaction (i.e. mass transfer between gas-liquid, liquid-solid phases, together with the effectiveness factor, η , for porous particles) are required. Owing to the difficulties of obtaining the above stated information, some assumptions have to be made for simplification of the reaction mechanism of the system. The concentration of the allyl alcohol is much greater than the dissolved hydrogen concentration in the present case, so both external and internal diffusion resistances for the allyl alcohol were reasonably neglected. Recently Ruether and Puri (32) reported in their study of mass transfer effects in hydrogenation in slurry reactors that the rate of hydrogenation

of allyl alcohol in water catalyzed by Raney nickel was approximately zero-order in substrate at substrate concentration greater than about 0.01 mole/l. The reaction order for hydrogen in the region of zero-order with respect to substrate was 0.96. If the intrinsic reaction orders are one and zero with respect to hydrogen and allyl alcohol concentrations respectively, the approximate amount of catalyst to be used can be estimated by using Condition (21), where the value of k' , equal to 6.147 ml/g cat-sec, was taken from Ruether and Puri's experimental data. The approximate value of k_L for various stirring speeds can be obtained from the result of oxidation experiments with the following assumption: $k_L \propto D^{0.5}$, and the value of diffusivity of hydrogen in water was used. Because the geometrical factors, fluid properties, and power input were all different between experiments of Ruether and Puri and the present work, the application of their experimentally obtained value of k' to the present system is not justified unless the external liquid-solid resistance is very small compared to other resistances in the liquid phase for both systems. Therefore, the amount of catalyst to be used to insure operation in the diffusional regime can be calculated only approximately from Condition (21).

III EXPERIMENTAL

1. Apparatus Description

The vessel used was a cylindrical glass tank of height 18 inches and diameter 12 inches. Four vertical baffles of width 1 inch and length $15\frac{1}{2}$ inches, were held in place $\frac{1}{8}$ inch from the vessel wall by top and bottom rings. A six-blade turbine impeller of five inches diameter, placed 3.75 inches above the vessel bottom, was driven by a variable speed explosion proof motor. The stirring speed was monitored with a stroboscope. The dimensions of the vessel and the stirrer are shown in Figure 3. A model 2010 oxygen analyzer, made by Delta Scientific Corp. was used to measure dissolved oxygen concentration in the vessel. The electrode was fastened to one of the baffles with its tip at the level of the impeller. A thermometer was also fastened to another baffle to indicate the liquid temperature.

For the oxidation experiments, the vessel was opened to atmosphere with air exposed above a stirred water surface. A pH meter was used to measure the pH value of the solution before and after a run.

For the hydrogenation experiments, a cover made of plexiglass with a hole drilled at its center large enough to let the stirrer shaft pass through was placed on the top of the vessel. The vessel was set inside a fumehood. A sketch of the apparatus is shown in Figure 4. Pure hy-

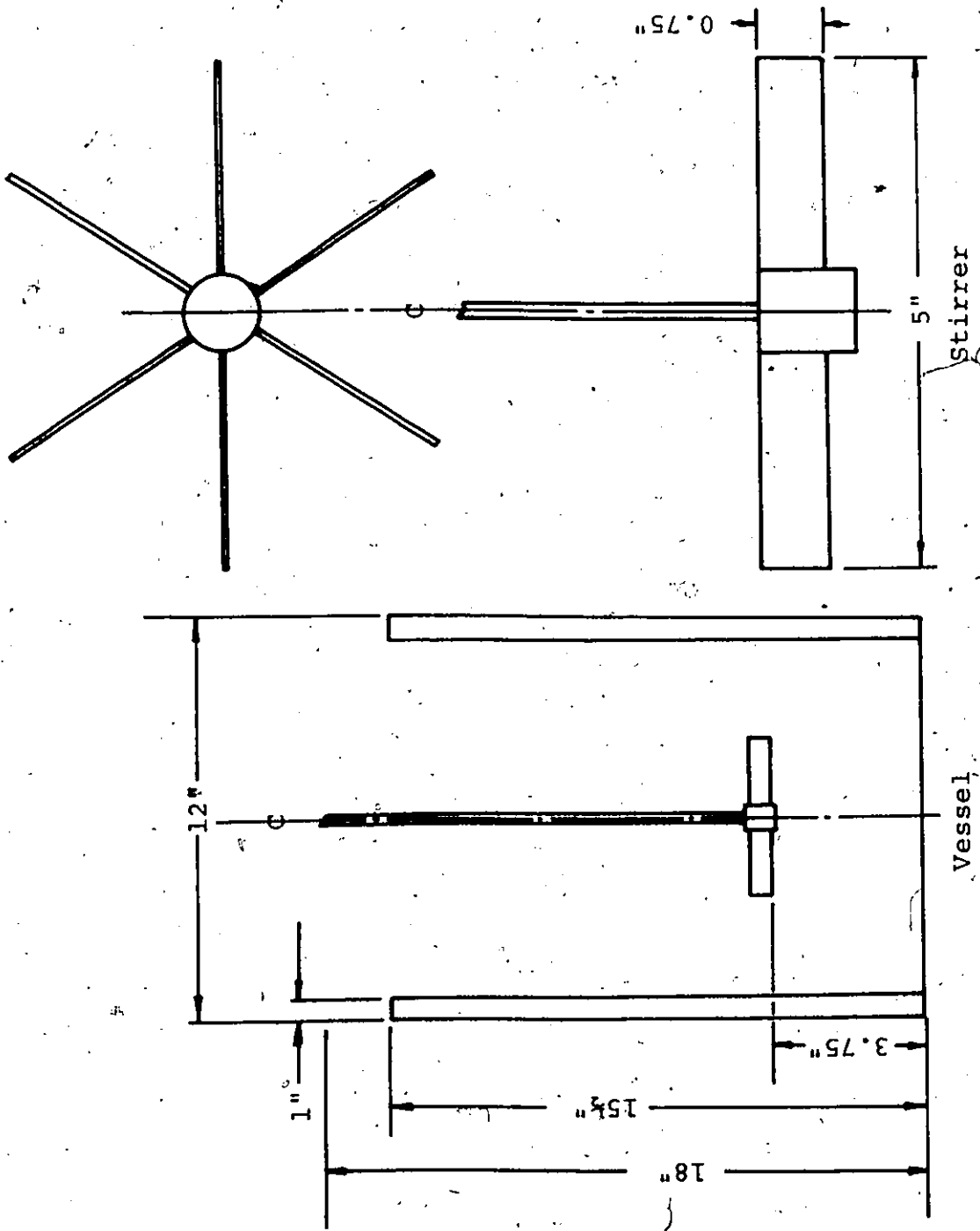


Figure 3. Schematic representation of the vessel and the stirrer

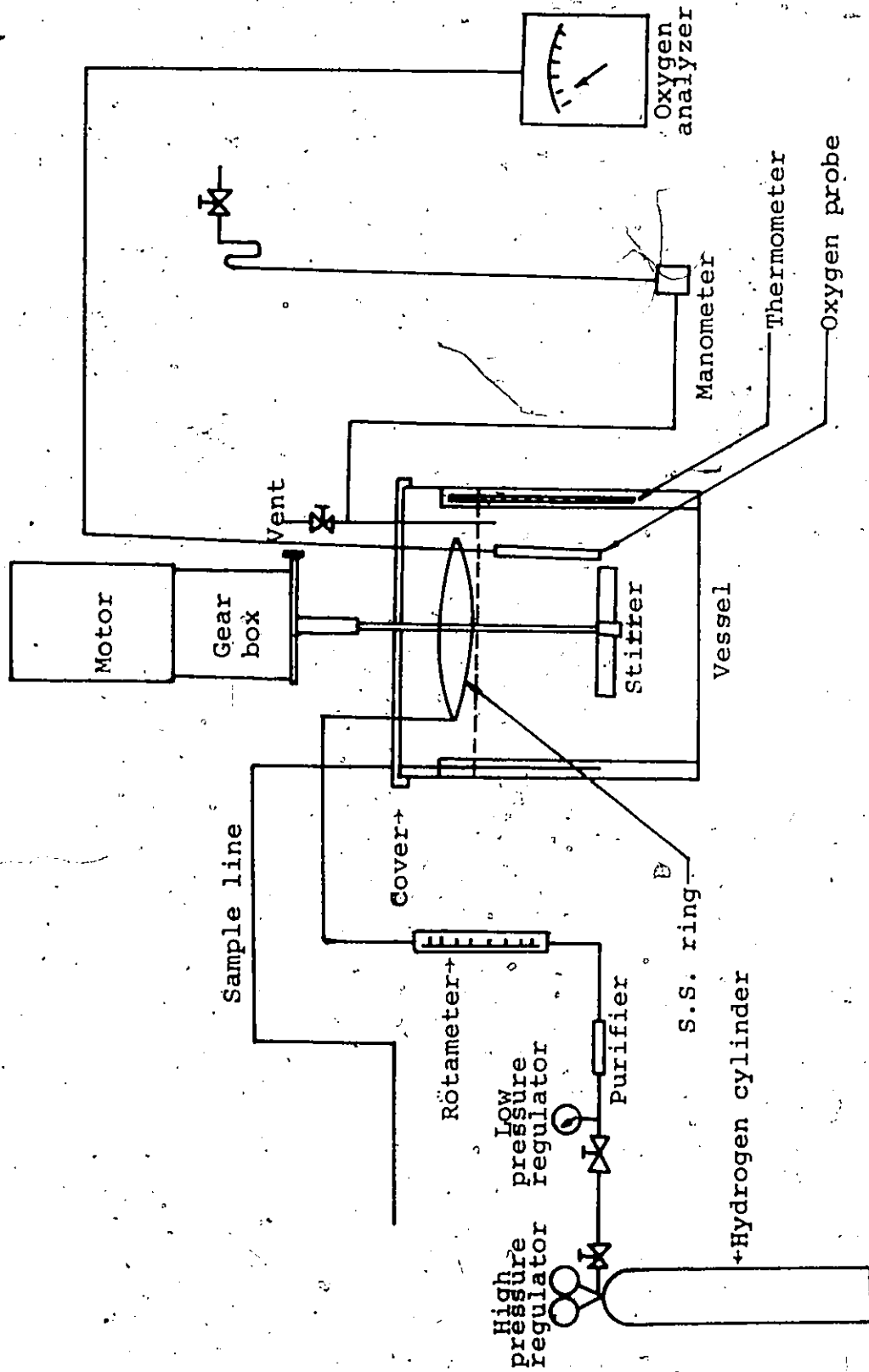


Figure 4. Apparatus for H₂ absorption studies

drogen gas for absorption was supplied from a cylinder and was fed through the holes of a tubing ring which was made by a 1/4 inch stainless steel tube with 36 holes about 1/32 inch in diameter evenly distributed at the positions all over both the outer and inner sides of the ring. The ring was placed about one inch above the liquid surface. The gas was purified before being fed to the vessel with a Deoxo catalytic purifier. A low range pressure regulator was used in series with a high pressure cylinder regulator to control the gas flow rate, which was indicated on a rotameter. The pressure in the vessel was slightly higher than atmospheric during experiments. The gas was allowed to leak out through the centre hole of the cover. A manometer was used to indicate the pressure inside the vessel. Samples were removed from the vessel by a 20 ml syringe through a 3 foot hypodermic needle of 1/32 inch diameter that extended from the vessel under the door of the hood. A model 1400 gas chromatograph with flame ionization detector and a model A-25 strip-chart recorder with integrator, both made by Varian Aerograph, were used for analyzing the concentration of propanol in solution samples.

2. Experimental Procedures

(a) Oxygen-sulphite system

The vessel was washed and rinsed before each run. It was filled with about 18 liters of distilled water. Cor-

rect amounts of analytical grade sodium sulphite and sodium sulphate, both supplied by the Fisher Scientific Company, Limited, were weighed and dissolved in the water to bring the solution to a value between 3×10^{-3} and 5×10^{-3} g mole/l in initial sulphite concentration, depending on the stirring speed used, and to a value of 0.1 g mole/l in total electrolyte concentration. The reason for the addition of sodium sulphate is to prevent significant changes in the kinetic rate constants, which might occur if the composition of the solution changed appreciably with the extent of reaction. In experiments with stirring speed higher than 181 rpm, preheated water was added to increase the initial liquid temperature from 1°C to 5°C , depending on the stirring speed. The raised liquid temperature produced a heat flow which would balance the heat generated from the agitator and reaction and kept the variation of temperature within $\pm 0.5^{\circ}\text{C}$ during an experiment. The range of the initial temperature was between 21°C and 28°C for all runs. The vessel was then filled to a 19 liter-mark with distilled water. The motor was started and the stirring speed was adjusted to the required value. The liquid was left in agitation for about 15 to 30 minutes before the experiment started to allow the system thoroughly mixed and to insure the complete dissolution of the salts. By using a 10 ml pipette, liquid samples were taken from the bulk liquid at various times during the experiment to measure the decrease of sulphite concentration by

iodometric titration method.

Standardized iodine solutions were used in iodometric titration. Sodium thiosulphate solutions were standardized against iodine solution before each run. Samples to be analyzed were pipetted into 25 ml of a slightly stronger iodine solution which had been made basic, about pH 8, by the addition of sodium bicarbonate powder. The mixture remained basic. It was desirable to keep the iodine solution alkaline, in order that the rate of oxidation of iodide ion to iodine was very slow. At least 10 minutes were allowed to elapse before titration to ensure complete reaction of sulphite ion to sulphate ion. The mixture was then made slightly acid, about pH 4, by the addition of acetic acid buffer, because thiosulphate must run in acid solution.

The dissolved oxygen analyzer used was calibrated with its full scale reading representing the saturated oxygen concentration of air-solution system at about 25°C and 1 atm. During the experiment, the oxygen content in the bulk of solution was indicated on the meter of the analyzer. Its reading was kept lower than one percent of the full scale, or, the value of saturation, at all times of the experiment. Temperature and pH were measured at the beginning and at the end of each run to ensure no significant changes occurred during a run. Atmospheric pressure was read from the manometer in each run.

The measurements were done at ten agitator speeds (109, 125, 132, 153, 164, 181, 225, 240, 258, and 272 rpm). At stirring speeds above 272 rpm the main gas-liquid interface was broken by vortexing action, and bubbles of gas were drawn into the bulk liquid. Thus the error by assuming the identification of the interfacial area with the cross sectional area of the vessel was much increased. In addition, the problem of the absorption from the entrained bubbles existed (5). At stirring speeds under 109 rpm the oxygen absorption rate was so slow that the initial concentration of the sulphite ion had to be very small in order to keep the reaction rate low enough for operation in the diffusional regime, Thus the determination of the decrease of sulphite concentration by iodometric titration became less accurate.

(b) Hydrogen-allyl alcohol system

The vessel was cleaned and filled with 19 liters of distilled water. Its temperature was adjusted as previously described in oxygen absorption experiments at high stirring speeds. The required amount of sodium sulphate was added to bring the solution to 0.1 g mole/l in sulphate concentration.

The Raney nickel is designated No. 28 Standard Active Nickel by the manufacturer, W. R. Grace and Co., and corresponds to a W-1 catalyst. The catalyst was stored at 10°C and was introduced by the following steps. A small beaker with the approximate amount of Raney nickel desired was filled with water to a mark. The beaker then was weighed and the value was denoted by W_m . This amount

of catalyst was then poured into the sulphate solution. The amount of Raney nickel used, W , can be calculated by the following expression which was derived by using the density of Raney nickel equal to 4.2 g/ml.

$$W = 1.3125 (W_m - W_w) \quad (28)$$

where W_w is the weight of the same beaker filled with water to the same mark.

By feeding hydrogen at a flow rate of about 15.2 cuft/hr, gas was entrained from above the surface in the highly agitating liquid for about one and half hours in order to saturate the catalyst and to drive out all the air in solution. The oxygen analyzer showed that the oxygen content dropped to zero within this time. The stirring speed was adjusted to the desired value using a stroboscope. About 65 ml of allyl alcohol was introduced into the solution through the sample line with a syringe. The system was allowed to come to steady state in half an hour, then samples, 10 ml each time, were taken through the sampling needle with time and analyzed by the gas chromatography method.

The gas chromatograph was calibrated before use and its power was kept on all the time to maintain a constant temperature. For determining the amount of propanol in sulphate solution, five μ l of the solution was injected into a 10' \times 1/8" O.D. stainless steel column having 10%

Carbowax 600 as the stationary phase. The carrier gas was helium and its flow rate was kept at 30 ml/min. Isothermal operation was used, and the column temperature being 80°C. The concentration of propanol in solution was shown on a recorder chart with the peak area measured by an electromechanical integrator. It was noted that the sample amplitude of the recorded peak was very sensitive to the various gas flow rates through the instrument and to temperature. The instrument was calibrated again if its power switch or any gas cylinder regulator had been turned off. A sample calibration curve is given in Appendix D.

The absorption rates were determined by the measured increase in concentration of propanol in solution. Because the Raney nickel contains hydrogen that may have caused production of propanol, it is necessary to ensure that all the absorbed hydrogen was consumed by the reaction and was the only hydrogen reacted. A test was made using nitrogen gas instead of hydrogen and it was found that no appreciable amount of propanol was produced within a normal operating time.

The measurement were done at seven agitator speeds (132, 153, 181, 225, 240, 258, and 272 rpm). At least three runs at each stirring speed were done with various amounts of catalyst added. In the diffusional regime the absorption rate is independent of the reaction kinetics. Hence the measured absorption rate was independent of the

amount of catalyst used. Experiments conducted in the diffusional regime were ensured when they gave a similar result.

VANIER LIP

IV METHOD OF CALCULATION AND RESULTS

Since all experiments were done with irreversible reaction in the diffusional regime, equations which will allow calculation of the mass transfer coefficient from the measured experimental data can be easily derived based on the physical absorption concept with a constant driving force ($C_I - 0$). The calculation of the mass transfer coefficient in both systems was carried out with the following assumptions:

i) Elimination of gas phase resistance

The chosen solute gases (O_2 and H_2) are both of low enough solubility to provide entirely liquid phase controlled system. Previous workers (33) have stated that gas phase resistance is negligible in aeration sulphite system. In hydrogenation of allyl alcohol, pure gas was used and no gas phase resistance need to be considered in the absorption process.

ii) Perfect mixing

Perfect mixing is assumed in both systems at all stirring speeds studied. Experimental samples were taken at different locations in the vessel and no significant difference in concentration was observed. In the hydrogenation system catalyst particles were suspended throughout the entire liquid solution even in the case of the slowest stirring speed, though some big lumps of Raney nickel were settled on the bottom of the vessel.

VANIER II

iii) Constant interfacial area

For convenience in calculating mass transfer coefficient from experimental absorption rate, the interfacial area with different stirring speeds was assumed constant and equal to the stationary liquid surface area. At stirring speeds lower than 181 rpm, interface area was increased very slightly by the concavity of the surface. At higher stirring speeds, more turbulence caused more error to this assumption, and it was no longer possible to identify the interfacial area with the cross sectional area of the vessel. Thus the mass transfer coefficients at high stirrer speeds calculated with this assumption would be overestimated. Fortunately, as shown in the later calculation, the degree of dependence of k_L on D , which is the main purpose of this work, is not affected by the value of interfacial area used.

iv) No interfacial turbulence effect

Interfacial turbulence induced by oxygen absorption in sodium sulphite solution under turbulent flow conditions was reported recently by Linek (34). This effect caused by oxygen chemisorption was insignificant and the value of the transfer coefficient was equal to the value of the physical absorption coefficient as long as the rate of oxygen absorption was lower than 2×10^{-8} mole/cm²-sec. The result in the present work showed that all the oxygen absorption rates were lower than the quoted value, and the

interfacial turbulence effect can be neglected. Thomas and Nicholl (35) suggested that the predominant cause of the interfacial turbulence for this absorption system with reaction was the buoyancy forces caused by an increase in density of the absorption solution at the interface. Linek (34) also suggested that buoyancy forces played the dominant role and the effect of interfacial turbulence on mass transfer coefficient was a function of the density difference. The density difference caused by the reaction of allyl alcohol to propanol is very small. Thus it is assumed that interfacial turbulence was also absent in the hydrogen absorption system.

v) Effect of solution composition on diffusivities

In the study of the influence of diffusivity on liquid phase mass transfer in solutions of electrolytes, Linek et al (36) assumed that the diffusivity data of various gases in water can be applied to calculate their experimental results in electrolyte solution. They supported their assumption from Gubbins' finding (37):

$$D/D_0 = 1 - \kappa f(x)$$

where the form $f(x)$ depends on the valence type of salt, and the value of constant κ depends on the salt used but is practically independent of the gas. From this they concluded that the slopes of a plot of $k_L A$, determined under the same conditions of absorption, vs the diffusivity D

in solution or the diffusivity D_0 in water plotted in logarithmic scale are the same in both cases. This assumption is followed by the present work and the diffusivity ratio of the two gases in water equals that in solution at the same temperature, or

$$(D/D_0)_{H_2} = (D/D_0)_{O_2}$$

vi) Same oxygen and hydrogen absorption conditions

To determine the degree of dependence of mass transfer coefficient on diffusivity, the absorption of the two different gases must occur under the same conditions. The measured transfer coefficients can then be compared. The requirements of the same conditions of absorption can be fulfilled only when the stirring speed, geometrical arrangement of the vessel, liquid used and its composition are the same in both oxygen and hydrogen absorption experiments. This assumption is plausible if we realize that any of the quantities which may influence the hydrodynamics of the liquid flow field at the interface, e.g. density, viscosity, surface tension, are identical in both cases. In the present work, the absorption conditions in experiments of absorption of the two different gases were identical except that a small amount of sodium sulphite was added to the solution in oxidation experiments, and allyl alcohol and Raney nickel catalyst were added to the solution in hydrogenation experiments. In the former case,

the added amount of sulphite were very small in comparison with the total concentration of electrolyte. The maximum concentration of sulphite in a run was 5×10^{-3} mole/l, and the total concentration of electrolyte was kept constant in every experiment at 0.1 mole/l. Therefore the change in hydrodynamic conditions caused by adding sodium sulphite in solution can be reasonably assumed negligible. For the case of allyl alcohol and Raney nickel catalyst added to the sodium sulphate solution, a few tests were done on physical absorption and desorption to study whether the mass transport rate would be affected by their presence. The detail of these tests are given in Appendix B. From the results of these tests, it was concluded that the addition of allyl alcohol and Raney nickel in the sodium sulphate solution in this work had an insignificant effect on the hydrodynamic conditions of the solution.

Solubilities of pure oxygen and hydrogen in 0.1 mole/l sodium sulphate solution between 20°C and 30°C have been obtained experimentally. The data from the experiments performed at various gas partial pressures were corrected to a uniform pressure of 720 mm Hg. The results are shown graphically in Figure 5.

The calculations and results of mass transfer coefficient in both systems are shown as follows:

(a) Oxygen-sulphite system

Preliminary experiments were done on sulphite oxida-

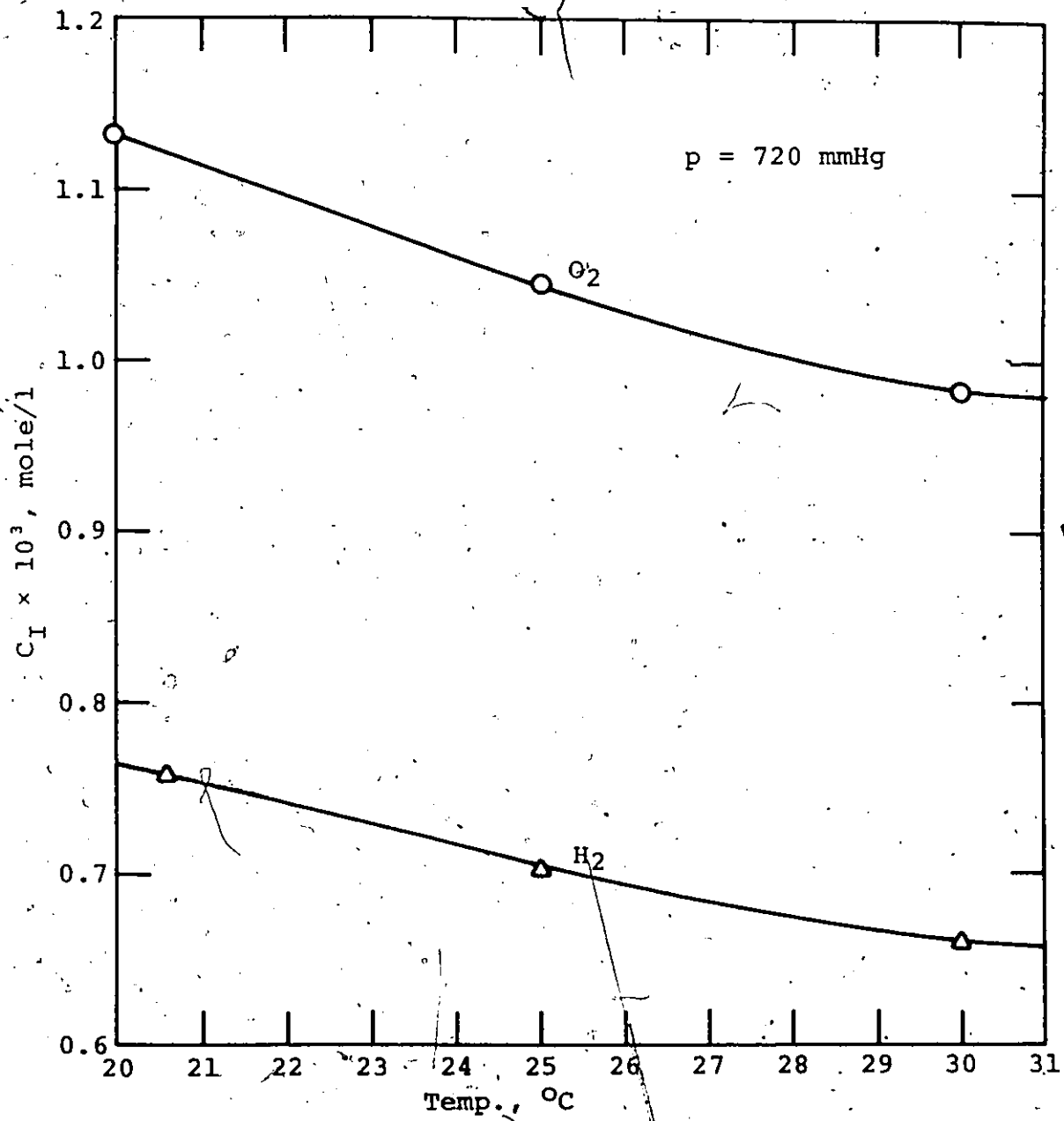


Figure 5. Solubilities of O₂ and H₂ in 0.1 M sodium sulphate solution

tion with and without cobalt sulphate used as catalyst. It was found that Equation (24) predicts a lower reaction rate than was experimentally observed. The difference in chemical kinetics between Yagi and Inoue (31) and the present system may have been due to the purity of the solution and added catalytic effect from the stainless steel components of the reaction vessel. Because many variables, which are not independent, influence the reaction rate, recent workers (29, 30) concluded that the kinetics of this reaction are not simple, and did not recommend to take up the rate data of the reaction from literature. It seems that to apply literature kinetic data of sulphite oxidation reliably it is necessary to use similar reaction conditions and the same degree of solution purity as was used in the original work. The lack of reliable kinetic data to be applied in the present work leads to the failure of using Equation (25) to find suitable reaction conditions for experiment and to ensure reaction occurred in the correct regime. Also, it prevents the way to find turbulent surface area at high stirring speeds by employing the chemical absorption method.

Fortunately, however, the diffusional regime can be identified by the independence of the rate of absorption on reaction kinetics. It is possible to infer from the results of an absorption experiment whether operation was in the diffusional regime. It is not necessary to know the kinetic expression

to determine the mass transfer coefficient by chemical method.

Equation (19) shows the rate of gas absorption with irreversible reaction in diffusional regime is

$$q_I = k_L C_I = \phi r_{C_B}$$

From stoichiometry, the reaction rate of oxygen r_{C_B} is equal to one half of reaction rate of sulphite ion,

$$r_{C_B} = -1/2 \frac{dC_{SO_3^{=}}}{dt} \quad (29)$$

By substituting the expression for r_{C_B} in the above absorption rate equation and integrating, a linear relation between $C_{SO_3^{=}}$ and \bar{t} is obtained:

$$C_{SO_3^{=}} = -\frac{2C_I k_L \bar{t}}{\phi} + B \quad (30)$$

where B is a constant from integration and is equal to the initial sulphite concentration at zero exposure time. The experimental results of sulphite concentration variation with time for each stirring speed are shown graphically in Appendix C. A straight line obtained in each run showed that the absorption rate was not affected by the sulphite concentration, thus the absorption experiments were ensured to perform in the diffusional regime. The slopes, which represent the sulphite oxidation rates, of the

curve for each stirring speed were determined by employing least squares method and were given in Table C-1 and C-2 of Appendix C.

The mass transfer coefficients were then calculated from the slopes obtained according to Equation (30). To make possible comparison of the mass transfer coefficients between different agitator speeds and in calculation of the degree of diffusion dependence, the values of k_L calculated from the results of the experimental runs made at 20.7°C to 28°C were corrected to a uniform temperature of 25°C by using King's equation for free surface mass transfer.

King (21) modified Calderbank and Moo-Young's (38) semi-empirical equation for liquid-particle interphase mass transfer by changing the power of the Schmidt number from -2/3 to -3/4 and applied it to the case of free surface mass transfer with eddy diffusion controlling. The equation is

$$k_L = 0.25 \left(\frac{\epsilon \mu}{\rho^2} \right)^{0.25} \left(\frac{\mu}{\rho D} \right)^{-0.75} \quad (31)$$

It has been stated (5) that the rate of energy dissipation is insensitive to temperature in a stirred vessel. By employing the simple relation, $D\mu/T = \text{constant}$, the above equation can be expressed as:

$$k_L \propto \left(\frac{\rho T^3}{\mu^5} \right)^{0.25} \quad (32)$$

The data for viscosity μ of water at different temperatures were used here and can be obtained from literature (39).

The use of Expression (32) may not be adequate to correct the temperature effect on the mass transfer coefficient if the absorption occurred in the region where surface renewal cannot be neglected. But since the temperature correction amounts to only a few degrees, the error caused by using Expression (32) should be small.

The calculated mass transfer coefficients with average values for each stirring speed are given in Table 1. The maximum rate of oxygen absorption was found from the fastest agitation rate where $q_{\max} = 8.49 \times 10^{-9}$ mole/cm²-sec. The value given is smaller than the quoted value 2×10^{-8} mole/cm²-sec for significant induced interfacial turbulence by chemisorption, thus no correction of interfacial turbulence on mass transfer coefficient need be considered.

Figure 6 gives the relation of mass transfer coefficient and stirring speed N plotted in logarithmic scale. It shows a linear relation at low turbulence intensities. The slope of the curve which increases sharply at stirring speed higher than 181 rpm is considered mainly caused by the error, of assuming a constant cross-sectional area. Because the surface area of the gas-liquid interface increased appreciably at N above 181 rpm, it became difficult

Table 1. Oxygen absorption coefficients

Stirring speed rpm	Run number	$k_L \times 10^2$ cm/sec	$k_{L,avg} \times 10^2$ cm/sec	Standard deviation %
109	144	0.270	0.272	1.00
	145	0.273		
125	150	0.334	0.350	7.67
	151	0.321		
	152	0.379		
	153	0.364		
132	137	0.343	0.360	4.16
	138	0.353		
	139	0.349		
	140	0.386		
	141	0.372		
	142	0.355		
	143	0.359		
153	155	0.468	0.448	3.52
	156	0.430		
	157	0.450		
	161	0.445		
164	149	0.467	0.467	----

Table 1. (Continued)

Stirring speed rpm	Run number	$k_L \times 10^2$ cm/sec	$k_{Lavg} \times 10^2$ cm/sec	Standard deviation %
181	158	0.571	0.570	2.81
	168	0.554		
	169	0.586		
225	159	0.898	0.896	1.19
	160	0.906		
	164	0.885		
240	148	1.186	1.178	2.13
	162	1.199		
	163	1.150		
258	154	1.668	1.669	2.39
	165	1.630		
	166	1.710		
272	146	1.819	1.826	0.34
	147	1.832		
	167	1.826		

to separate the k_L from the interfacial area reliably. The increased area due to the high turbulence at the interface increases the absorption rate directly, thus the calculated values of k_L are considered overestimated. The slope of the curve at low turbulence range indicates the relation $k_L \propto N^{1.5}$. This is in agreement with some other investigations (40, 41).

(b) Hydrogen-allyl alcohol system

Experimental absorption rate in this part was determined by measuring the concentration of propanol increase with time. From stoichiometry, the hydrogen reaction rate is equal to the rate of producing propanol,

$$r_{CB} = \frac{dC_{C_3H_7OH}}{dt} \quad (33)$$

With similar procedures as the sulphite oxidation in part (a), an equation which will allow calculation of the mass transfer coefficient from the measured experimental variables was derived:

$$C_{C_3H_7OH} = \frac{k_L C_I}{\phi} \bar{t} + B \quad (34)$$

Experimental results obtained for the rate of hydrogen absorption are given in Appendix C. A sample calculation with one of the concentration indicating peak from gas chromatography in a run of 132 rpm is given in Appendix D. Similar absorption rates obtained from different runs with different amounts of catalyst used in a stirring

speed indicates that the absorption processes were independent of diffusional and kinetic resistances associated with the catalyst particles. Thus the experiments were performed in the diffusional regime.

The mass transfer coefficients of the main body of runs made at 25°C to 27°C were calculated from the expression: $k_L = \phi \times \text{slope}/C_I$, and then were corrected to 25°C by the procedure used in the sulphite oxidation part. The results are given in Table 2.

The relation between k_L and N for allyl alcohol hydrogenation is also given in Figure 6. The mass transfer coefficient increased linearly with stirring speed at low turbulence intensities and then increased much more rapidly when stirring speed higher than 181 rpm. The slope of the linear portion indicates a 1.4 power of dependence of k_L on N , about 7% lower than the power obtained from the oxygen absorption experiments.

(c) Dependence of k_L on D

Based on most of the proposed models the dependence of mass transfer coefficient on diffusivity can be generally expressed in the form: $k_L \propto D^m$. The exponent m is a constant value, equal to 1/2, 2/3, or 1 in individual model respectively, suggested by some authors, or is a variable value which changes with hydrodynamic conditions suggested by the others. The value of m , followed from the above expression, can be calculated from the obtained

Table 2. Hydrogen absorption coefficients

Stirring speed rpm	Run number	$k_L \times 10^2$ cm/sec	$k_{Lavg} \times 10^2$ cm/sec	Standard deviation %
132	261	0.591	0.597	3.90
	235	0.572		
	260	0.596		
	236	0.628		
153	249	0.683	0.725	5.23
	266	0.724		
	267	0.724		
	265	0.769		
181	248	0.925	0.918	1.98
	247	0.918		
	256	0.894		
	246	0.937		
225	242	1.401	1.415	3.39
	245	1.386		
	230	1.358		
	229	1.449		
	233	1.401		
	251	1.460		
	237	1.372		
268	1.496			

Table 2. (Continued)

Stirring speed rpm	Run number	$k_L \times 10^2$ cm/sec	$k_{Lavg} \times 10^2$ cm/sec	Standard deviation %
240	238	1.783	1.827	2.50
	231	1.817		
	254	1.870		
	253	1.786		
	239	1.880		
258	257	2.548	2.545	0.85
	259	2.522		
	252	2.565		
272	262	2.807	2.714	5.76
	263	2.695		
	264	2.853		
	269	2.502		

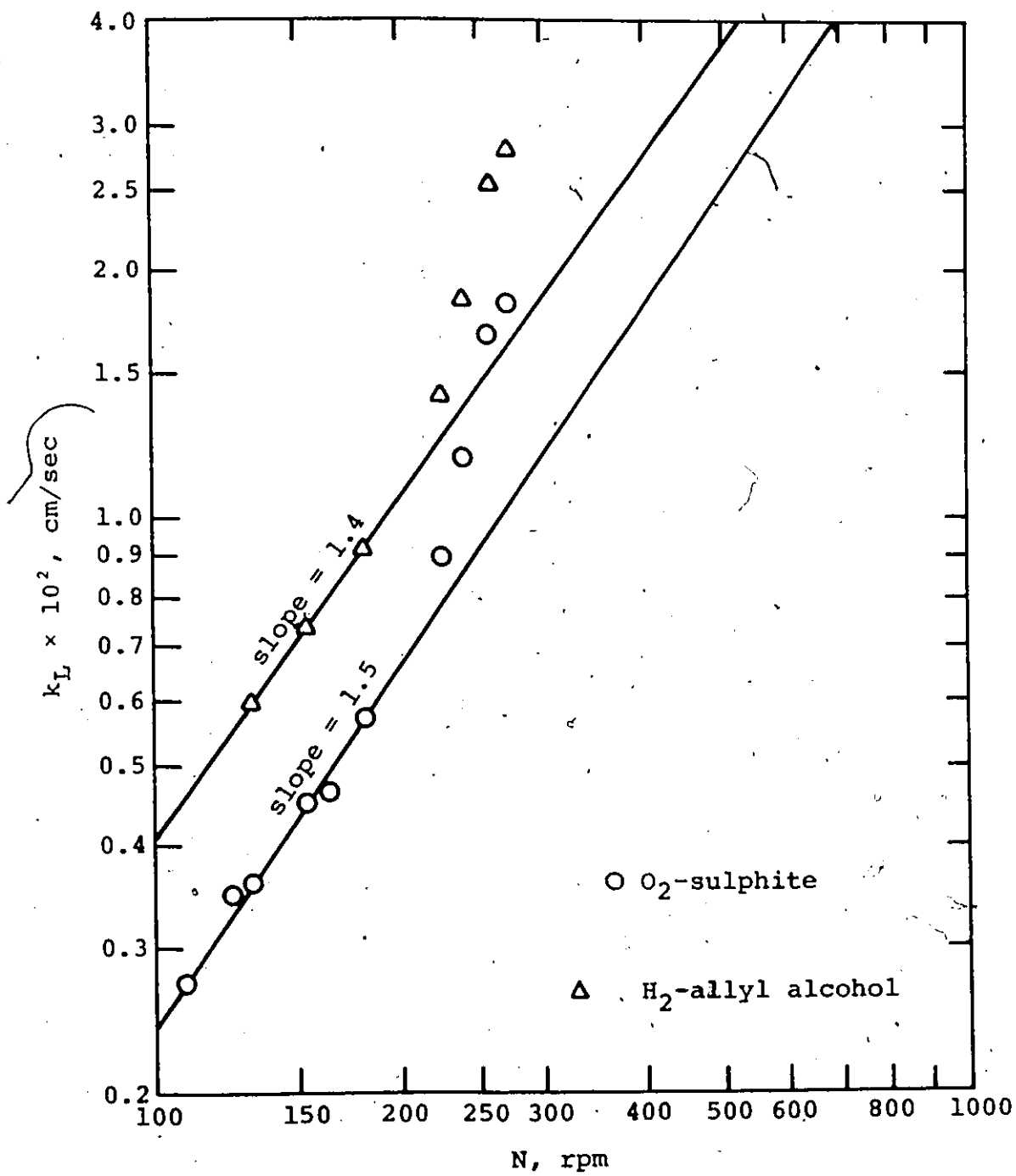


Figure 6. The influence of stirring speed upon k_L

mass transfer coefficient data in a fixed fluid flow field with diffusivity being the only variable factor by the following expression:

$$m = \frac{\Delta \ln k_L}{\Delta \ln D}$$

where m is a constant or its value changes only when the hydrodynamic conditions are altered.

To apply the above expression to the present work with oxygen and hydrogen absorptions in the same transfer conditions, the mass transfer coefficient data in part (a) and part (b) were used and were substituted in the following equation:

$$m = \frac{\ln k_{LH_2} - \ln k_{LO_2}}{\ln D_{H_2} - \ln D_{O_2}} \quad (35)$$

The accuracy of the diffusivity data used is obviously affecting the result of m value calculated. Owing to the lack of gas diffusivity data available for sodium sulphate solution, the oxygen-water and hydrogen-water diffusivities were used on the basis of assuming that the ratio (D/D_0) is constant for both gases at the same temperature. The published diffusivity data of hydrogen in water show a poor agreement. The recent data available from Vivian and King (42) were used in the present work because they seem most reliable and show agreement among different experimental techniques.

As stated in previous parts the values of mass trans-

fer coefficients calculated from the measurement of experimental absorption rate at various temperatures were corrected to 25°C by employing King's equation where $k_L \propto D^{0.75}$. In order to obtain more accurate values of diffusivity dependence on m at various stirring speeds, the values of k_L in both oxygen and hydrogen absorption experiments can be back-calculated for the temperature effect by using the resulting m values inserted in Equation (31) instead of using $m = 0.75$. The new obtained values of mass transfer coefficient can in turn be used to calculate a more accurate value of m . A trial and error method was used in a computer program and the value of m for each stirring speed was calculated up to a value where the difference between two consecutive values was less than one percent. New values of k_L for both systems were also obtained from this computation and can be used to check the previously resulted values of k_L where the temperature was corrected on the basis of $k_L \propto D^{0.75}$. The maximum deviation being about 1 % indicates that the assumption of $m = 0.75$ in correcting the temperature effect on mass transfer coefficients in part (a) and (b) is considered acceptable.

The obtained values of m are given in Table 3. A variation of m with stirring speed shown in this table indicates that only the theoretical models for free surface mass transfer with the value of m being a variable

Table 3. The values of apparent exponent m
for various stirring speeds

Stirring speed rpm	$k_{L_{O_2}} \times 10^2$ cm/sec	$k_{L_{H_2}} \times 10^2$ cm/sec	m
132	0.359	0.597	0.738
153	0.448	0.725	0.701
181	0.569	0.920	0.696
225	0.893	1.419	0.671
240	1.181	1.836	0.641
258	1.670	2.558	0.619
272	1.839	2.738	0.574

can interpret the absorption mechanism in the present work. Belonging to this group of models are the film-penetration theories of Toor and Marchello (18), and Dobbins (19), the random distance eddies model of Harriott (20), and parallel molecular and eddy diffusivities model of King (21). An examination of these models reveals that the discontinuity in the turbulent flow field near the interface and the defined film thickness L in the film-penetration theories is unclear in physical meaning. Harriott's model postulates the concept that not all the eddies accomplishing the transfer of the dissolved substance into the bulk liquid can penetrate directly to the surface, but the effects of turbulence do not include the concept of eddy diffusion based on the structure of the turbulent flow. Also the value of application of this model is questionable for its complexity. With introduction of a damped eddy diffusivity, King's model gives a simplified but reasonable picture of transport across a free surface. The variation of the m values being within the limits of 0.5 and 0.75 supports the choice of this model. An abstract of King's model is given in Appendix E and its parameters were calculated from the present experimental data.

(d) Parameter evaluation in King's model

There are three parameters n , a , and t in King's model (see Appendix E). These parameters have to be

evaluated for application of quantitative analysis of free surface mass transfer. As suggested by King, n equals four for gas absorption. This is in agreement with present experimental result in which m was within values of 0.5 and 0.75, the values of low and high τ asymptotes respectively in King's mass transfer model.

From the finding of m being a variable in the experiment of the desorption of helium and oxygen from electrolyte solutions (36), Linek and Mayrhoferova (43) interpreted their results by King's model and concluded that the experiments were performed in the region of transition between steady state transfer and penetration asymptotes (see Appendix E). They estimated the values of m from the expression $m = \frac{\Delta \ln k_L}{\Delta \ln D}$. The corresponding values of a and t were then evaluated by employing the graphical solutions for mass transfer coefficient and for exponent on diffusivity in King's paper (21). However, it was found that the correctness of the resulting values of parameters a and t is questionable on the basis of the following theoretical argument.

King (21) defined the apparent exponent of diffusivity dependence in the form:

$$m = \frac{d \ln k_L}{d \ln D} \quad (36)$$

If a gas absorption process is operated in the steady

state transfer asymptote, the distribution of ages will be unimportant and the value of m equals 0.75. On the other hand, if a gas absorption process is operated in the penetration control asymptote, the eddy diffusion will be unimportant and the value of m equals 0.5. If an experiment of gas absorption with various gases of different diffusivities absorbed into a turbulent liquid in a given condition is performed in either one of these two asymptotes, Equation (36) can be simplified to $m = \frac{\Delta \ln k_L}{\Delta \ln D}$. If the resulting values of mass transfer coefficient are plotted against diffusivity logarithmically, a straight line will be given with its slope equal to m . But when the same sort of experiment is performed in the transition region between the asymptotes, m is no longer a constant but is a function of D even though all the hydrodynamic conditions, which may have influence upon mass transfer, are unaltered. A logarithmic plot of k_L against D in this region will give a curve instead of a straight line. Thus the form of equation $m = \frac{\Delta \ln k_L}{\Delta \ln D}$ is not identical with the form $m = \frac{d \ln k_L}{d \ln D}$, and it is concluded that the former expression is not adequate in use to estimate m in the transition region. There should be different values of parameter m , also τ and ψ corresponding to each diffusivity, for each gas, while parameters a and t should have the same value for all gases used in a given absorption condition. Different results from Linek and Mayrho-

ferova's evaluation of a and t would be expected to be obtained if the data of mass transfer coefficient in helium absorption in their experiment are available and applied.

A new procedure was developed as follows to evaluate the model parameters a and t from experimental data of k_L when the transition region is considered.

With $n = 4$, for the mass transfer of gas across a free liquid interface the definitions of dimensionless parameters τ and ψ given by King can be expressed as :

$$\psi = \frac{k_L}{a^{0.25} D^{0.75}} \quad (37)$$

$$\tau = \sqrt{aDt} \quad (38)$$

For the case of more than two gases used in a gas absorption experiment, a procedure similar to Linek and Mayrhoferova's can be used for evaluating parameters a and t . If the results show m being a variable with the process performed in the region of transition between high and low τ asymptotes, a curve should be shown on a logarithmic plot of k_L vs. D for each absorption condition. A value of m can be obtained from the curve for a chosen gas. The graphical solutions for k_L and m in King's paper (21) then give the corresponding values of τ and ψ , and the parameters a and t can be obtained by using Equation (37) and (38). The resulting values of these para-

meters should be independent of the gas chosen.

For the case of only two gases absorbed in a turbulent liquid as in the present experiment, a trial and error method can be used to evaluate the model parameters a and t . Figure 7, which was reproduced from King's paper (21), gives the relation between the dimensionless surface age τ and the dimensionless mass transfer coefficient ψ . This figure shows that if the τ and ψ ratios of the two gases are given, the values of τ and ψ of both gases in an absorption condition will be fixed and can be obtained by trial and error method. Equation (37) and (38) show that τ and ψ are proportional to \sqrt{D} and $k_L/D^{0.75}$ respectively in a given absorption condition. The required ratios for τ and ψ of the two gases can be obtained if their diffusivities and mass transfer coefficients are known. Equation (37) and (38) can then be used to calculate values of a and t by substituting the obtained values of τ and ψ of any one of the two gases.

In the present work, the result of m being a variable indicates that the absorption experiments were performed in the region of transition between the two asymptotes, where $\frac{d \ln k_L}{d \ln D} \neq \frac{\Delta \ln k_L}{\Delta \ln D}$. The parameters a and t were evaluated by the above stated method. The ratios for τ and ψ of O_2 and H_2 are

$$\tau_{O_2}/\tau_{H_2} = \sqrt{D_{O_2}/D_{H_2}} = 0.71 \quad (39)$$

$$\psi_{O_2}/\psi_{H_2} = \frac{k_{LO_2}}{k_{LH_2}} \times \left(\frac{D_{H_2}}{D_{O_2}}\right)^{0.75} = 1.68 \frac{k_{LO_2}}{k_{LH_2}} \quad (40)$$

The gas diffusivity data for water were used in Equation (37) and (38). Owing to the low electrolyte content (0.1 mole/l) in solution, the difference in diffusivity between water and solution should be small, and the use of the diffusivity data for water in these equations is considered not causing significant error. The obtained parameters a and \bar{t} are given in Table 4 where \bar{t} presented the average age of surface elements was considered. Table 4 shows that as turbulence, represented by stirring speed N , increases, the eddy diffusion activity a increases and the average surface age \bar{t} decreases.

Further more, to relate the parameters with known experimental conditions, values of energy dissipation rate per unit volume ϵ were estimated by using Bates et al's (44) power number correlation for stirred vessel and are given in Table 5. Plots of a vs. ϵ and \bar{t} vs. ϵ on a log x log scale show practically two straight lines of slope 1.73 and 1.07 respectively in the low turbulence range where experimental results are considered not to be affected by the stationary surface area assumed (Figure 8). Thus for the system considered the following empirical relations can be written:

$$a = X\epsilon^\alpha \quad (41)$$

$$\bar{t} = Y\epsilon^\gamma \quad (42)$$

Table 4. The parameters of King's model

$$n = 4$$

N	τ_{H_2}	τ_{O_2}	ψ_{H_2}	ψ_{O_2}	$a \times 10^{-4}$	\bar{t}
rpm	_____	_____	_____	_____	1/cm ² -sec	sec
132	1.82	1.29	0.99	1.00	1.20	2.40
153	1.75	1.24	0.99	1.01	2.81	1.51
181	1.50	1.06	1.00	1.03	6.61	0.84
225	0.62	0.44	1.13	1.20	21.80	0.19
240	0.50	0.36	1.17	1.26	54.83	0.10
258	0.44	0.31	1.20	1.31	186.70	0.05
272	0.40	0.28	1.23	1.35	244.21	0.04

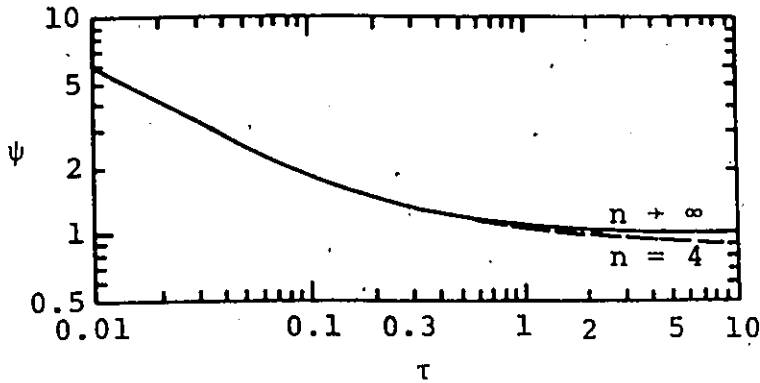


Figure 7. General model for uniform lifetime surface age distribution

Table 5. Values of specific energy dissipation rate at various stirring speeds

<u>N, rpm</u>	132	153	181	225	240	258	272
<u>ε, watt/ml</u>	12.10	18.84	31.19	59.91	72.71	90.33	105.85

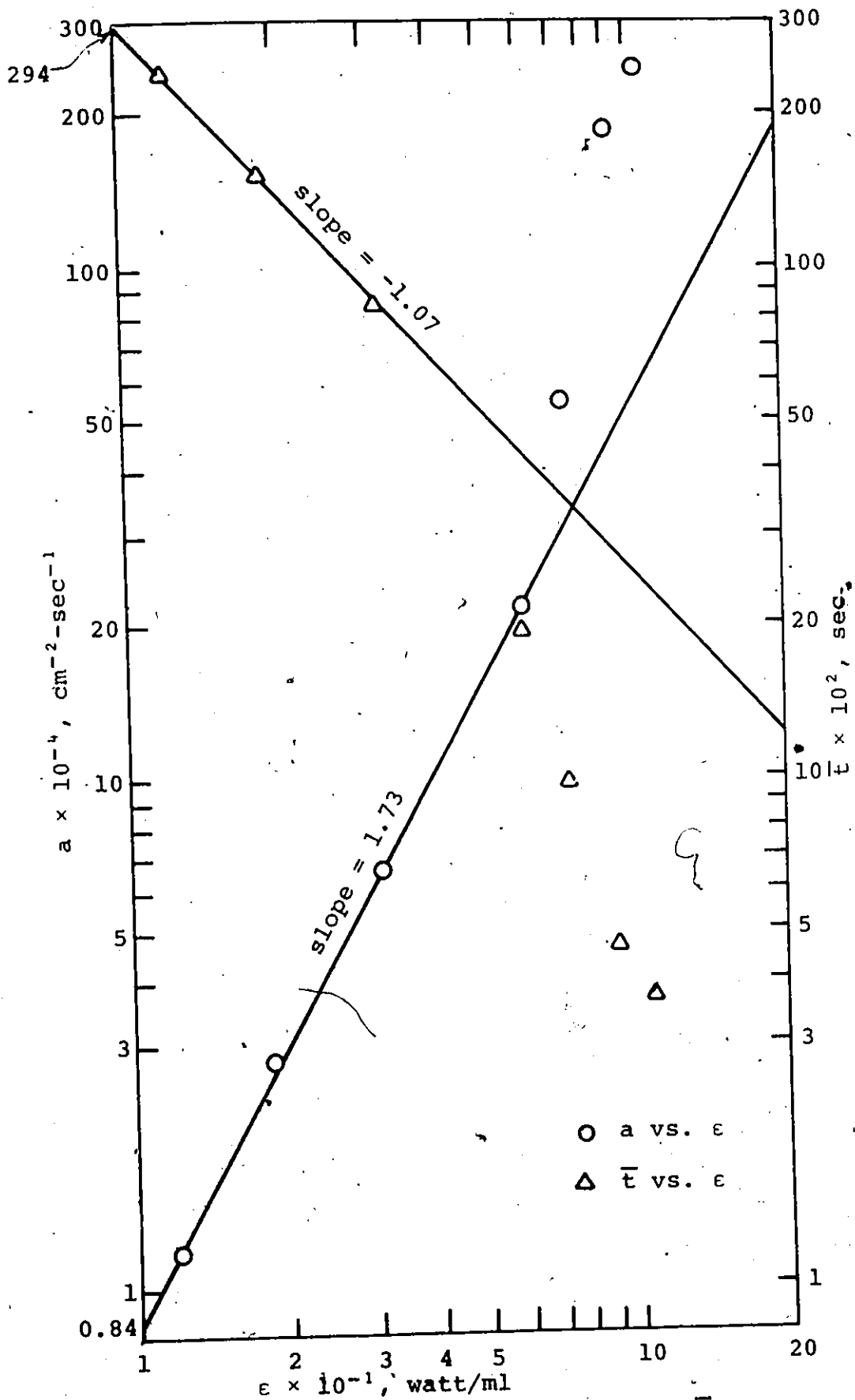


Figure 8. The dependence of parameters a and \bar{E} on ϵ .

where $\alpha = 1.73$, $\gamma = -1.07$, $X = 0.84 \times 10^4$, and $Y = 2.94$.

Bates et al's correlation shows that the power number becomes independent of Reynolds number when the latter exceeds 10^4 . The Reynolds number for all runs in the present work are all larger than this quoted value, therefore, the energy dissipation rate per unit volume ϵ is proportional to the stirring speed N to the third power. Applying this relation to Equation (41) and Equation (42), the following expressions were obtained:

$$a \propto N^{5.19} \quad (43)$$

$$\bar{t} \propto N^{-3.21} \quad (44)$$

V DISSCUSSION

1. Transport Mechanism

As shown by the above stated experimental results, the degree of dependence of k_L on D varies with the mixing intensity. Differences in the apparent exponent m between stirred levels in the present work and between the various past studies may be interpreted by King's model (21) which removes the contradictions between the earlier mass transfer models by suggesting a damped profile of eddy diffusivity with surface renewals near the interface. The decrease of m as the agitating speed increases is in accord with a continuous transition from a steady state transport regime towards a penetration control regime.

It is well known that except molecular diffusion, other transport mechanisms (eddy diffusion and surface renewal) considered in King's model increase their intensities with increasing agitation power. However, the variation direction of m with N , or ϵ is indefinite unless the relative effect of the two power dependent mechanisms is known. The experimental results of a previous investigation (5) of gas absorption in a continuous flow stirred vessel showed that m increased as stirrer speed increased. Recently Linek et al. (36) stated that King's model predicted that the value of exponent m rises with rising energy dissipation. The contradiction between the

above statement and the present experimental results can be cleared by examining King's theoretical approach which shows that m is a function of both parameters a and t for a given absorbed gas, where a is a measure of eddy diffusivity and t is the surface age of an fluid element. In a turbulent flow field, more turbulence will give a bigger value of a , but at the same time, it will give a shorter total surface age to an element. Thus an increase in turbulence of a flow field could cause m either to increase or to decrease, according to which factor, a or t , has a more effect on m . It has been pointed out by King (21) that the small and large eddies, which are related to a and t respectively, are affected by the geometrical nature of equipments in extremely different degree. The geometrical difference between the present batch system and the flow system used in Kozinsky and King's experiment (5) probably is the reason why m went to opposite directions with increasing degree of turbulence in the two experimental results.

In the present case, the effect of surface renewal on mass transfer was larger than the effect of eddy diffusion when the condition of turbulence was changed. If the experiment can be run at a higher level of agitation, surface renewal would be expected in controlling the transport mechanism. On the other hand, if the experiment can be run at a lower level of agitation, steady

state mass transfer may be achieved in which case the surface age of the liquid elements would no longer be important. From the results of parameter evaluation, the effects of these two important characteristic factors can be combined to give a relation indicating which regime the transport mechanism will tend towards with increasing power. The dimensionless parameter τ , which characterizes the region of transport mechanism that applies, relates to a and \bar{t} by definition as: $\tau \propto \sqrt{a\bar{t}}$ when $n = 4$. By substituting values of a and \bar{t} from equations (41) and (42), the relation between τ and ϵ can be shown as $\tau \propto \epsilon^{-0.2}$. The negative sign of the exponent indicates that the mechanism will move towards the penetration regime when the specific rate of energy dissipation is increased. By studying the results of past mass transfer investigations in a stirred vessel, Kozinsky and King (5) stated that surface renewals are less important at lower stirring rates than in the intermediate range of agitation. This is in agreement with the present experimental findings.

Some further support for King's model comes from other studies of the effect of diffusivity on mass transfer coefficient. Table 6 gives some previous investigations for free surface mass transfer in various systems in which at least two gases were used. Except for the lower limit of Hutchinson and Sherwood's experiment (41), resulting values of m , which were recalculated on the

Table 6. Summary of measurements of m values

Gas-liquid contactor	Gas	$k_L \times 10^2$ cm/sec	m	Reference
Packed column	H ₂ , He		0.48	Vivian and King (7)
	O ₂ , CO ₂		to	
	C ₃ H ₆		0.54	
Wetted-wall column	H ₂ , He	1.27	0.54	Lamourelle and Sandall (8)
	O ₂ , CO ₂	to		
		5.08		
Turbulent jets	H ₂ , CO ₂	1.80	0.55	Davies and Ting (9)
		to		
		8.40		
Continuous flow stirred vessel	H ₂ , He	1.80	0.51	Kozinsky and King (5)
	O ₂ , CO ₂	to	to	
	A	3.70	0.58	
Stirred flask	SO ₂ , O ₂	0.01	0.04	Hutchinson and Sherwood (41)
	Cl ₂ , N ₂	to	to	
	CO ₂ , H ₂	0.21	0.62	
	He, C ₂ H ₂			
Agitated vessel	N ₂ , He	0.09	0.47	Dobbins (4)
		to	to	
		3.60	0.71	
Stirred vessel with bubbles dispersion	O ₂ , He	3.41	0.46	Linek et al (36)
		to	to	
		5.00	0.69	
Stirred vessel	O ₂ , H ₂	0.36	0.61	Present work
		to	to	
		1.84	0.74	
Stirred vessel	H ₂ , He	0.09	0.46	Davies et al (6)
	O ₂ , CO ₂	to	to	
		1.94	0.82	

*Values for O₂, N₂, or CO₂ absorption

basis of Vivian and King's diffusivity data, are reasonably within the experimental errors of the high and low τ asymptotes. The apparent exponent on diffusivity at low turbulence obtained by Hutchinson and Sherwood being much lower than 0.5 probably is due to the imperfect mixing produced by their special agitator arrangement in the vessel. The value of m does not vary with the magnitude of the mass transfer coefficient shown in Table 6. This suggests that the regime of controlling mass transfer mechanism that obtains - asymptotic surface renewal, asymptotic eddy diffusion, or somewhere in between - is determined by the size and frequency of the eddies in the region of the gas-liquid interface. The relatively higher values of m resulting from Linek's experiments and the present work are considered to be partly due to the surface renewals occurring less frequently, caused by the effect of existed electrolytes as pointed out by Linek and Mayrhoferova (43). The same reason of suppressed surface renewal applied to the Davies et al's (6) experiments where tangential interfacial motion was suppressed by counterrotating stirrers and surface elasticity was formed by adding surfactant. The difference in geometry is the other reason for different values of m obtained. It was observed that the mechanism of transport for the flow systems, such as pack column, wetted wall column, and continuous flow stirred tank, are close to or within

the penetration controlling asymptote, m being close to 0.5 and nearly constant, which indicates that surface renewal is more important than eddy diffusion in these systems. For batch stirred vessels, Table 6 shows that the mechanism of transport is in the transition region where both penetration and eddy diffusion are important.

There is still no such a confirmed theory of attenuation of turbulent eddies close to an interface. The idea of a severe damping effect of surface tension on the finer transverse pulsation is generally accepted. This suggests that the role of molecular diffusion in mass transfer processes is important even at highly turbulent conditions. Only Kishinevsky's model gives $k_L \propto D^0$ for high turbulence mass transfer. This proposal seems incorrect in describing the picture of interphase mass transfer and has not been confirmed by experiments. King (21) suggested that eddy diffusivity varies as the fourth power of distance from the free surface which is based on the maximum values of m in the equation: $n = (1 - m)^{-1}$, (see Appendix E), where m was shown to have a maximum value of 0.75 in some previous works. However, there are experimental data testifying in favor of $n = 3$ (43) and $n = 2$ (8). It is well known that the data of diffusivity used when analyzing mass transfer data will influence the estimated value of m , or, in alternative, will influence the determination of the value of n from the above equation. The values of

m calculated from Vivian and King's diffusivity data in Table 6 support $n = 4$ even though it is impossible to assert that value of exponent on distance for free surface eddy diffusion has been established with complete accuracy.

2. Specific Energy Dissipation Rate and Stirring Speed Effects

Equations (41), (42) and Figure 8 give the following relations between specific energy dissipation rate and the model parameters a and \bar{t} , which characterize the influence of hydrodynamic conditions upon mass transfer, in this work: $a \propto \epsilon^{1.73}$, $\bar{t} \propto \epsilon^{-1.07}$.

The mass transfer coefficient dependence upon stirring speed N in stirred vessels with a gas-liquid interface studied by many previous workers has been shown by Kozinsky and King (5), where k_L varies as N to a power of 0.6 to 1.2 in various experimental works. Recently Davies (45) also showed that exponent on N varies from 0.8 to 1.4 by observing work done on stirred cells with a plane surface. The results of present experiment together with other previous findings (40, 41), give k_L depending on N to a power of 1.4 to 1.5 at low turbulence levels. Obviously the geometries of the stirrer and vessel have an important bearing on the exponent of N as well as on the absolute magnitude of k_L , since the turbulence from the stirrers is inhomogeneous and nonisotropic.

Though the present experiments were performed in the transition region, the relations between mass transfer coefficient and specific energy dissipation rate, or stirring speed, in both asymptotes can be derived through Equations (41), (42), (43), and (44) as follows.

In the case of penetration control, the classical equation for mass transfer coefficient is

$$k_L = \sqrt{(D/\pi \bar{t})} \quad (45)$$

Comparison of this equation with Equation (42) and (44) shows that:

$$k_L \propto \epsilon^{0.53} \propto N^{1.6} \quad (46)$$

In work reviewed by Davies (45), the exponent on N has a value of 1.2 and 1.4 depending on stirrer position.

For steady state transfer, King's model gives the following equation for $n = 4$:

$$k_L = 0.9a^{0.25}D^{0.75} \quad (47)$$

By substituting Equations (41) and (43) to the above equation, one can obtain

$$k_L \propto \epsilon^{0.43} \propto N^{1.3} \quad (48)$$

Equation (31), which was derived through the Calderbank and Moo-Young's correlation for fixed surface mass transfer, predicts a $N^{0.75}$ dependence for k_L which does not

agree with the present result. Probably the use of the analogy between eddy diffusivity profiles near a fixed surface and near a free surface is not adequate.

Equations (46) and (48) show that there are different values of the exponent on N for mass transfer occurring in different asymptotes in a given geometry. This value should vary from one end to another in the transition region. In the present work, the degree of dependence of k_L on N was in the limits of 1.3 and 1.6. The difference in diffusivity of the two gases caused this dependence has a higher value for the oxygen absorption system than the hydrogen absorption system at the same agitation level.

If in a particular case where the exponent on N of both asymptotes has the same value, the dimensionless surface age τ according to Equations (38), (41), and (42) will no longer depend on the energy dissipation rate and equal to \sqrt{DXY} in a given gas-liquid contactor. Thus the mechanism of transport depends on the diffusivity of the absorbed gas only. The condition required for such a case existed is: $\alpha = -2\gamma$, where α and γ are the exponents on ϵ in the relations of a and ϵ , and \bar{t} and ϵ respectively. This probably is the case for Linek et al's (36) experiment which gives a result that m varied with changing electrolyte concentration in the solution but remained constant with changing stirring speed or gas flow rate. A more likely explanation to this result is afforded by

consideration of the fact that both parameters a and \bar{t} are a very weak function of ϵ in absorption from gas bubbles. The value of τ can vary only with changing solution properties in absorption of a gas in a given geometry. It has been noted by Bull and Kempe (46) that there are differences in mechanism between the gas absorption from dispersed bubbles and through a free interface. In addition, experimental results show that in bubble absorption k_L is nearly unaffected by degree of turbulence and ionic strength (36) which, however, are important factors for k_L in free surface absorption. The differences between the two systems prevents further comparison of model parameters a and \bar{t} of Linek and Mayrhoferova's and the present work.

3. Correlation of Data on k_L

It has been stated previously that m is a function of D in the transition region of gas absorption. Figure 9 shows qualitatively the relation between k_L and D in a given hydrodynamic condition on a logarithmic plot. The curve shown in the middle part of the figure indicates that the usual power form of the relation $k_L \propto D^m$ is not adequate in use in the transition region of free surface mass transfer. This means that the experimental data relating to such a region cannot be correlated by means of correlations of the type $N_{Sh} \propto N_{Re}^\sigma N_{Sc}^\delta$. Furthermore, if the isotropic theory of turbulence is adequate in use to

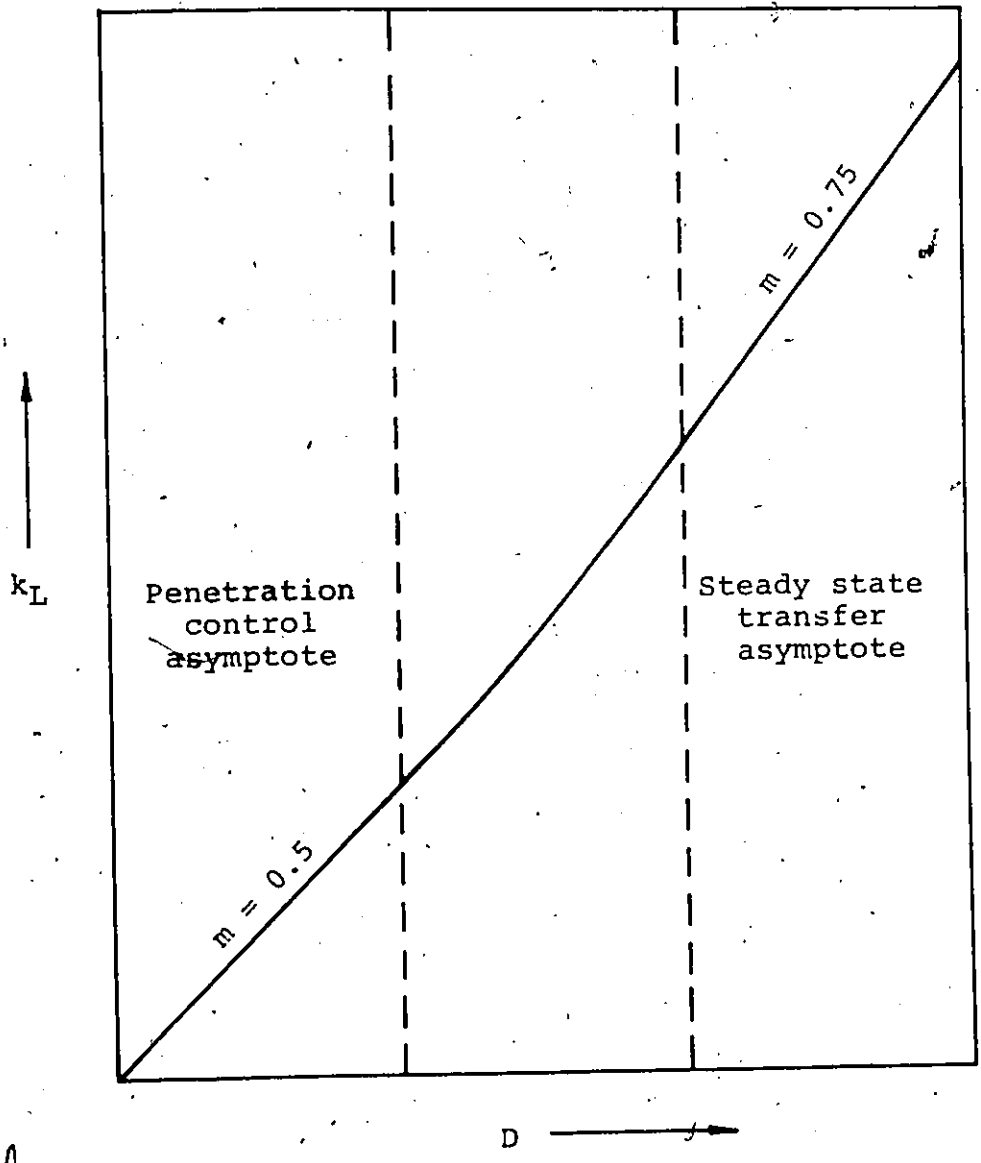


Figure 9. Dependence of mass transfer coefficient on diffusivity

explain the hydrodynamics near the free interface, or, if there is a significant difference between the geometric effects on the large and small eddies which control the surface renewal and eddy diffusions respectively, a small change in geometrical arrangement will change the relative effects of eddy diffusion and surface renewal on mass transfer. Thus the exponents on D and on ϵ may be shifted from one value to another. Both exponents σ and δ on the groups of Reynolds number and Schmidt number are uncertain unless the transfer process is known to be in either the steady state transfer asymptote or the penetration control asymptote in a given geometry.

Therefore it is not recommended to use the existing empirical correlation for k_L to predict rate of mass transfer across a free interface directly. Parameters a and \bar{t} have to be estimated beforehand and then k_L obtained by using Figure 7. Because the geometrical factors and the liquid properties are important to absorption rate, it should be noted that Equations (41) and (42) can be applied to the systems having conditions similar to the present work only.

VI CONCLUSIONS AND RECOMMENDATIONS

The results obtained in this study for mass transfer across a free gas-liquid interface into a turbulent liquid indicate that the dependence of mass transfer coefficient on molecular diffusivity is a variable. The value of apparent exponent, m , decreases with an increasing stirring speed from the value of about 0.74 to about 0.57. This finding suggests that King's mass transfer model most closely describes the actual physical phenomena of gas absorption into turbulent liquids.

According to this model, the mechanism of gas absorption is controlled by the concepts of molecular diffusion, eddy diffusion, and surface renewal. The dependence of k_L on D depends on the relative effect of these three transport mechanisms. Except the molecular diffusion, the transfer is generated by the turbulent eddies. It is generally accepted that the specific rate of energy dissipation has a direct effect on the mass transfer rate. How the energy is distributed and ultimately dissipated, however, is most important. For this reason, the effect of the geometry of an absorption system on the energy dissipation, which is in turn affecting the transport mechanism, must be considered.

For gas absorption in agitated vessels, the results from the present work and the other previous investigations show that the transfer process is usually performed in the region of transition between the steady state transfer and

the penetration asymptotes of King's model. The usual power form of the relation $k_L \propto D^m$ is inadequate in use. Some previous correlations (8, 47) for mass transfer coefficient give k_L related to ϵ , N , or N_{Re} to a certain power. However, it is noted that not only these exponents are affected by geometrical factors, but also, k_L may relate to a different power on ϵ , N , or N_{Re} if absorption is performed in different transfer asymptotes in a given geometry. If the detailed features of the theory of King's model are confirmed, further gas absorption studies should give correlations on model parameters a and t instead of k_L itself. More experimental evidences in a wide agitation range and different geometries are required to confirm the transport mechanism. Also, reliable diffusivity data for gases in different liquids and solutions are needed to be determined experimentally for supporting the mass transfer studies.

The kinetic theory of liquids presents notorious difficulties. It is not surprising, therefore, that there are no satisfactory methods of predicting absorption rate in turbulent liquid systems from first principles. There are still many problems on turbulence transport such as the size and frequency effect of an eddy, the way of the distribution and the dissipation of the energy, the interfacial turbulence effects caused by local changes of surface tension or density, the damping effect to the turbulent

pulsations by a surface, etc. The solution of these problems is necessary for the postulation of a theory of mass transfer which is required for the transfer rate prediction. These problems are very complex in nature and in mathematical analysis. Expenditures of great joint efforts by scientists are required.

VII NOMENCLATURE

- a proportionality constant in eddy diffusivity expression, $\text{cm}^{-2}\text{-sec}^{-1}$
- a_p external particle surface area per unit mass of catalyst, cm^2/g
- A total area of interface, cm^2
- b constant in Equation (7); eddy diffusivity at the interface, cm^2/sec
- B integration constant in Equation (30) or (34); initial concentration of sodium sulphite or propanol at zero absorption time, mole/cm^3
- C gas solute concentration in liquid, mole/cm^3
- C_e chemical equilibrium concentration of gas solute, mole/cm^3
- C_G hypothetical liquid phase concentration that would be in equilibrium with gas of partial pressure p_G , mole/cm^3
- D molecular diffusivity, cm^2/sec
- D_e eddy diffusivity, cm^2/sec
- D_o diffusivity in pure water, cm^2/sec
- H Henry's law constant, $\text{atm}\text{-cm}^3/\text{mole}$
- k_1 first order or pseudo-first order rate constant, $\text{cm}^3/\text{g}\text{-sec}$
- k_2 second order rate constant, $\text{cm}^3/\text{mole}\text{-sec}$
- k_G gas phase mass transfer coefficient, $\text{mole}/\text{cm}^2\text{-sec-atm}$

k_L	liquid phase mass transfer coefficient, cm/sec
k_p	liquid particle mass transfer coefficient, cm/sec
L	liquid film thickness, cm
m	defined by Equation (36)
n	exponent on distance in eddy diffusivity expression
N	stirring speed, rpm
p	partial pressure of soluble gas, atm
q	flux of gas solute in liquid phase, mole/cm ² -sec
r	rate of reaction, mole/cm ³ -sec
r_{C_I}	rate of reaction with gas reactant concentration C_I , mole/cm ³ -sec
r_{C_B}	rate of reaction with gas reactant concentration C_B , mole/cm ³ -sec
s	fractional rate of surface renewal, sec ⁻¹
t	age of an element of surface, sec
\bar{t}	average surface age, sec
\bar{t}	experimental absorption time, sec
t_D	diffusion time defined by Equation (14), sec
t_r	reaction time defined by Equation (13), sec
T	temperature, °K
V	liquid volume, cm ³
w	catalyst mass per unit volume of liquid, g/cm ³
W	amount of Raney nickel used, g
W_m	total weight of becker with Raney nickel and water, g
W_w	weight of becker with water alone, g
X	constant in Equation (41)

y distance from interface, cm
 Y constant in Equation (42)

Greek letters

α defined by Equation (41)
 γ defined by Equation (42)
 ϕ liquid volume per unit interfacial area, cm
 ϵ specific rate of energy dissipation, watt/ml
 η particle internal effectiveness factor
 κ constant in Gubbin's equation of diffusivity
for electrolyte solutions
 μ viscosity, poise
 ρ density, g/cm³
 θ uniform surface age, sec
 σ exponent on Reynolds number in mass transfer
correlation
 δ_1 exponent on Schmidt number in mass transfer
correlation
 τ dimensionless surface age
 ψ dimensionless mass transfer coefficient

Subscripts

B bulk liquid
 f liquid film
 I interface
 O_2 oxygen

H₂ hydrogen
Na₂SO₃ sodium sulphite
CoSO₄ cobalt sulphate
SO₃⁼ sulphite ion
C₃H₇OH propanol
S particle external surface

VIII BIBLIOGRAPHY

- (1) Lewis, W. K., and Whitman W. G., Ind. & Eng. Chem., 16, 1215 (1924).
- (2) Rozen, A. M., and Krylov, V. S., International Chem. Eng. 6, 3, 429 (1966).
- (3) Kishinevskii, M. K., and Serbryansky, V. T., Zh. prikl. khim. SSSR 29, 27 (1956).
- (4) Dobbins, W. E., International Conference on Water Pollution Research, Pergamon Press (1962).
- (5) Kozinski, A. A., and King, C. J., A.I.Ch.E. Journal, 12, 1, 109 (1966).
- (6) Davies, J. T., Kilner, A. A., and Ratcliff, G. A., Chem. Eng. Sci., 19, 583 (1964).
- (7) Vivian, J. E., and King, C. J., A.I.Ch.E. Journal, 10, 2, 221 (1964).
- (8) Lamourelle, A. P., and Sandall, O. C., Chem. Eng. Sci., 27, 1035 (1972).
- (9) Davies, J. T., and Ting, S. T., Chem. Eng. Sci., 22, 1539 (1967).
- (10) Sherwood, T. K., and Holloway, F. A. L., Am. Inst. Chem. Engrs., 36, 39 (1940).
- (11) Calderbank, P. H., Trans. Instit. Chem. Eng. (37, 173 (1959)).
- (12) Levich, V. G., "Physicochemical Hydrodynamics," Prentice-Hall, Englewood Cliffs, N. J. (1962).

- (13) Higbie, R., Trans. A.I.Ch.E. 31, 365 (1935).
- (14) Danckwerts, P. V., Ind. Eng. Chem. 43, 1460 (1951).
- (15) Perlmutter, D. D., Chem. Eng. Sci., 16, 287 (1961).
- (16) Hanratty, T. J., A.I.Ch.E. Journal, 2, 359 (1956).
- (17) Davies, J. T., Proc. R. Soc. A290, 515 (1966).
- (18) Toor, H. L., and Marchello, J. M., A.I.Ch.E. Journal, 4, 1, 97 (1958).
- (19) Dobbins, W. E., in "Biological Treatment of Sewage and Industrial Wastes," W. L. McCabe and W. W. Eckenfelder, eds., Pt. 2-1, Reinhold, New York (1956).
- (20) Harriott, P., Chem. Eng. Sci., 17, 149 (1962).
- (21) King, C. J., Ind. Eng. Chem. Fundamentals, 5, 1, 1 (1966).
- (22) Fortescue, G. E., and Pearson, J. R. A., Chem. Eng. Sci., 22, 1163 (1967).
- (23) Lamont, J. C., Scott, D. S., A.I.Ch.E. Journal, 16, 4 513 (1970).
- (24) Sharma, M. M., Danckwerts, P. V., Brit. Chem. Eng., 15, 4, 522 (1970).
- (25) Astarita, G., "Mass transfer with chemical reaction," Elsevier Publishing Co., Amsterdam (1967).
- (26) Danckwerts, P. V., "Gas-Liquid Reactions," McGraw-Hill, New York (1970).
- (27) Westerterp, K. R., van Dierendonck, L. L., and de Kraa, J. A., Chem. Eng. Sci., 18, 157 (1963).
- (28) de Waal, K. J. A. and Beek, W. J., Chem. Eng. Sci., 22, 585, (1967).

- (29) Linek, V., and Mayrhoferova, J., Chem. Eng. Sci., 25, 787 (1970).
- (30) Wesselingh, J. A., and Van't Hoog, A. C., Trans. Instr. Chem. Engrs., 48, T69 (1970).
- (31) Yagi, S., and Inoue, H., Chem. Eng. Sci., 17, 411 (1962).
- (32) Ruether, J. A., and Puri, P. S., Canadian Journal of Chem. Eng., 51, 3, 345 (1973).
- (33) Schultzi, S. and Gaden, E. L. Ind. Eng. Sci., 48, 2209 (1956).
- (34) Linek, V., Chem. Eng. Sci., 27, 627 (1972).
- (35) Thomas, W. J., and Nicholl, E. McK., Chem. Eng. Sci., 22, 1877 (1967).
- (36) Linek, V., Mayrhoferova, J., and Mosnerova, J., Chem. Eng. Sci., 25, 1033 (1970).
- (37) Gubins, K. F., Bhathia, K. K., and Walker, R. D., A.I.Ch.E. Journal, 12, 548 (1966).
- (38) Calderbank, P. H., and Moo-Young, M. B., Chem. Eng. Sci., 16, 39 (1961).
- (39) Perry's, J. H., "Chemical Engineers' Handbook", 4th Edition (1963).
- (40) Poon, C. P. P., and Lee, F. M., Water and Sewage Works, 116, 262 (1969).
- (41) Hutchinson, M. H., and Sherwood, T. K., Ind. Eng. Chem., 29, 7, 836 (1937).
- (42) Vivian, J. E., and King, C. J., A.I.Ch.E. Journal, 10, 220 (1964).

- (43) Linek, V., and Mayrhoferova, J., Chem. Eng. Sci., 26, 1319 (1971).
- (44) Bates, R. L., Fonday, P. L., and Fenic, J. G. in "Mixing" Uhl, V. W. and Gray, J. B., eds., Vol. 1, Chap. 3, Academic Press, New York (1966).
- (45) Davies, J. T., "Turbulence Phenomena" Academic Press, New York (1972).
- (46) Bull, D. N., and Kempe, L. L., Biotech. and Bioeng., 13, 529 (1971).
- (47) Frasher, B. D., Chem. Eng. Sci., 28, 1230 (1973).

IX APPENDICES

Appendix A

Heterogeneous Mass Transfer with Reaction:

Conditions for Diffusional Regime

The following derivation applies to gas-liquid reactions with finely divided catalyst particles in liquid phase. It is restricted to the reaction of first order or pseudo-first order with respect to gas solute and zero order with respect to substrate.

1. Minimum Speed of Reaction for Diffusional Regime

There are three resistances encountered in the case of heterogeneous mass transfer with reaction. There are mass transfer between gas and liquid phases; external liquid particle mass transfer; and intraparticle diffusion with reaction. If all three steps act in series with each other, their rates must be equal under steady conditions. By assuming uniform composition in bulk liquid, the gas absorption flux can be written:

$$\begin{aligned}
 q &= k_L (C_I - C_B) \\
 &= \phi k_p a_p w (C_B - C_S) \\
 &= \phi \eta k_1 w (C_S - C_e)
 \end{aligned}
 \tag{A1}$$

By adding and rearranging, the equation becomes

$$C_I - C_e = q \left(\frac{1}{k_L} + \frac{1}{\phi k_p a_p w} + \frac{1}{\phi \eta k_1 w} \right)$$

or

$$\frac{C_I - C_B}{C_I - C_e} = \frac{1/k_L}{\left(\frac{1}{k_L} + \frac{1}{\phi k_p a_p w} + \frac{1}{\phi \eta k_1 w} \right)}
 \tag{A2}$$

Define the total liquid phase mass transfer coefficient as:

$$k' = \frac{k_p a_p \eta k_l}{k_p a_p + \eta k_l}$$

Equation (A2) can be expressed in terms of k' as:

$$\frac{C_I - C_B}{C_I - C_e} = \frac{1}{1 + k_L / \phi k' w}$$

For essentially the entire concentration driving force employed for absorption,

$$\frac{C_I - C_B}{C_I - C_e} \approx 1$$

Requirement is that:

$$1 \gg k_L / \phi k' w \quad (A3)$$

as the criterion for minimum catalyst loading.

2. Maximum Speed of Reaction for Diffusional Regime

Liquid in vicinity of gas-liquid interface has higher concentration of absorbing gas than bulk liquid. Reaction taking place on catalyst in this vicinity will have a higher rate than reaction in bulk. If the amount of reaction that occurs in the vicinity of the gas-liquid interface is appreciable compared to the reaction occurring in the entire absorber, then in fact chemical reaction in this vicinity is significantly affecting the diffusion

of the gas through the liquid boundary, and Equation (A1) is no longer applicable.

(a) Condition derived on the basis of film theory.

From the film theory point of view, the amount of reaction in the gas-liquid diffusion film must be negligible compared to the amount of reaction in the bulk liquid. The condition can be written

$$l \gg \frac{r_{C_I} \times (\text{Volume of film})}{r_{C_B} \times (\text{Bulk liquid volume})}$$

or,

$$l \gg \frac{k'w(C_I - C_e)V_f}{k'w(C_B - C_e)V_B}$$

The relative rates of reaction in the film and the bulk are given by the ratio of the respective concentration driving forces. Also the fraction of liquid in the diffusion film is expressed in terms of the film thickness L and ϕ :

$$l \gg \frac{(C_I - C_e)L}{(C_B - C_e)\phi} \quad (A4)$$

In the situation under consideration Condition (A3) will apply. Also, chemical reaction in the vicinity of the gas-liquid interface is insignificant by definition, so Equation (A1) can be used and gives:

$$1 + \frac{\phi w k'}{k_L} = \frac{C_I - C_e}{C_B - C_e}$$

Also, $L = D/k_L$. Then Condition (A4) becomes:

$$1 \gg \left(1 + \frac{\phi w k'}{k_L}\right) \frac{D}{\phi k_L}$$

or,
$$1 \gg \frac{k' w D}{k_L^2} \quad (A5)$$

(b) Condition derived on the basis of penetration theory.

Following Astarita's (25) derivation, the conditions prescribing chemical absorption can be derived from the point of view of the penetration theory, employing the concepts of reaction time, t_r , and diffusion time, t_D . Reaction time is the time required for a significant degree of reaction and is given by:

$$t_r = 1/k'w$$

Diffusion time is the time available for diffusion and is given by:

$$t_D = D/k_L^2$$

The condition for insignificant chemical reaction in the vicinity of the gas-liquid interface is:

$$t_r \gg t_D$$

which gives Condition (A5).

By combining Conditions (A3) and (A5), the condition for diffusional regime can be written:

$$k_L^2/D \gg k'w \gg \phi k_L/\phi \quad (A6)$$

Appendix B

Supporting Experiments

1. Experiments with Transfer Rate Measured by Physical Method

There are two purposes in doing these experiments. The first one is to find out whether the hydrodynamic condition in the boundary of the liquid surface would be affected by adding the required amount of allyl alcohol and catalyst in the solution. The dependence of k_L on D is determined by comparison of the measured mass transfer coefficients of the two absorbing gases at the same hydrodynamic conditions. It is necessary to ensure that the different contents in the two systems, H_2 -allyl alcohol and O_2 -sulphite, provide insignificant difference in hydrodynamic conditions. The second purpose is to select a suitable material as catalyst used in hydrogenation experiments. It was noted from preliminary runs that palladium on carbon has a much higher activity in catalytic allyl alcohol hydrogenation reaction than Raney nickel. Only about 1/20 of the amount of Raney nickel used is required for palladium on carbon to have a similar activity in reaction. Also, the particles of palladium on carbon are more finely divided and less dense than Raney nickel. All particles were thoroughly suspended even at lowest stirring speed used when this catalyst was used. This gives another advantage in using palladium on carbon over Raney nickel as catalyst: that the effective amount used can be clearly known. However, the insignificance of the

addition of catalyst particles to the hydrodynamic conditions is most important. The selection of which catalyst to be use was based on the results of the following described experiments.

The same apparatus as the hydrogenation experiments in the main part of this work was used in these runs except for the addition of a Honeywell Electronik 194 laboratory recorder, which was in connection with the oxygen analyzer, to record the concentration of oxygen varying with time. The procedure of these experiments was divided to two parts. In the oxygen desorption part the vessel was closed by the cover and nitrogen was fed on the top of the liquid surface. With agitation the oxygen content in the liquid was driven out gradually. The decrease in oxygen concentration was indicated on the analyzer and was recorded on the recorder. Following this, the oxygen absorption process started with a very low oxygen concentration in solution resulting from the desorption process. The cover was removed with the agitated liquid surface open to atmosphere. Oxygen was absorbed from air and the increasing oxygen concentration of the solution was recorded. The desorption part was performed in the agitation of 240 rpm, and the absorption part was performed in 132 rpm. Sodium sulphate solution with 0.1 mole/l in concentration was used with the addition of one of the assigned testing materials in each run.

Allyl alcohol, Raney nickel, and palladium on carbon were tested, with the amount used depending on the requirements for the hydrogenation experiments. The resulted mass transfer rates for the solutions with each of these material added were compared to the transfer rate for the solution without adding any material on the basis of equal oxygen concentration levels. In the experiment of testing Raney nickel, the dissolved oxygen concentration dropped when the catalyst particles were added. Also, a slower absorption rate and a faster desorption rate, in comparison with the results of the case where pure sodium sulphate solution was used were found apparently on the recorder. This is considered due to the strong affinity for oxygen of the catalyst particles. The Raney nickel catalyst was left over night with the solution to saturate the particles with oxygen. The experiment was then performed again the next day. The results showed that the Raney nickel was inactive to oxygen. In the case of testing palladium on carbon, faster absorption and desorption rates were found apparently. No attempt has been made to explain this observation.

The results for allyl alcohol and Raney nickel are given in Table B-1. The maximum change in transfer rate being 1.5 % and 2.3 % for the addition of allyl alcohol and Raney nickel respectively shows that both materials have no significant effect on the hydrodynamic conditions

of the liquid. In addition, the presence of allyl alcohol in a concentration of 0.05 mole/l in a 0.1 mole/l sodium sulphate solution was found to have a negligible effect on the solubility of hydrogen and oxygen, and on the solution viscosity.

Table B-1. Values of t^* in various material added solutions

Stirring speed rpm	Pure sodium sulphate solution	Material added solution	
		Allyl alcohol (65 ml)	Raney nickel (28.71 g)
132	102.9	101.4	100.5
240	33.5	33.2	33.3

* t' = the time in minute required for oxygen concentration changing its value between marks of 20 and 80 of a 0-100 chart scale.

For the reason of avoiding any possibility of any significant changing of hydrodynamic conditions by the addition of catalyst, it was decided to use Raney nickel as catalyst in later hydrogenation experiments. Also, the catalytic activity of Raney nickel was found more stable than palladium on carbon for the hydrogenation of allyl alcohol.

It is not possible to make the same test for sodium

sulphite because oxygen will be consumed by the reaction. The concentration of sulphite ion was kept very low compared to the total electrolyte concentration in the oxidation experiments. It was considered that no further attempt to ensure the ineffectiveness of the addition of sodium sulphite to the solution is necessary. The same conclusion was applied to the solution with propanol which was produced in the hydrogenation experiments. The content of propanol was very small in comparison to allyl alcohol.

2. Experiments with Transfer Rate Measured by the Chemical Method at a Condition other than Diffusional Regime

In addition to experiments performed in diffusional regime in hydrogen-allyl alcohol system, experiments have been done in the situation where Condition (A3) cannot be fulfilled. In this case the reaction is not fast enough to drop C_B close to zero.

Following previous assumptions for catalytic hydrogenation of allyl alcohol, Equation (A1) can be used and was expressed in terms of k'

$$q = k_L(C_I - C_B) = \phi k' w C_B$$

or,

$$\frac{C_I}{q} = \frac{1}{k_L} + \frac{1}{\phi k' w} \quad (B1)$$

Equation (B1) gives a linear relation in a plot of C_I/q vs. $1/w$. The reciprocal value of mass transfer coeffi-

cient can be obtained at $1/w$ equal to zero.

To achieve this the amount of catalyst used must be less than the minimum amount required for diffusional regime. Two runs were performed in this condition with different amount of Raney nickel used in the same stirring speed, 225 rpm. The results of propanol concentration increasing with time were given in Figure B-1. The absorption rates can be calculated from the slope of these straight lines.

$$q = \phi \times \text{slope} \quad (B2)$$

A plot of C_I/q against $1/w$ is shown in Figure B-2 which gives $k_L = 1.346 \times 10^{-2}$ cm/sec after temperature correction has been done from 26°C to 25°C . This value is about 4.13 percent lower than the average value obtained by the experiments performed in the diffusional regime.

The application of this method in determining mass transfer coefficient requires the insurance of the hydrogenation reaction to be first order or psuedo-first order with the absorbing gas. Also, owing to the reaction kinetics and solubility concerned, temperature has to be controlled to a fixed value for all experimental runs in a given stirring speed. This may not be achieved with the apparatus in the present work. In addition, the accuracy of the value of the catalyst amount, w , used is important in this case. Because some big lumps of particles were

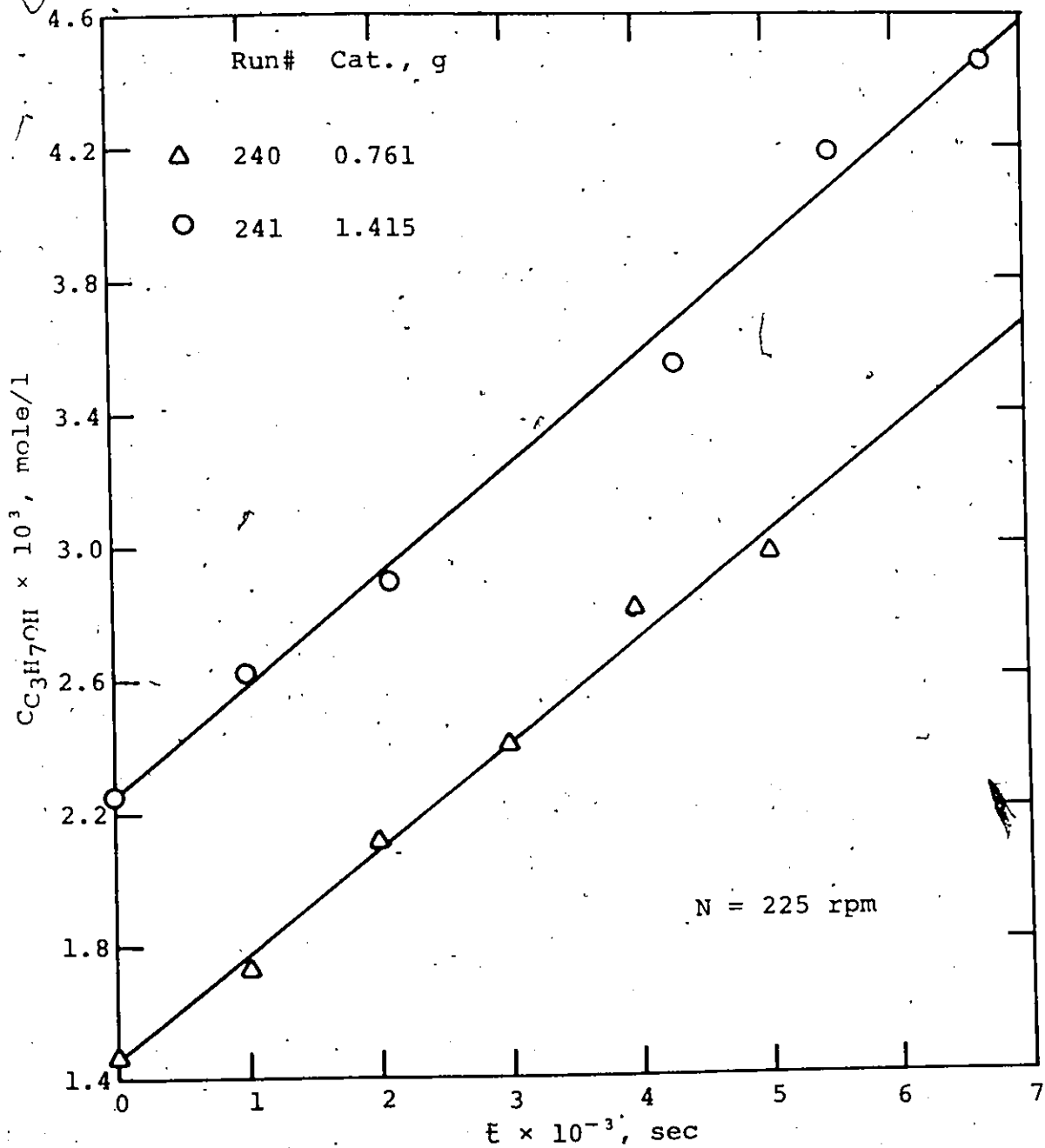


Figure B-1 Propanol concentration vs. time for hydrogenation of allyl alcohol at a condition where $C_B \neq 0$

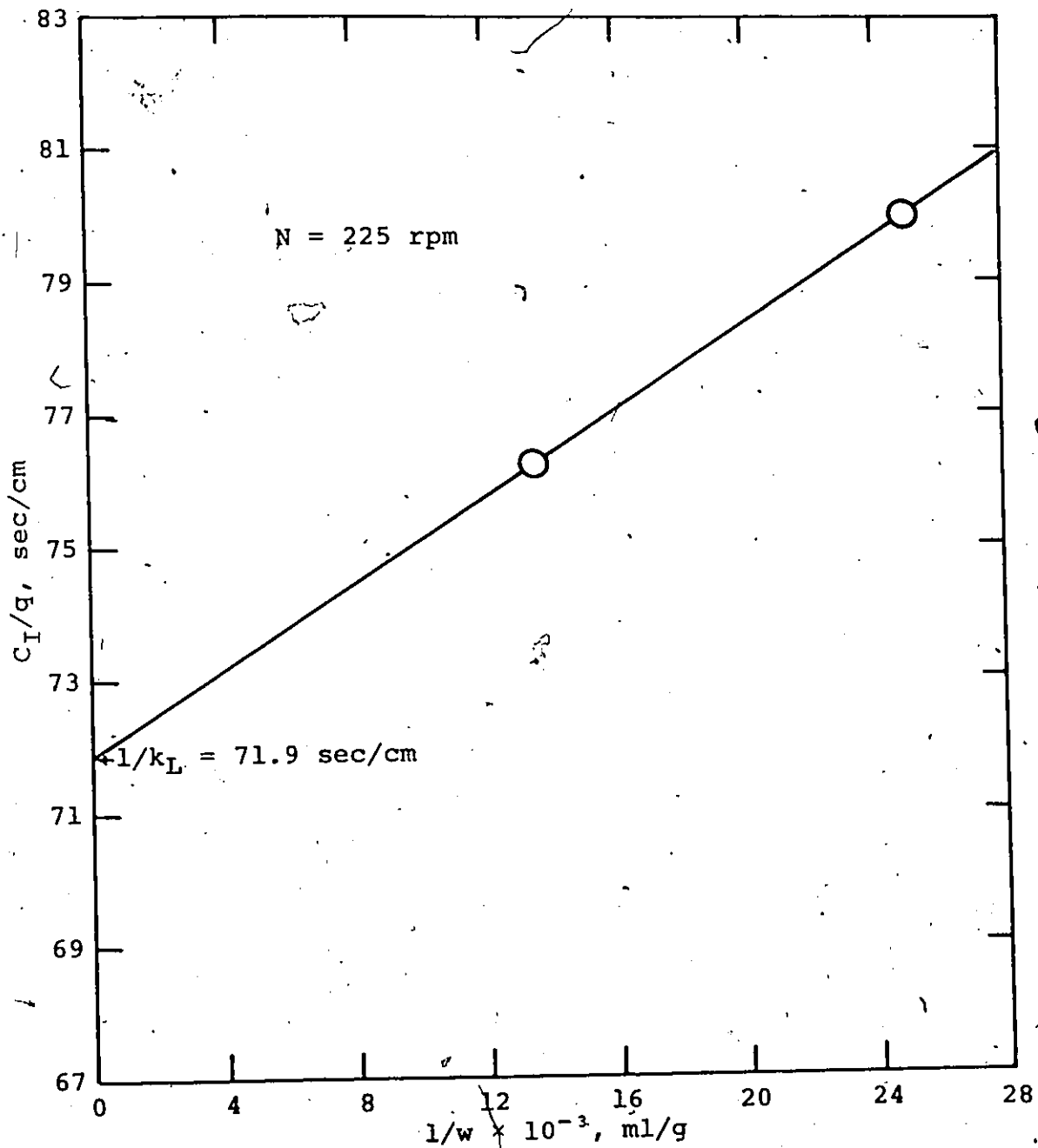


Figure B-2. Determination of mass transfer coefficient for absorption of hydrogen according to Equation (B1)

found under the stirrer in experiments, the effective value of w cannot be obtained accurately. For these reasons, the above stated method was rejected, and values of k_L were measured in experiments performed in diffusional regime only.

The values of k_L calculated from the diffusional regime equations covering all the experiments done on 225 rpm are given in Figure B-3 together with the amount of catalyst used. This figure shows that all experiments were performed in the diffusional regime (not affected by the amount of catalyst used) except the two experiments with lowest amount of Raney nickel used.

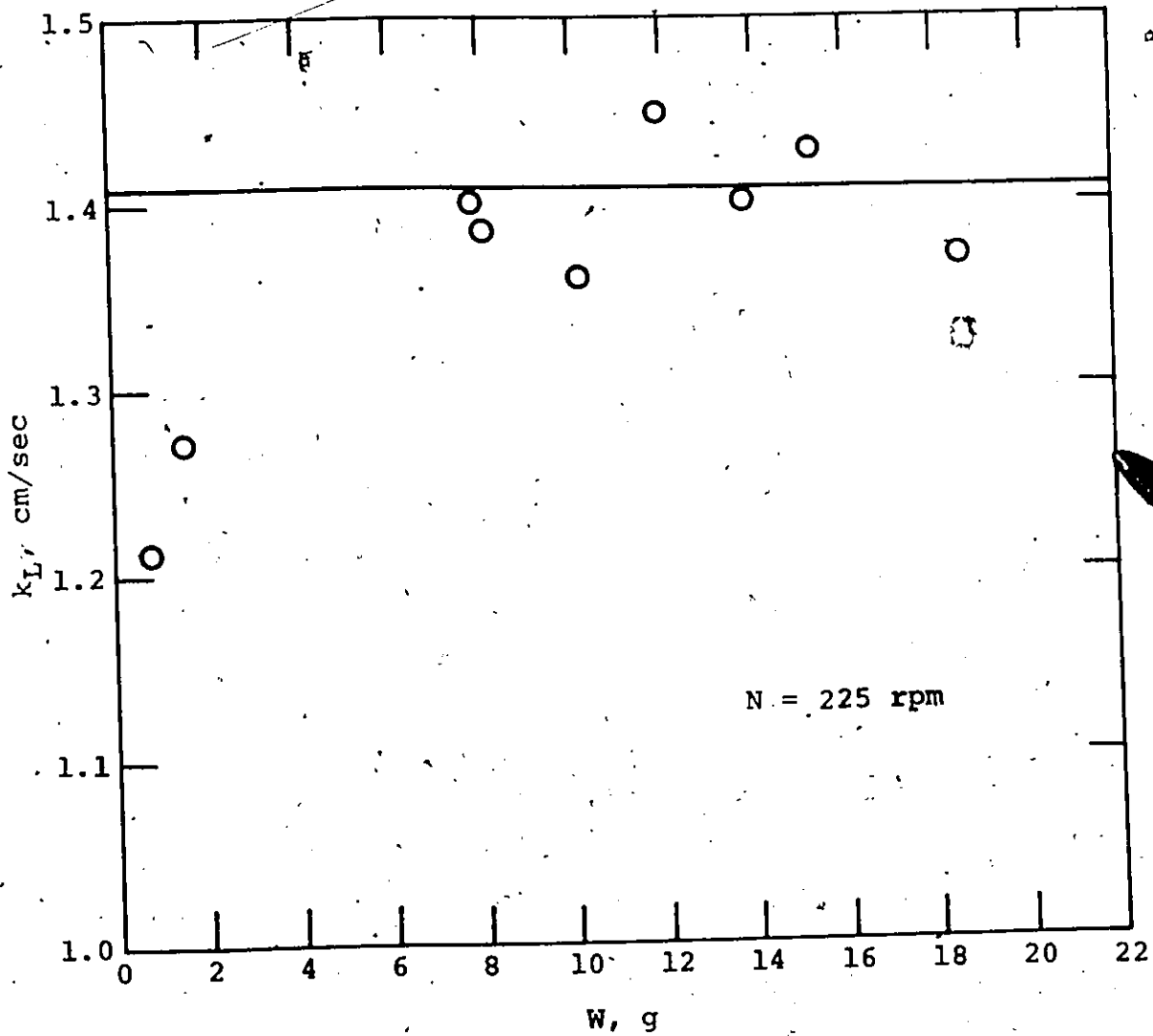


Figure B-3. Mass transfer coefficient* vs. amount of Raney nickel used

* Values of k_L were calculated according to the equation for diffusional regime.

Appendix C

Experimental Results

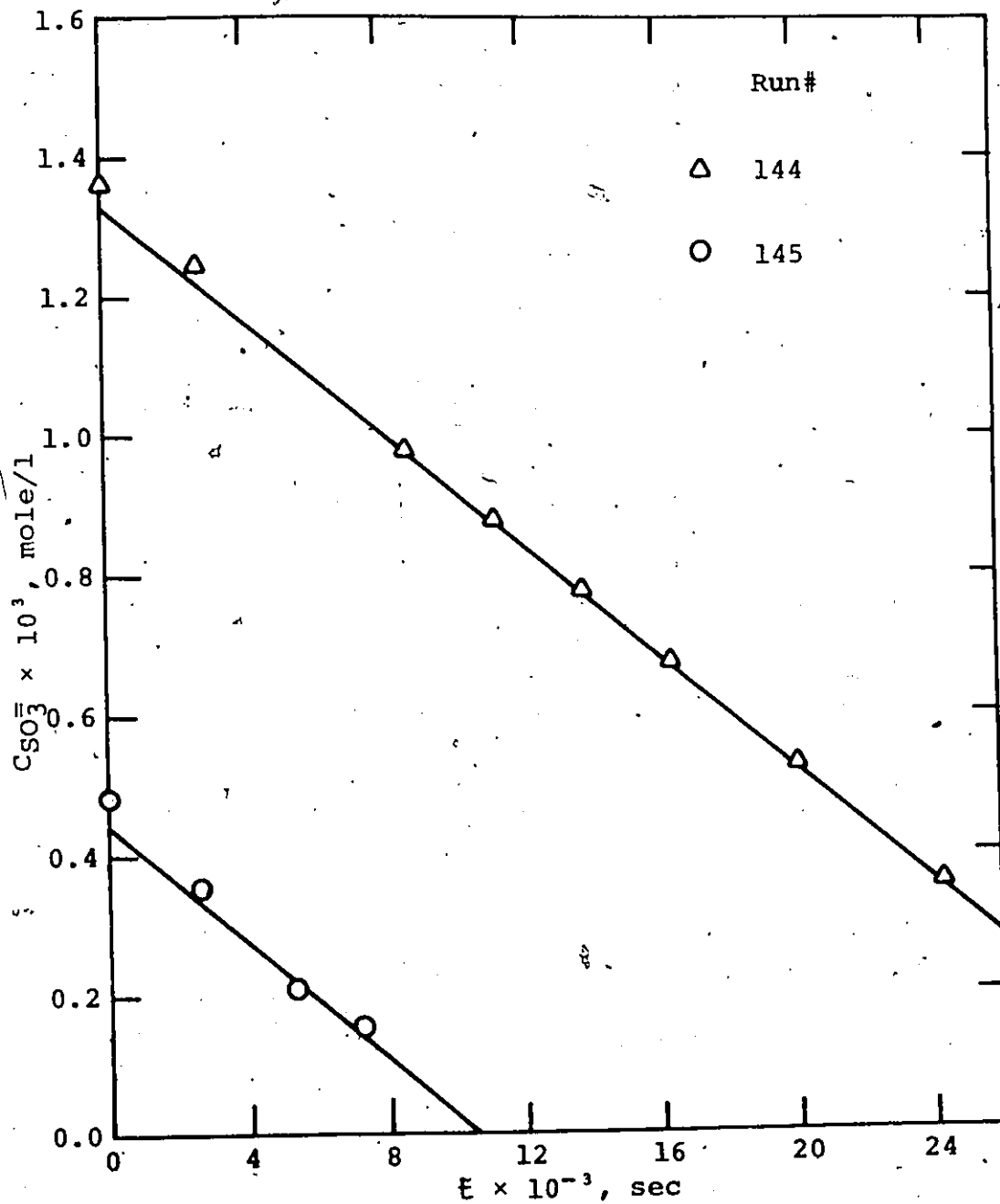


Figure C-1. Sulphite concentration vs. time for oxidation of sodium sulphite at a stirring speed of 109 rpm

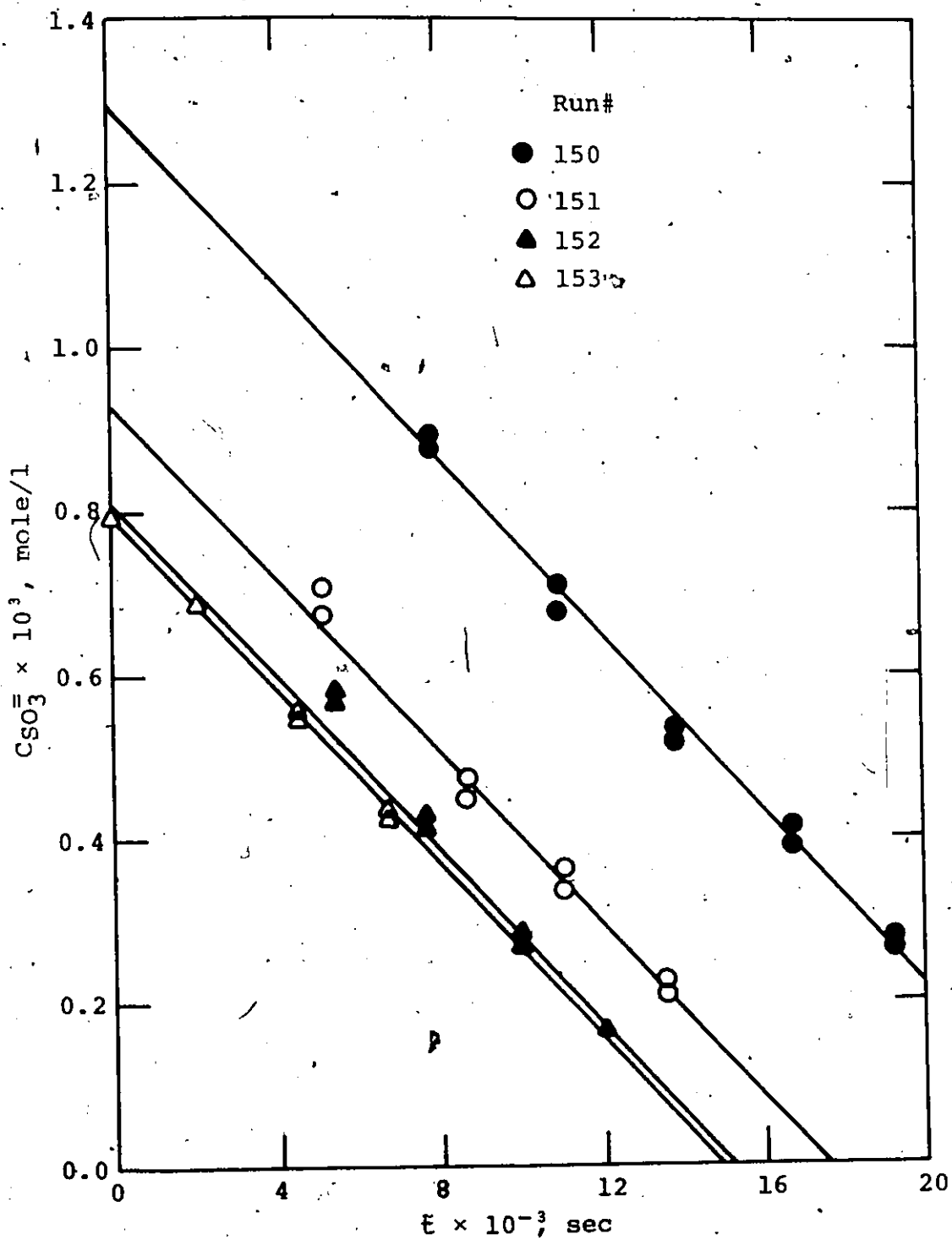


Figure C-2. Sulphite concentration vs. time for oxidation of sodium sulphite at a stirring speed of 125 rpm

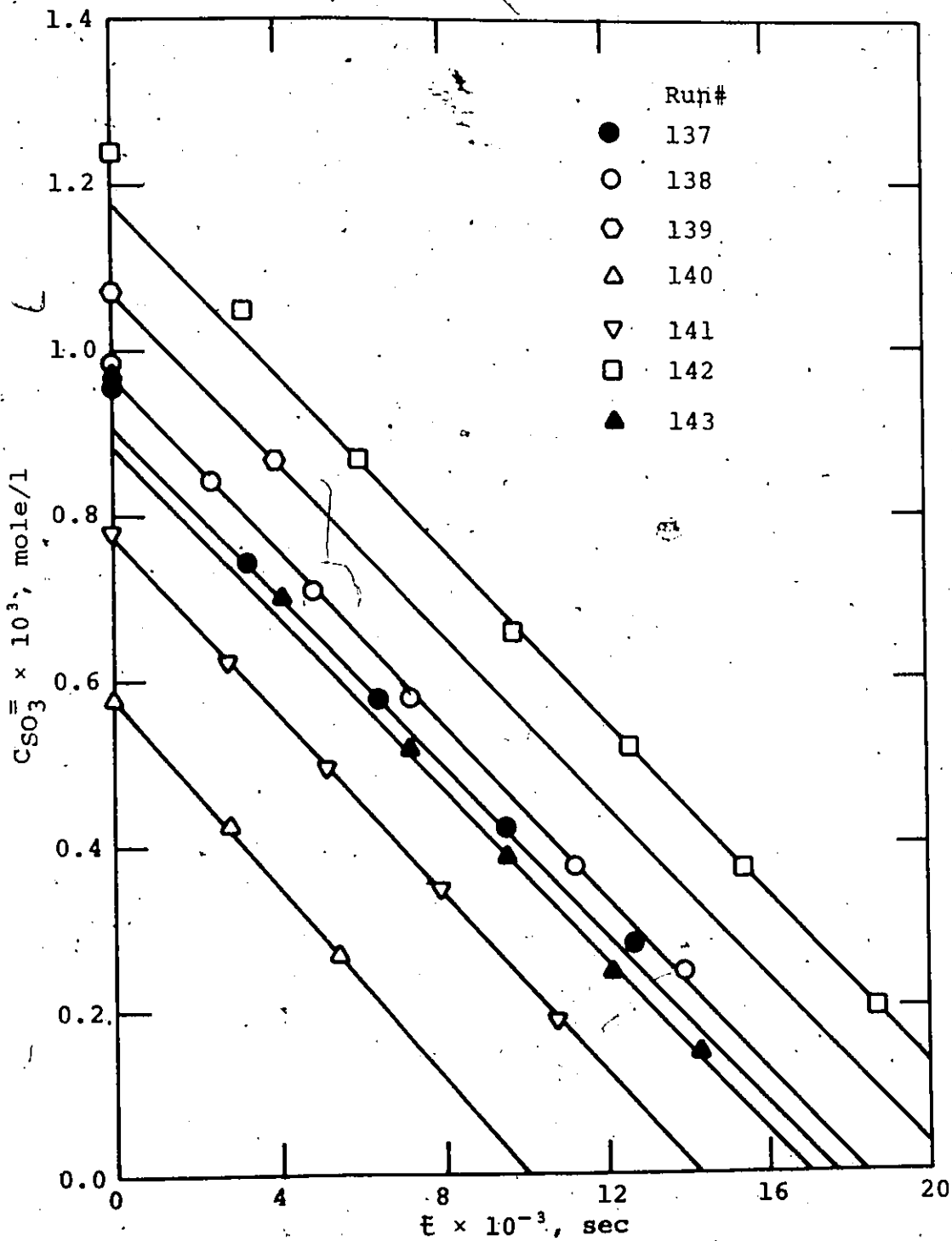


Figure C-3. Sulphite concentration vs. time for oxidation of sodium sulphite at a stirring speed of 132 rpm

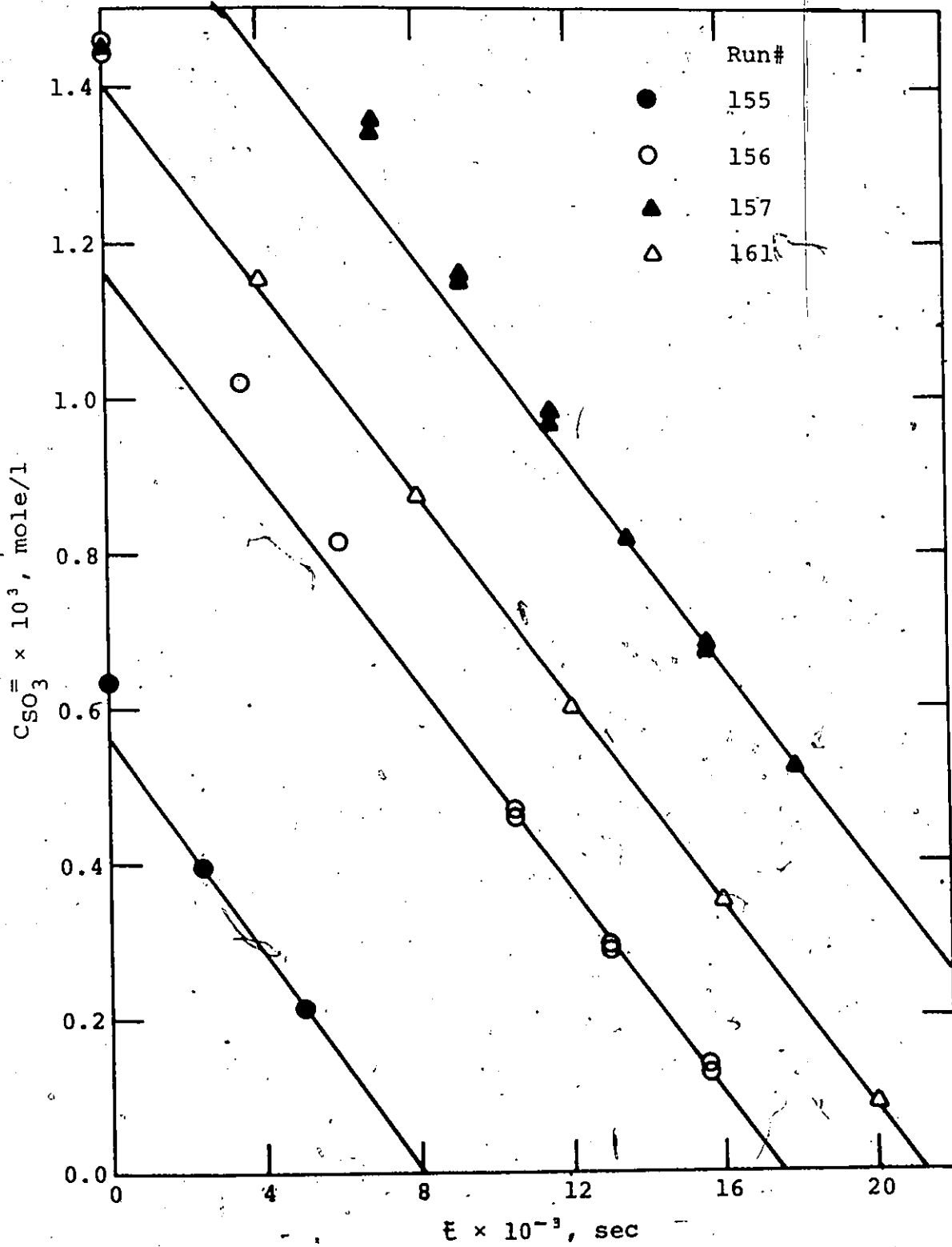


Figure C-4. Sulphite concentration vs. time for oxidation of sodium sulphite at a stirring speed of 153 rpm

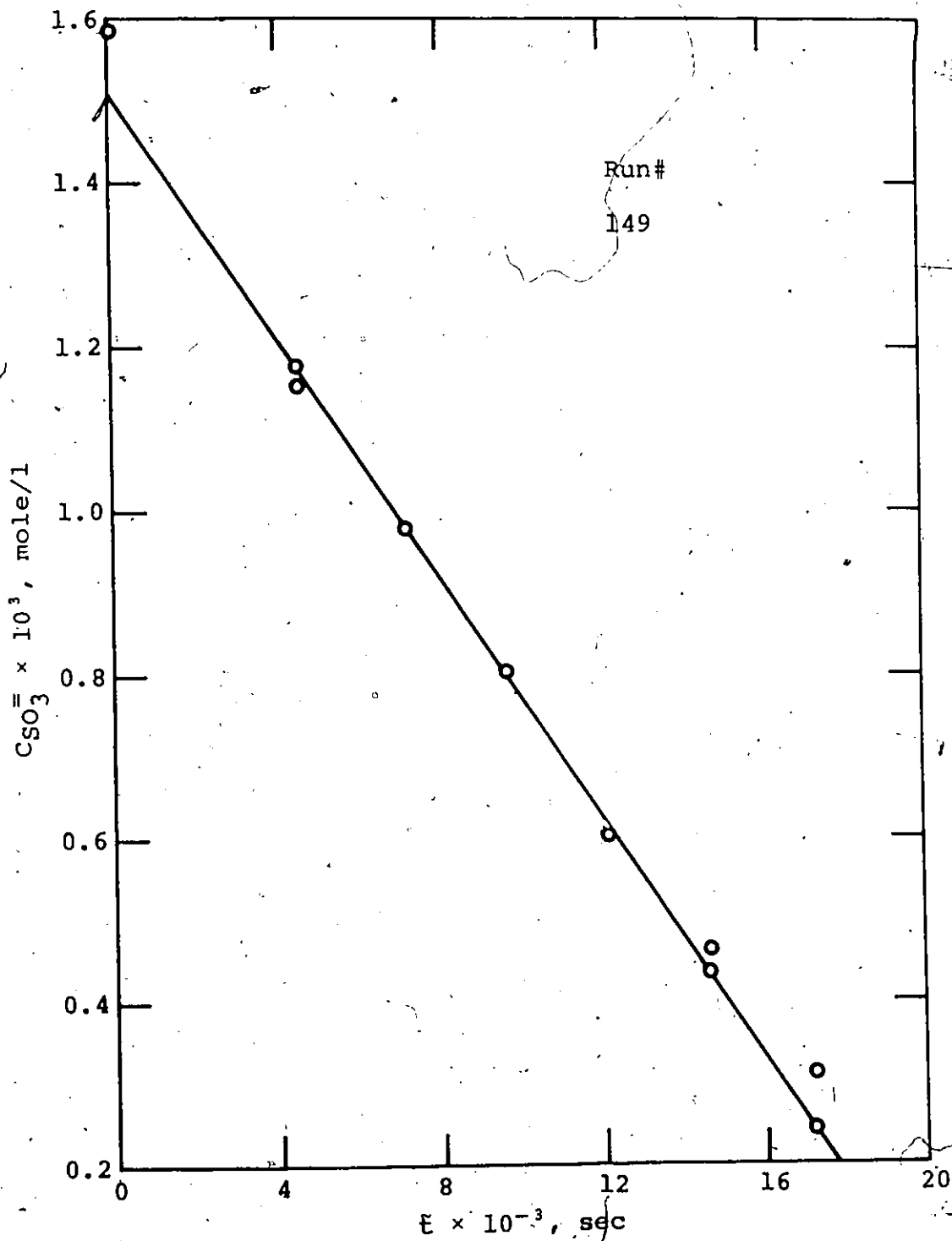


Figure C-5. Sulphite concentration vs. time for oxidation of sodium sulphite at a stirring speed of 164 rpm

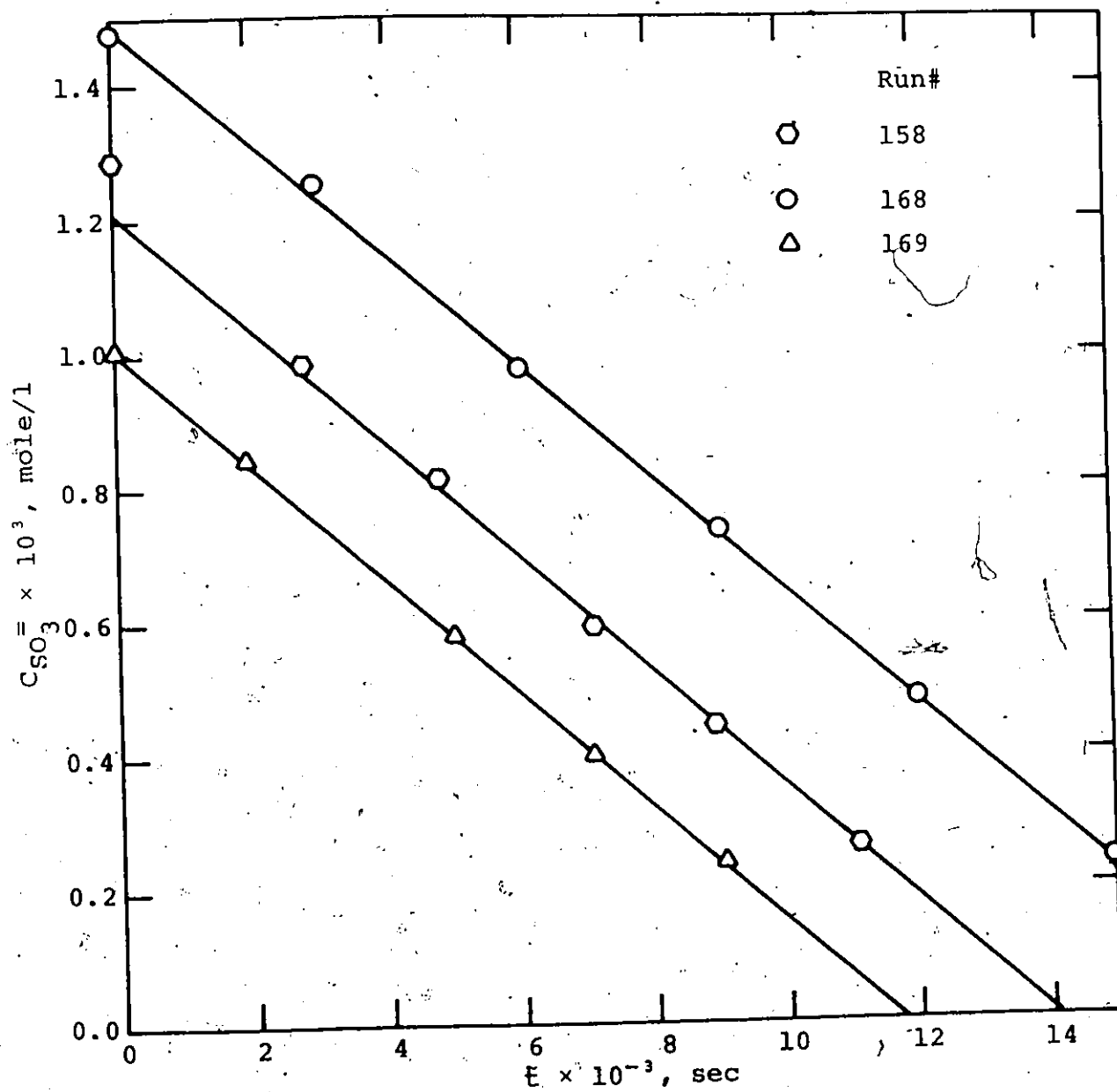


Figure C-6. Sulphite concentration vs. time for oxidation of sodium sulphite at a stirring speed of 181 rpm

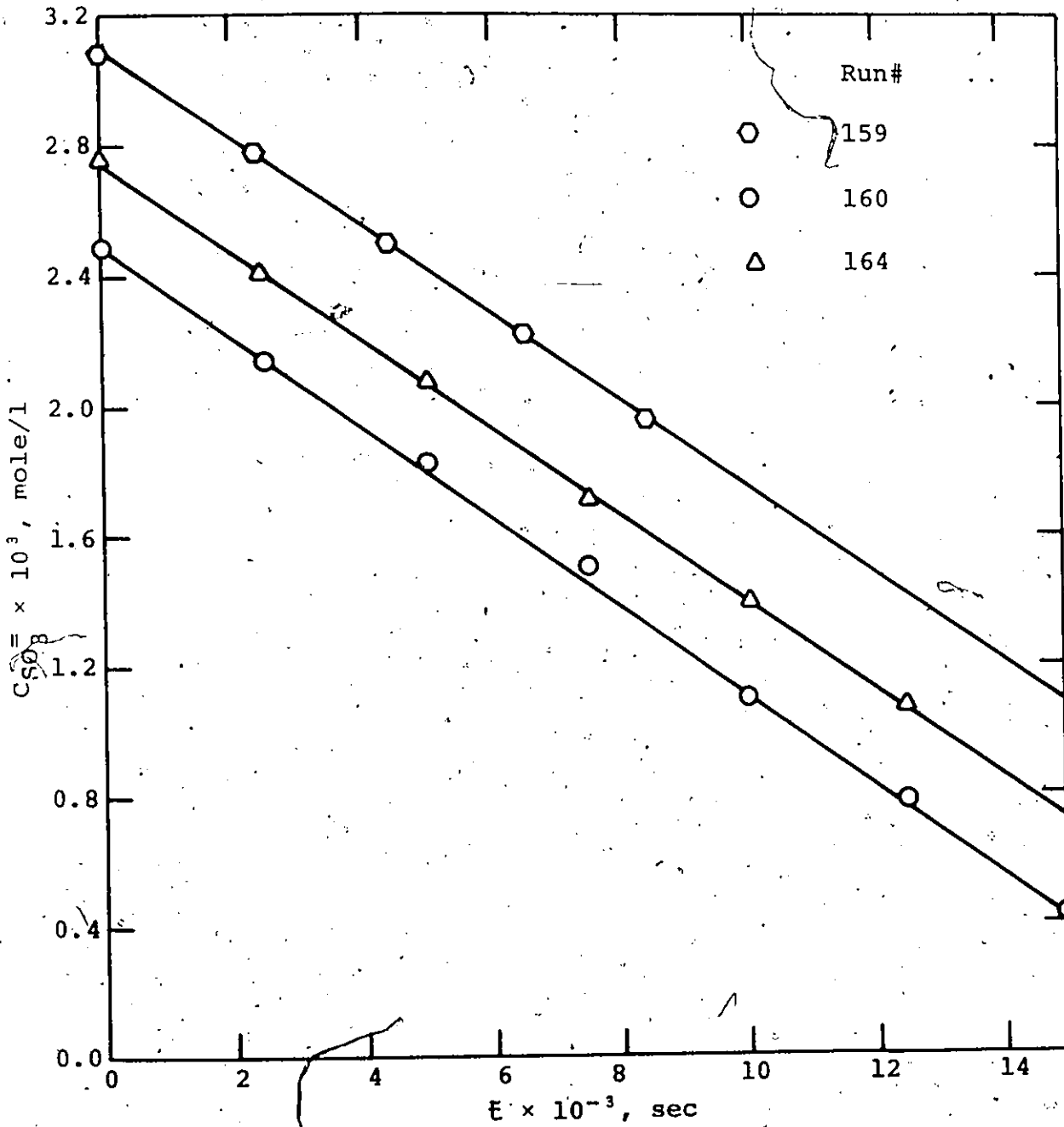


Figure C-7. Silphite concentration vs. time for oxidation of sodium sulphite at a stirring speed of 225 rpm

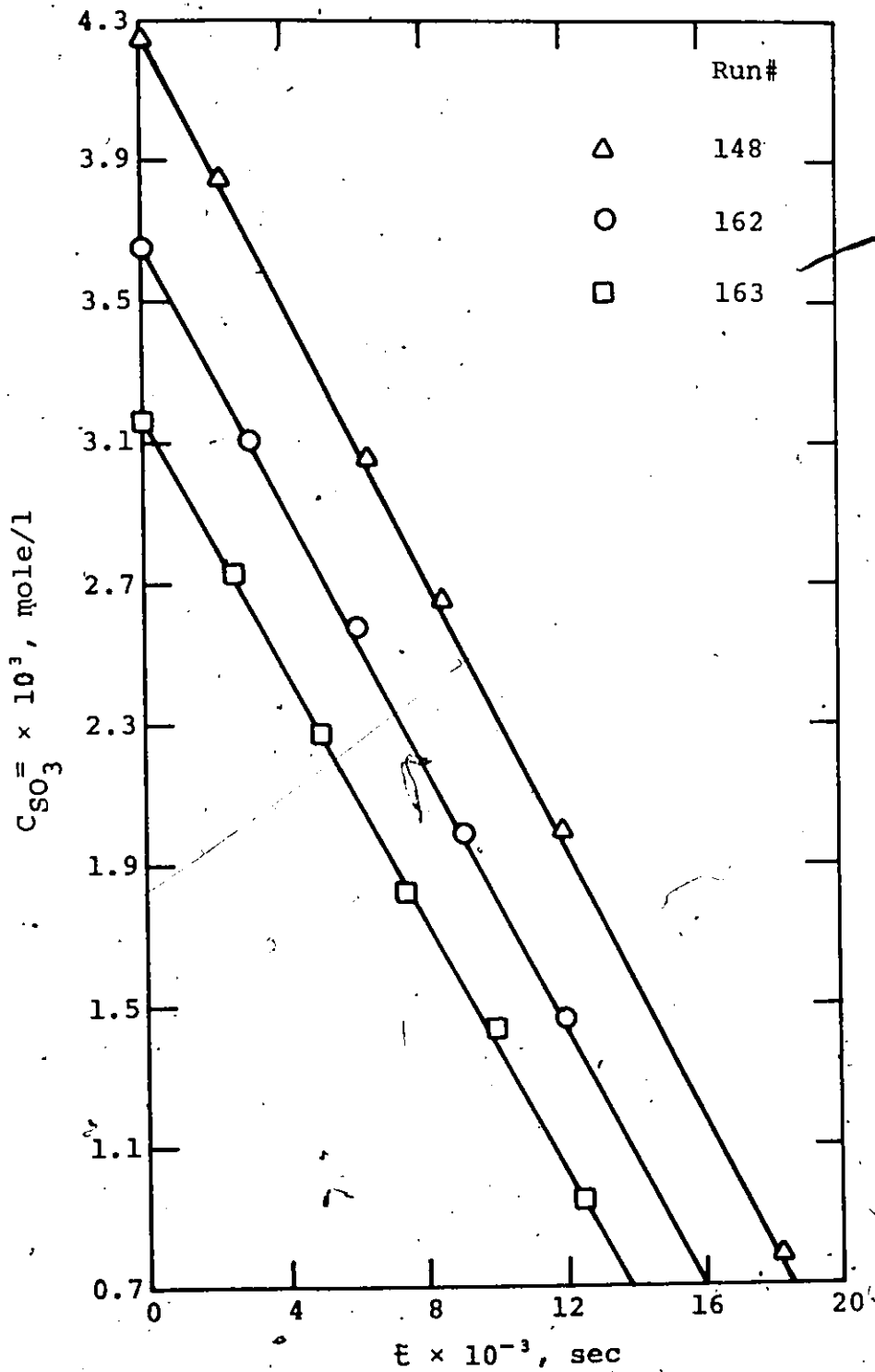


Figure C-8. Sulphite concentration vs. time for oxidation of sodium sulphite at a stirring speed of 240 rpm

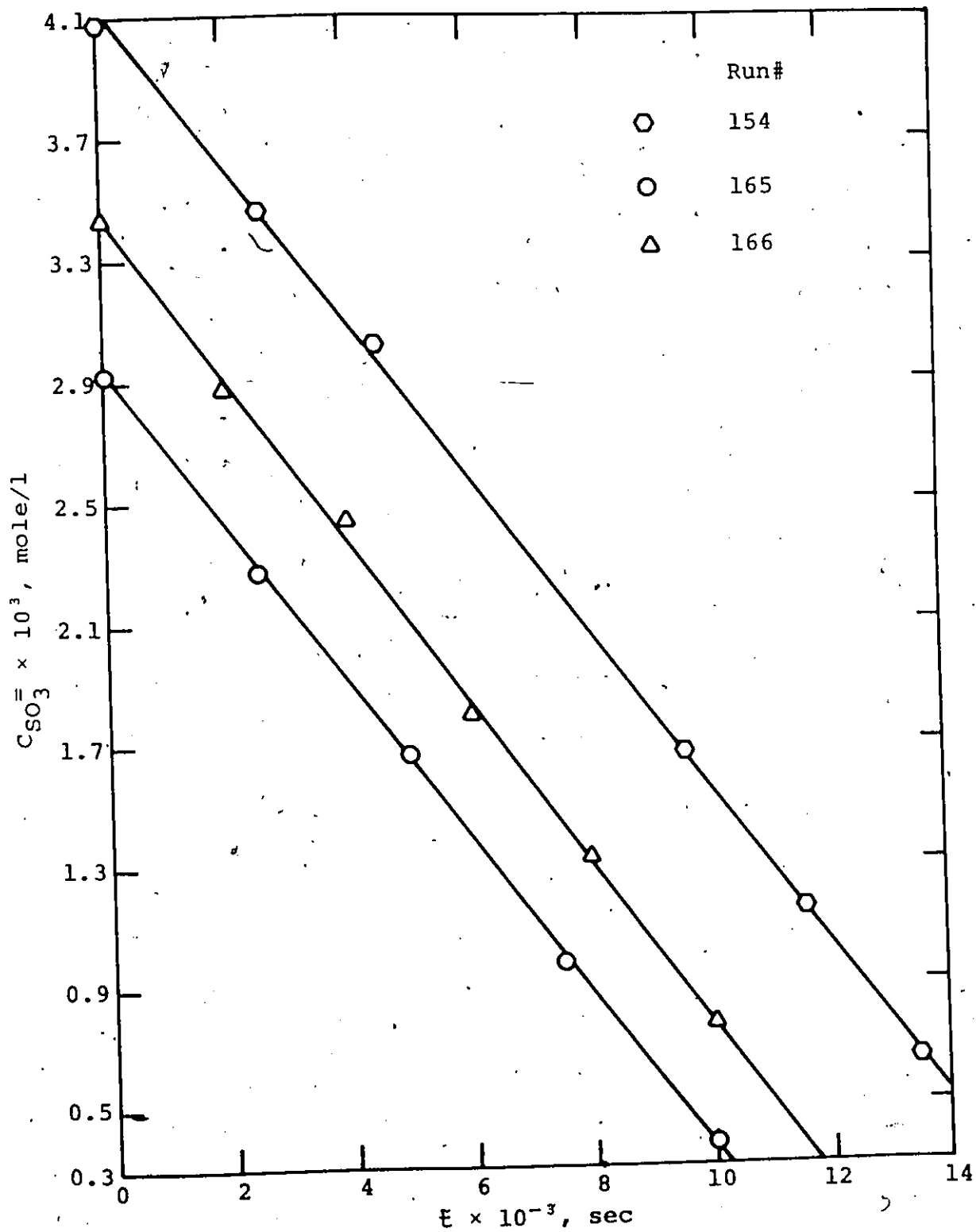


Figure C-9. Sulphite concentration vs. time for oxidation of sodium sulphite at a stirring speed of 258 rpm

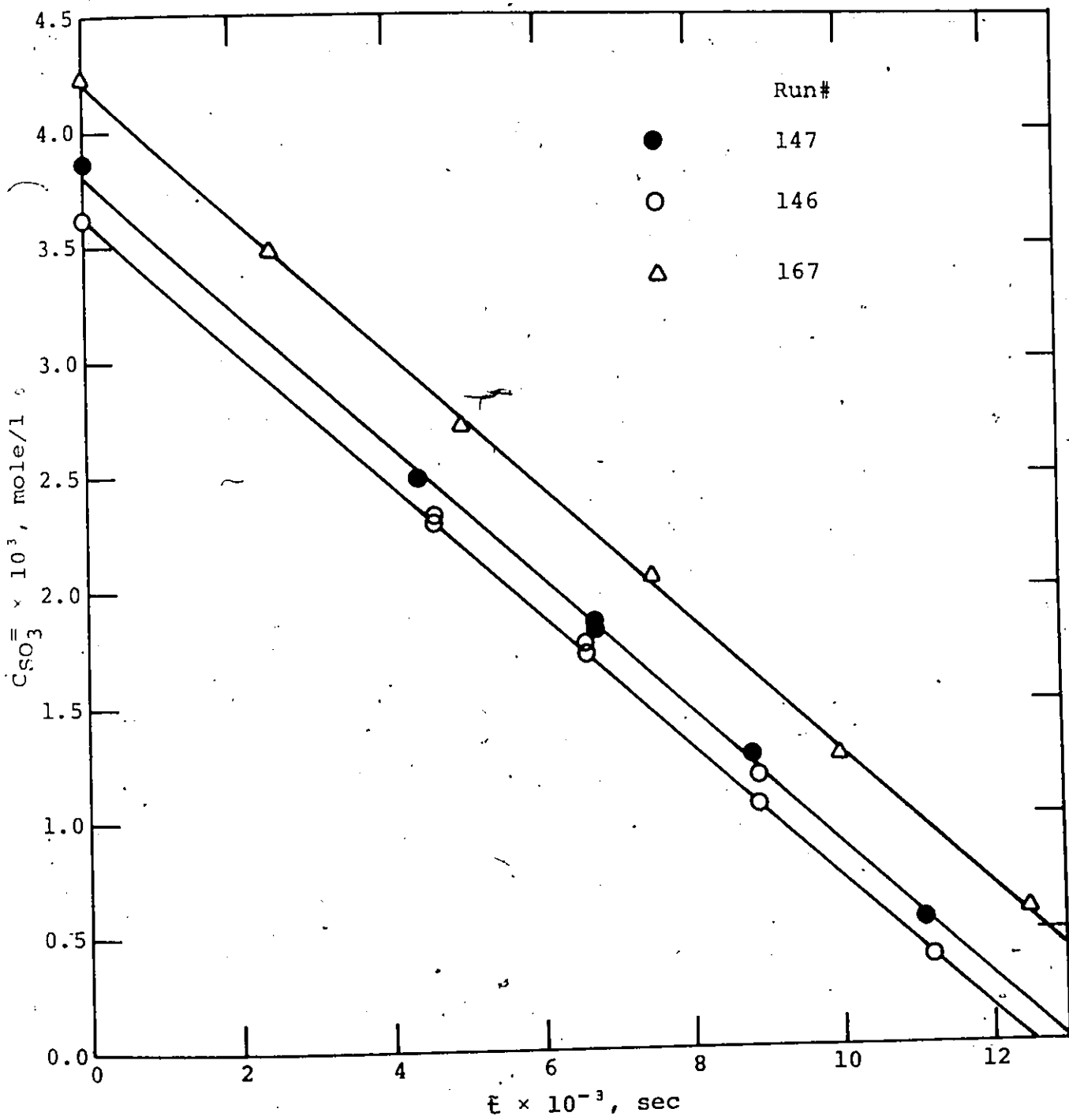


Figure C-10. Sulphite concentration vs. time for oxidation of sodium sulphite at a stirring speed of 272 rpm

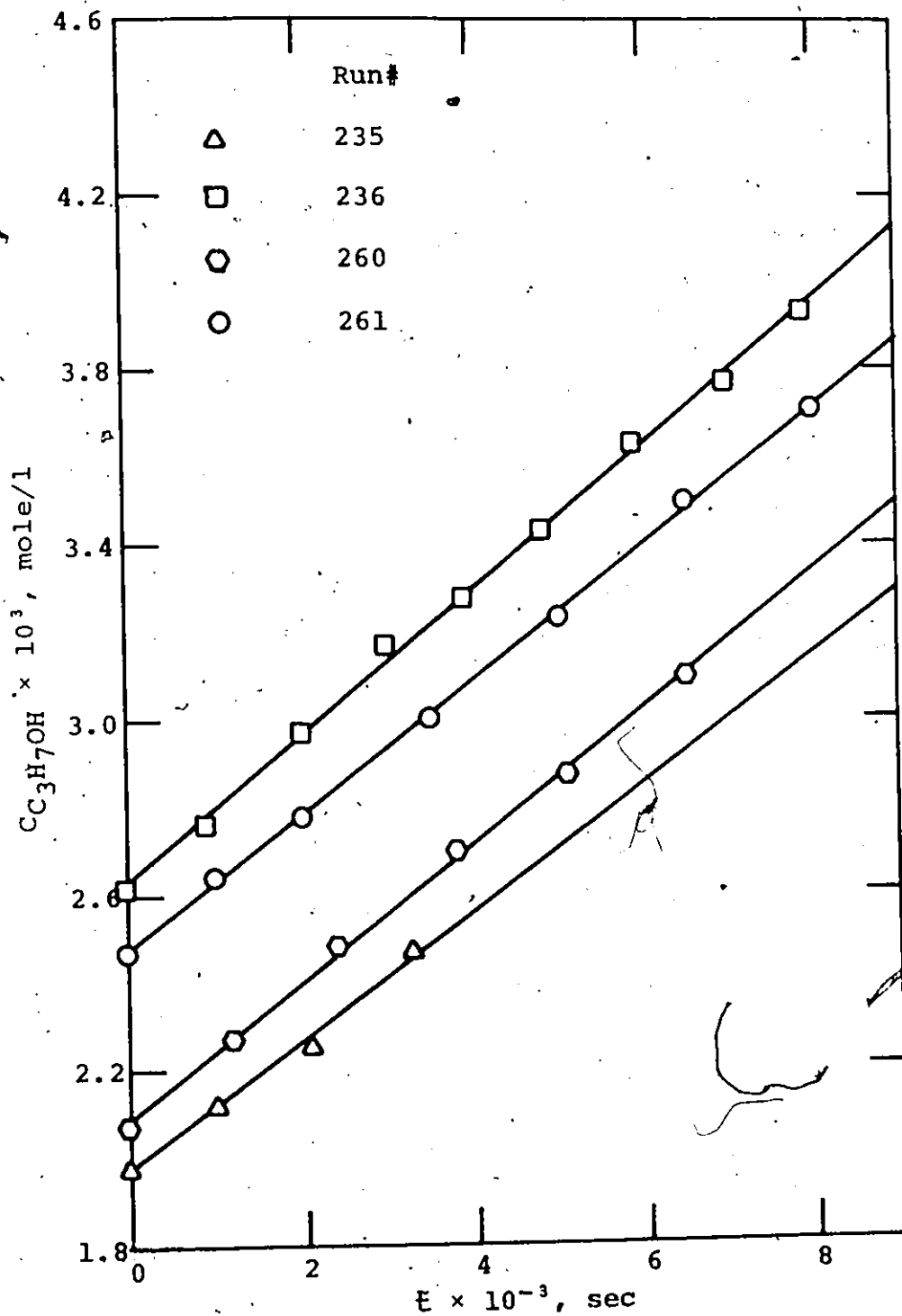


Figure C-11. Propanol concentration vs. time for hydrogenation of allyl alcohol at a stirring speed of 132 rpm

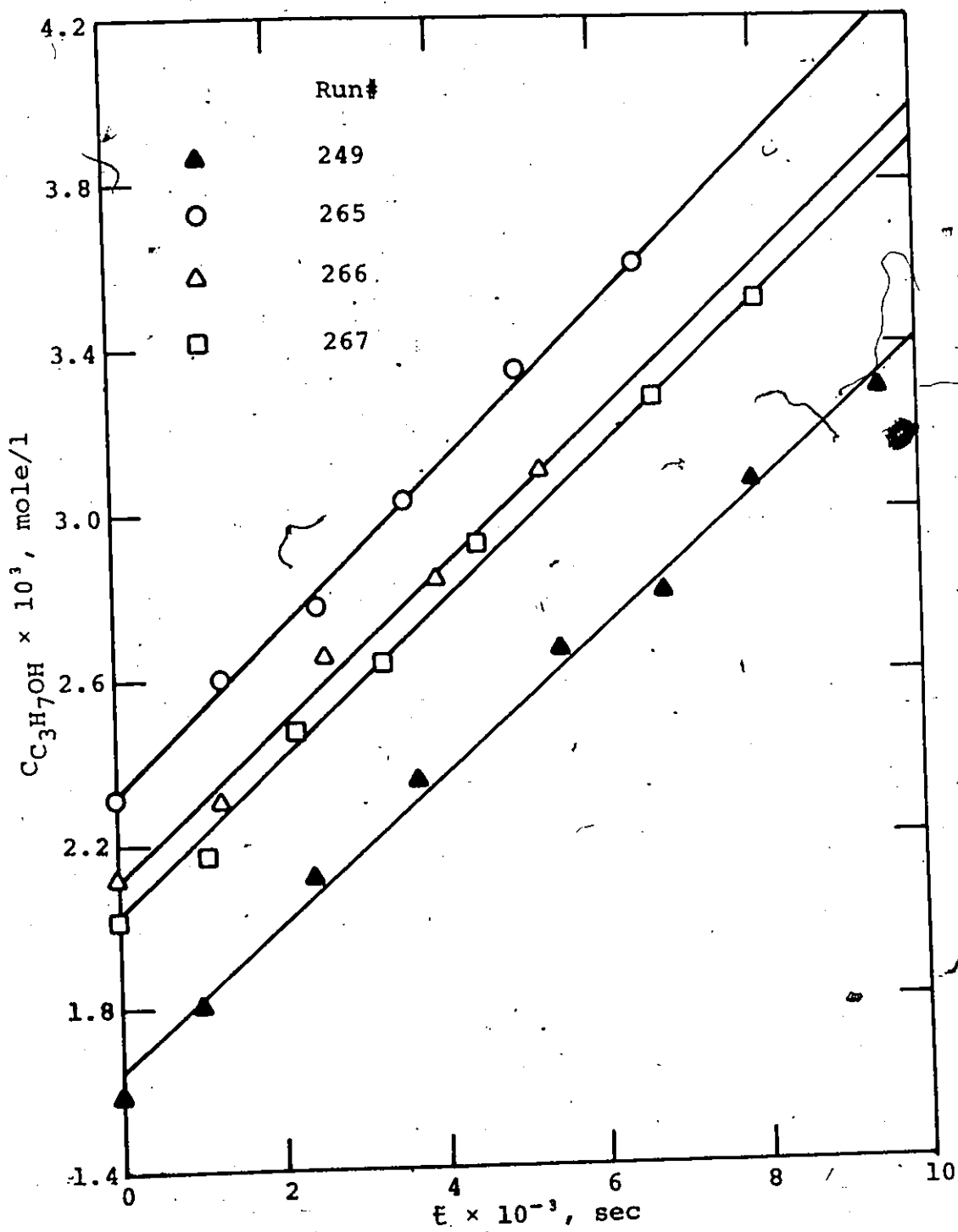


Figure C-12. Propanol concentration vs. time for hydrogenation of allyl alcohol at a stirring speed of 153 rpm

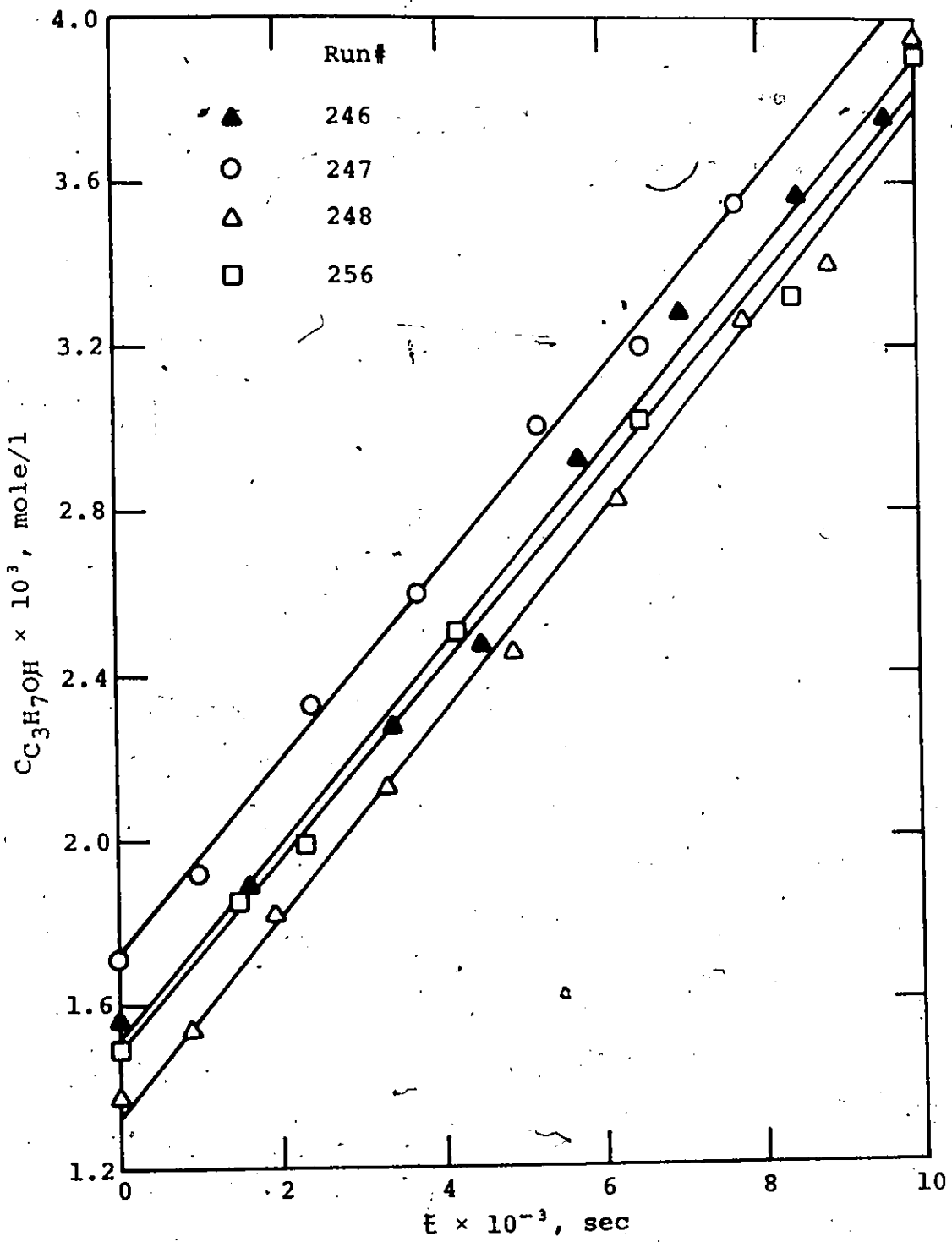


Figure C-13. Propanol concentration vs. time for hydrogenation of allyl alcohol at a stirring speed of 181 rpm

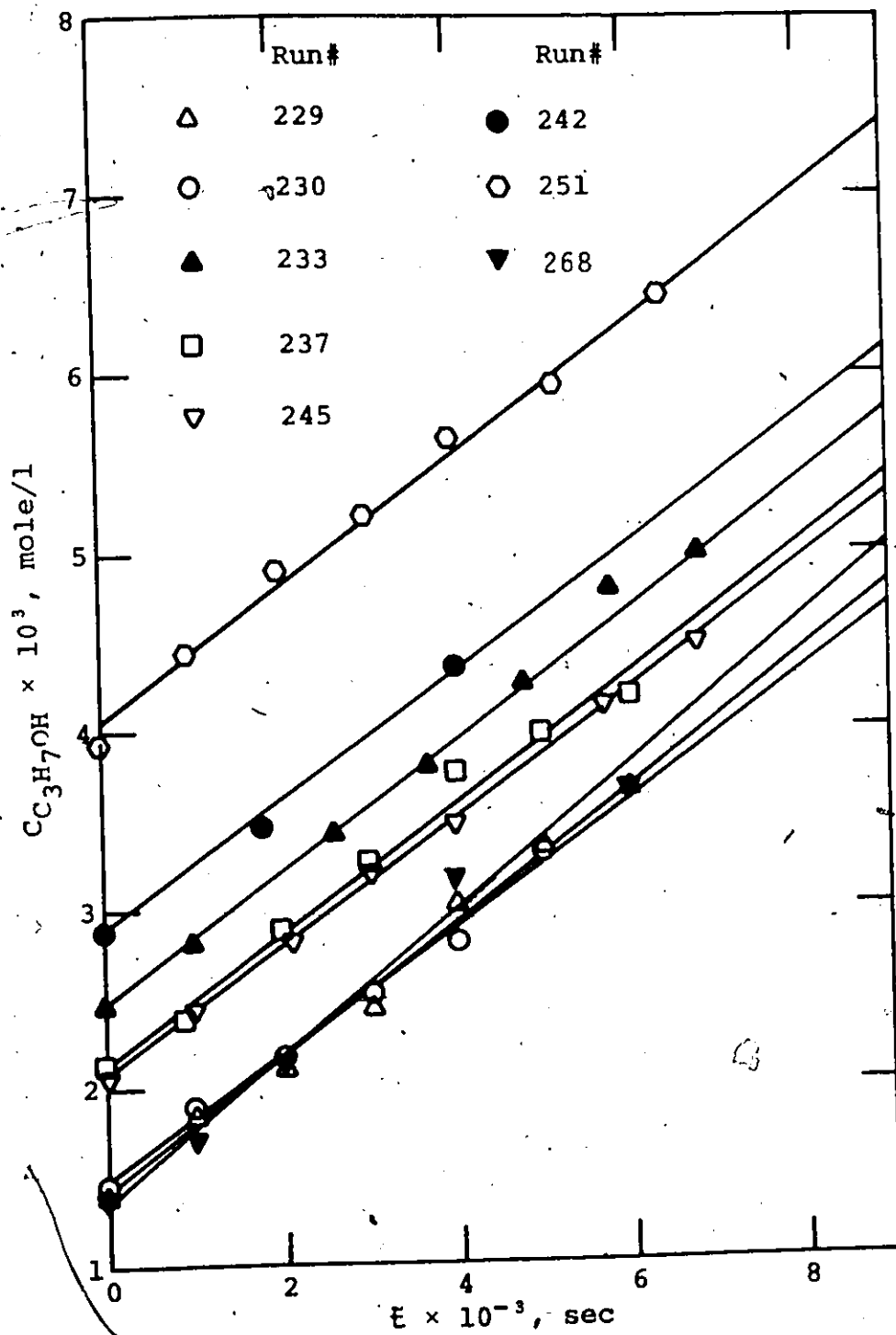


Figure C-14. Propanol concentration vs. time for hydrogenation of allyl alcohol at a stirring speed of 225 rpm

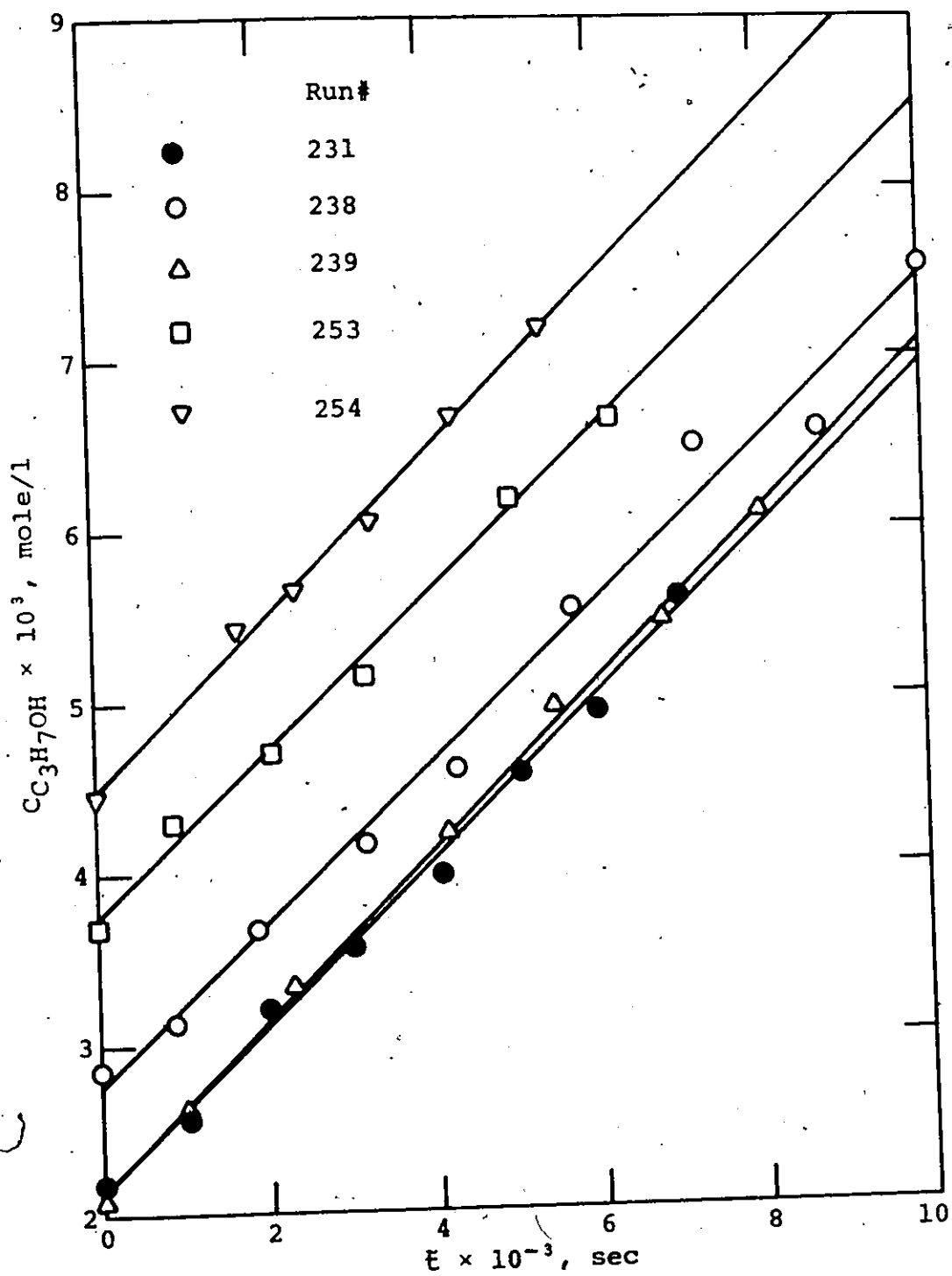


Figure C-15. Propyl alcohol concentration vs. time for hydrogenation of allyl alcohol at a stirring speed of 240 rpm

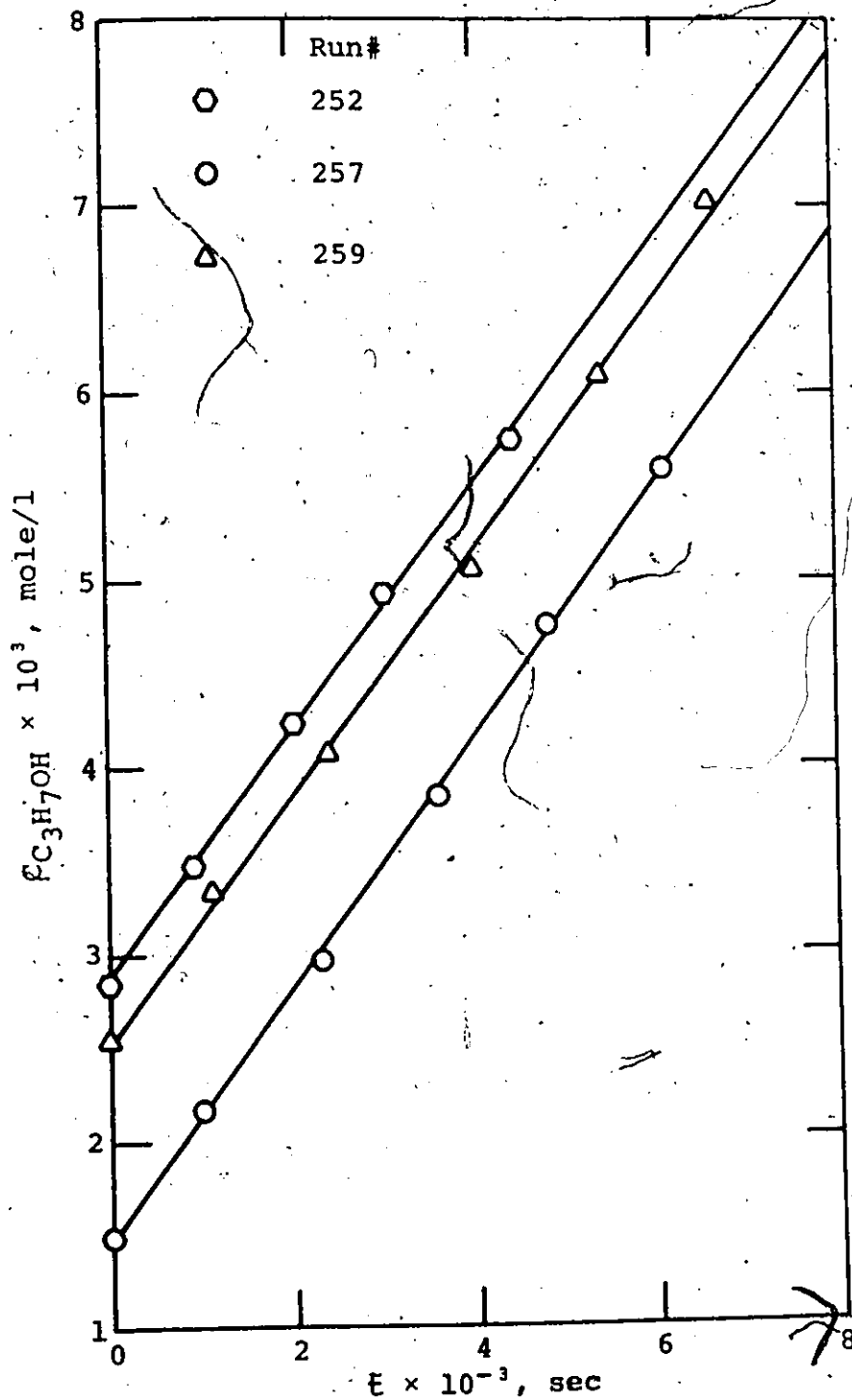


Figure C-16. Propanol concentration vs. time for hydrogenation of allyl alcohol at a stirring speed of 258 rpm

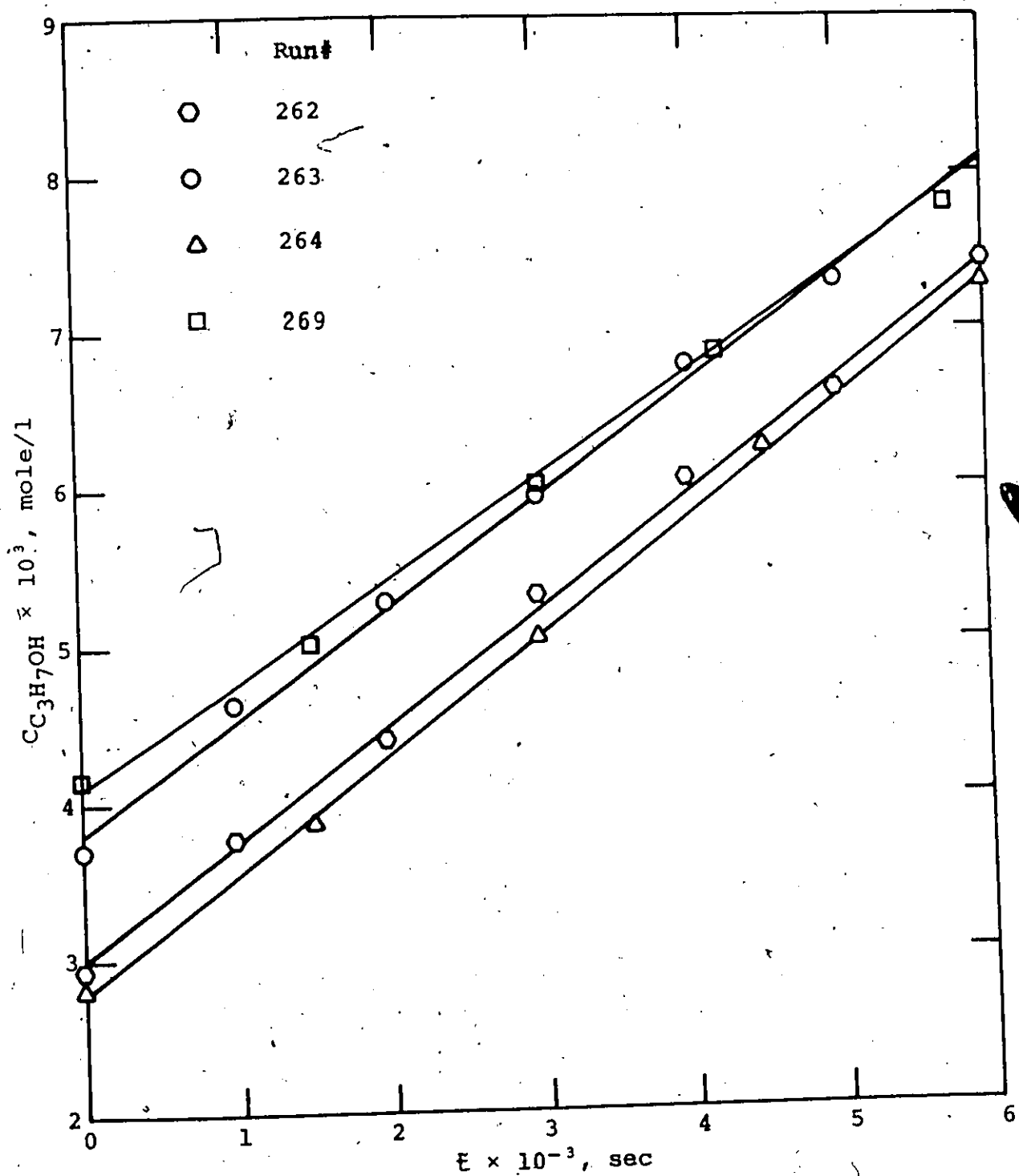


Figure C-17. Propanol concentration vs. time for hydrogenation of allyl alcohol at a stirring speed of 272 rpm

Table C-1. Experimental results for
oxygen-sulphite system
 $P_{O_2} = 152 - 157 \text{ mmHg}$

Stirring speed rpm	Run number	Temperature $^{\circ}\text{C}$	Slope $\times 10^7$ mole/l-sec
109	144	23.0	-0.404
	145	24.9	-0.423
125	150	23.4	-0.506
	151	24.5	-0.496
	152	23.0	-0.571
	153	23.8	-0.552
132	137	22.5	-0.514
	138	21.8	-0.529
	139	20.7	-0.518
	140	22.3	-0.576
	141	21.0	-0.543
	142	22.0	-0.523
	143	21.0	-0.522
153	155	23.0	-0.712
	156	23.1	-0.643
	157	23.0	-0.668
	161	23.0	-0.661
164	149	22.9	-0.704

Table C-1. (Continued)

<u>Stirring speed rpm</u>	<u>Run- number</u>	<u>Temperature °C</u>	<u>Slope × 10⁷ mole/l-sec</u>
181	158	24.6	-0.875
	168	23.8	-0.838
	169	24.3	-0.860
225	159	22.8	-1.347
	160	23.8	-1.374
	164	24.0	-1.353
240	148	28.0	-1.907
	162	24.5	-1.835
	163	24.5	-1.764
258	154	24.3	-2.567
	165	26.0	-2.568
	166	25.0	-2.664
272	146	26.5	-2.890
	147	27.9	-2.951
	167	27.0	-2.908

Table C-2. Experimental results for hydrogen-allyl alcohol system

$$P_{H_2} = 742 - 769 \text{ mmHg}$$

Stirring speed rpm	Run number	Temp. °C	Raney nickel g	Slope $\times 10^7$ mole/l-sec
132	261	25.9	1.073	1.543
	235	26.0	1.504	1.461
	260	26.0	2.481	1.564
	236	25.9	3.291	1.655
153	249	25.3	1.392	1.773
	266	25.4	2.832	1.876
	267	25.5	4.212	1.879
	265	25.4	6.537	1.990
181	248	26.1	5.218	2.470
	247	26.0	8.645	2.374
	256	26.1	9.947	2.337
	246	25.2	12.372	2.396
225	242	26.1	7.83	3.598
	245	25.9	8.093	3.592
	230	26.0	10.132	3.561
	229	25.4	11.871	3.785
	233	26.1	13.764	3.682
	251	26.0	15.210	3.773
	237	26.9	18.440	3.655
268	26.4	16.340	3.980	

Table C-2. (Continued)

<u>Stirring speed rpm</u>	<u>Run number</u>	<u>Temp. °C</u>	<u>Raney nickel. g</u>	<u>Slope × 10⁷ mole/l-sec</u>
240	238	26.1	14.280	4.723
	231	27.0	15.719	4.836
	254	27.0	18.082	5.021
	253	26.6	20.881	4.715
	239	26.4	24.494	5.002
258	257	26.2	19.076	6.760
	259	27.0	25.348	6.688
	252	26.1	29.659	6.626
272	262	27.0	25.732	7.474
	263	27.0	31.158	7.182
	264	27.0	37.120	7.595
	269	27.0	28.327	6.662

Appendix D

Sample Calculations

1. Oxygen-Sulphite System

Calculation of mass transfer coefficient for run no. 148:

Initial sulphite concentration = 5×10^{-3} mole/l

Total electrolyte concentration ($\text{SO}_4^{2-} + \text{SO}_3^{2-}$) = 0.1 mole/l

Temperature = 28°C

Atmospheric pressure = 748.8 mmHg

(a) Calculation of sulphite concentration for a sample taken at 2200 sec:

Iodine solution used for titration = 0.01N

Sodium thiosulphate solution used was standardized against

0.01N iodine solution:

25 ml I_2 = 25.67 ml $\text{Na}_2\text{S}_2\text{O}_3$

Volume of sodium thiosulphate solution used to titrate

10 ml sample with 25 ml iodine solution = 17.77 ml

The sulphite concentration was then calculated:

$$C_{\text{SO}_3^{2-}} = (1 - 17.77/25.67) \times 25 \times 10^{-3}/2 = 3.874 \times 10^{-3} \text{ mole/l}$$

(b) Calculation of mass transfer coefficient at experiment temperature:

The slope of the curve of $C_{\text{SO}_3^{2-}}$ vs. t (see Figure C-8) was calculated by least squares method. The result is

$$\text{slope} = -1.91 \times 10^{-7} \text{ mole/l-sec}$$

$$k_1 = \phi \text{slope} / 2C_I$$

where

$$\phi = 19 \times 10^3 \times 4 / (3.14 \times 29^2) = 28.78 \text{ cm}$$

C_I was obtained through Figure 5 and correction for the oxygen partial pressure:

$$\begin{aligned}C_I &= 1.006 \times 10^{-3} \times P_{O_2}/720 \\&= 1.006 \times 10^{-3} \times 0.21(748.8 - 28.35)/720 \\&= 2.114 \times 10^{-4} \text{ mole/l}\end{aligned}$$

$$\begin{aligned}k_L &= 0.5 \times 1.91 \times 10^{-7} \times 28.78/2.114 \times 10^{-4} \\&= 1.298 \times 10^{-2} \text{ cm/sec}\end{aligned}$$

(c) Correction for k_L to 25°C

$$\begin{aligned}k_L &\propto (T^3/\mu^5)^{0.25} \\k_{L25^\circ\text{C}} &= k_{LT} \left(\frac{298.16}{T}\right)^{0.75} \left(\frac{\mu_T}{\mu_{25^\circ\text{C}}}\right)^{1.25} \\&= 1.298 \times 10^{-2} \left(\frac{298.16}{301.16}\right)^{0.75} \left(\frac{0.836}{0.894}\right)^{1.25} \\&= 1.186 \times 10^{-2} \text{ cm/sec}\end{aligned}$$

2. Hydrogen-Allyl Alcohol System

Calculation of mass transfer coefficient for run no. 261

Sodium sulphate concentration = 0.1 mole/l

Initial allyl alcohol concentration = 0.05 mole/l

Amount of Raney nickel used = 1.073 g

Stirring speed = 132 rpm

Temperature = 25.9°C

Hydrogen pressure = 760.5 mmHg

(a) Calculation of propanol concentration for a sample taken at 2000 sec:

A calibration curve of the gas chromatograph for propanol concentration is given in Figure D-1. The peak obtained on recorder chart with attenuation = 8 is shown in Figure D-2. The propanol concentration was then calculated:

$$C_{C_3H_7OH} = 1031 \times 8 \times 3.372 \times 10^{-7} = 2.782 \times 10^{-3} \text{ mole/l}$$

(b) Calculation of k_L at experiment temperature:

The slope of the curve of propanol vs. time (see Figure C-11) was calculated by least squares method. The result is

$$\text{slope} = 1.543 \times 10^{-7} \text{ mole/l-sec}$$

$$\begin{aligned} k_L &= \text{slope} \times \phi / C_I \\ &= 1.543 \times 10^{-7} \times \frac{28.78 \times 720}{6.929 \times 10^{-4} \times 760.5} \\ &= 0.607 \times 10^{-2} \text{ cm/sec} \end{aligned}$$

(c) Temperature correction for k_L to 25°C

$$\begin{aligned} k_{L25^\circ C} &= 0.607 \times 10^{-2} \times \left(\frac{273.16 + 25}{273.16 + 25.9} \right)^{0.75} \times \\ &\quad \left(\frac{0.877}{0.894} \right)^{1.25} \\ &= 0.591 \times 10^{-2} \text{ cm/sec} \end{aligned}$$

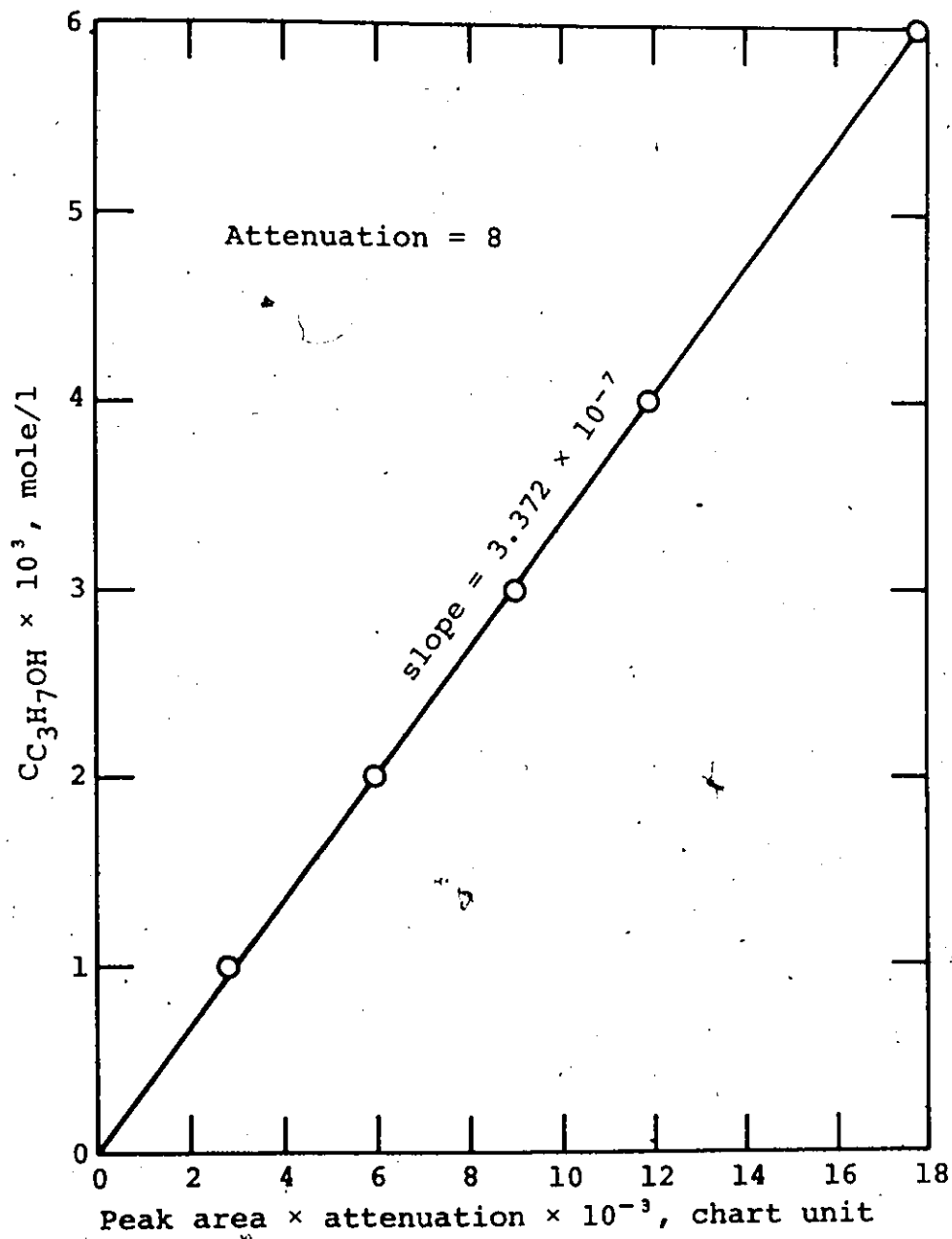


Figure D-1. Calibration of propanol concentration

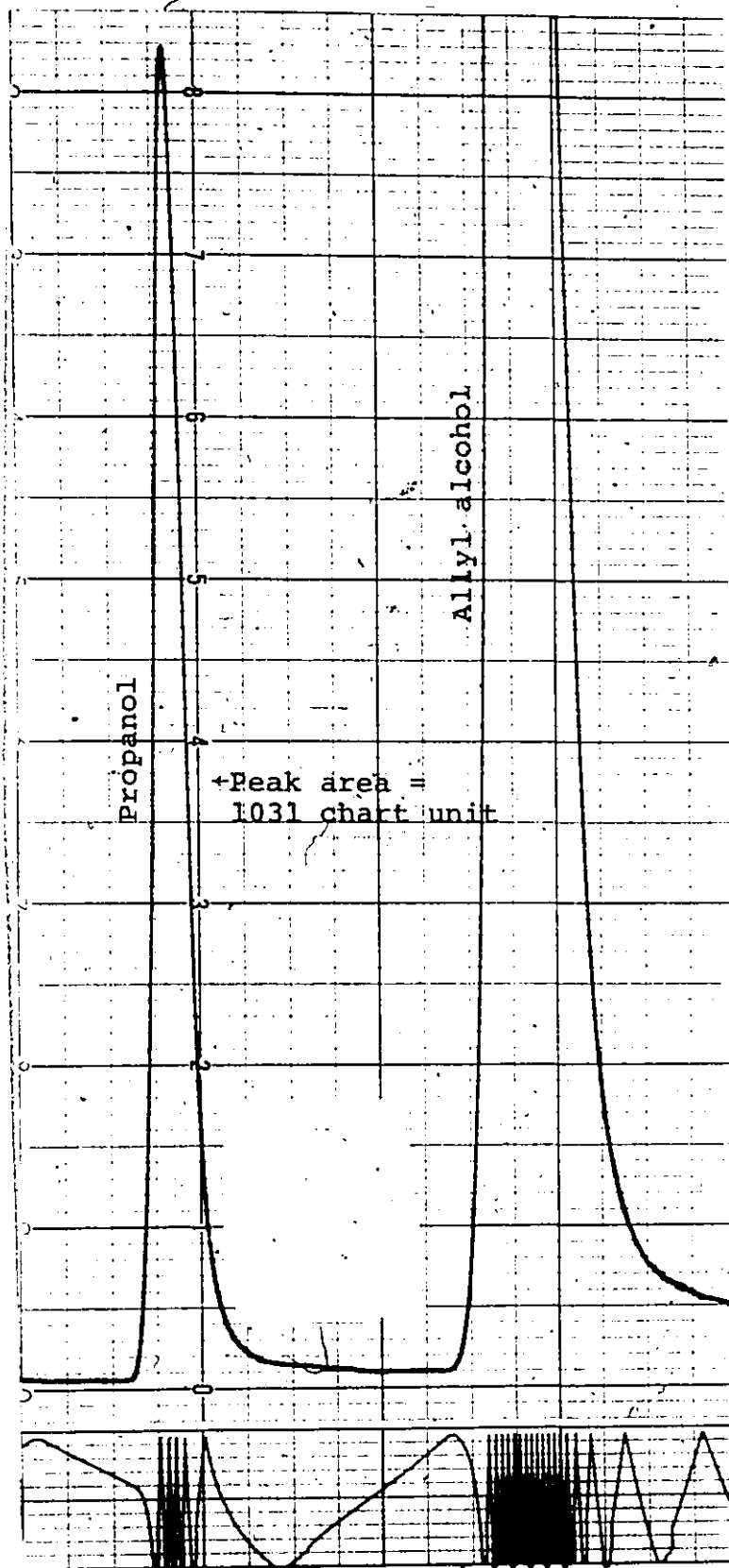


Figure D-2. Typical analysis of propanol by gas chromatography

Appendix E

Abstract of King's Model

King (21) in his treatment of turbulent liquid phase mass transfer at a free gas-liquid interface gives a general model which involves concepts of surface renewals and of a damped eddy diffusivity profile in the vicinity of the surface. By considering that molecular and turbulent diffusion work in parallel, the general equation of unsteady state mass transfer is as follow:

$$\frac{\partial C}{\partial t} = \frac{\partial}{\partial y} \left\{ (D + D_e) \frac{\partial C}{\partial y} \right\} \quad (E1)$$

The value of eddy diffusivity is governed by a limiting law of attenuation and is given by $D_e = ay^n + b$. By assuming that D_e would be damped out at the surface for liquids of high surface tension such as water, the constant b is equal to zero. Equation (E1) becomes

$$\frac{\partial C}{\partial t} = \frac{\partial}{\partial y} \left\{ (D + ay^n) \frac{\partial C}{\partial y} \right\} \quad (E2)$$

with the following boundary conditions:

$$\begin{aligned} C &= C_B \quad \text{at} \quad t = 0, \quad y > 0 \\ C &= C_B \quad \text{at} \quad t > 0, \quad y \rightarrow \infty \\ C &= C_I \quad \text{at} \quad t > 0, \quad y = 0 \end{aligned} \quad (E3)$$

With the consideration of k_L depending upon D , a , n , and t alone in a dimensional analysis, the following expression is given:

$$\frac{k_L}{a^{1/n} D^{1-1/n}} = f\left(\frac{a^{2/n} t}{D^{2/n-1}}, n\right)$$

or, $\psi = f(\tau, n)$

where ψ is the dimensionless mass transfer coefficient and τ is the dimensionless surface age.

It is not possible to obtain a general solution to Equation (E2) for all values of n in any simple fashion. Solutions for special cases for k_L through dimensional analysis and specific solution of Equation (E2) with (E3) are given as follows:

(a) steady state mass transfer asymptote

$$\psi = \frac{n}{\pi} \sin(\pi/n) \quad \text{for } \tau \gg 1 \quad \text{and } n > 1;$$

(b) penetration control asymptote

$$k_L = \sqrt{(D/\pi t)}$$

or $\psi = 1/\sqrt{(\pi t)}$ for $\tau \ll 1$ and $n > 0$;

(c)

$$k_L = \sqrt{(D + a)/\pi t}$$

or $\psi = \sqrt{(2/\pi t)}$ at $n = 0$;

(d)

$$\psi = \frac{2}{\pi^2} \int_0^\infty \frac{\exp(-\tau \xi^2/4) d\xi}{\xi \{J_0^2(\xi) + Y_0^2(\xi)\}} \quad \text{at } n = 1$$

where J_0 is the Bessel function of first kind and zero order and ξ is the dummy variable.

(e) $\psi = k_L/\sqrt{aD}$

$\tau = at$ at $n = 2$

(f) $\psi = k_L\lambda/D$

$\tau = Dt/\lambda^2$ at $n \rightarrow \infty$

All cases at $n = 0, 1, 2,$ and ∞ can be shown graphically by plotting ψ - τ curves which are given in Figure E-1. For other values of n King suggested that the curves will undergo a smooth transition between high and low τ asymptotes. Curves for $n = 3$ and $n = 4$ are also given in Figure E-1 under this consideration.

With the definition for apparent exponent on diffusivity, $m = d\ln k_L/d\ln D$, Figure E-2 is adapted from Figure E-1 and shows m being a function of τ and n .

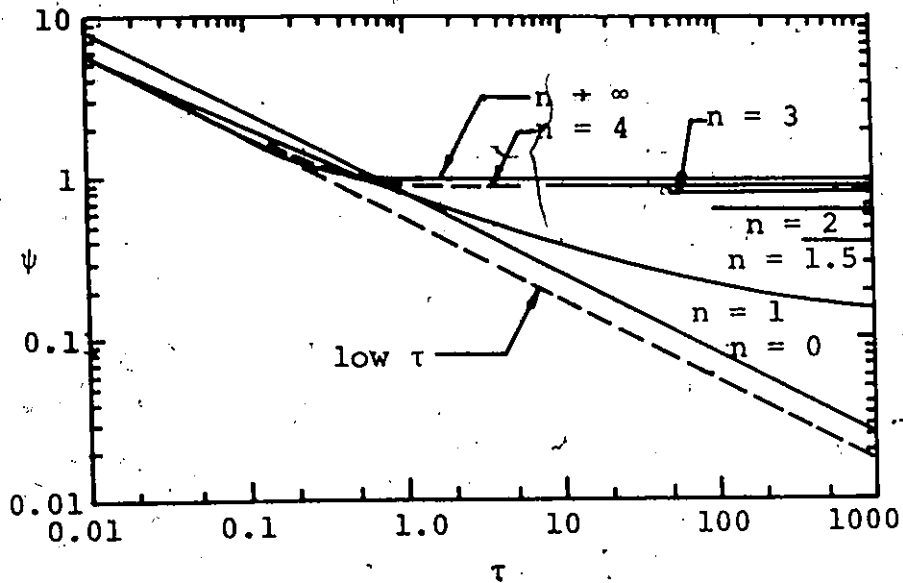


Figure E-1. General model for free surface mass transfer

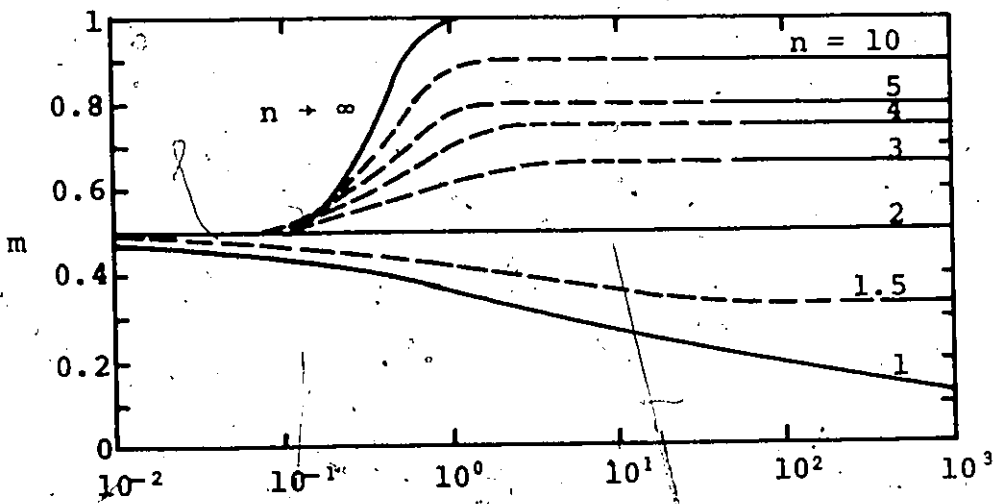


Figure E-2. Exponent on diffusivity vs. dimensionless surface age